INL/EXT-19-55090
Revision 0

Light Water Reactor Sustainability Program

Evaluation of Non-electric Market Options for a Light-water Reactor in the Midwest

August 2019

U.S. Department of Energy

Office of Nuclear Energy

INL/EXT-19-55090

Evaluation of Non-electric Market Options for a Light-water Reactor in the Midwest

Richard Boardman, Jong Suk Kim, Stephen Hancock, Hongqiang Hu, Konor Frick, Daniel Wendt, Cristian Rabiti, Shannon Bragg-Sitton, Idaho National Laboratory

Amgad Elgowainy, Argonne National Laboratory

Robert Weber, Jamie Holladay, Pacific Northwest National Laboratory

August 2019
Idaho National Laboratory
Idaho Falls, Idaho 83415

http://www.inl.gov

Prepared for:
Department of Energy Light Water Reactor Sustainability Program
Under DOE Idaho Operations Office
Contract DE-AC07-05ID14517

EXECUTIVE SUMMARY

This report addresses new market opportunities for nuclear energy at a time when existing light-water reactors (LWRs) are experiencing diminishing revenues in the electricity market. This initial technical/economic assessment indicates LWR hybrid operations can increase the revenue of LWR power-generation stations.

A hybrid system provides an offtake for energy produced by an LWR power-generation station when the price offered for committing electricity to the grid is lower than the cost of producing this electricity. A secondary user benefits by purchasing electrical power, steam, or thermal energy directly from the LWR site at a cost that is lower than it can be purchased from the grid at either the electricity transmission-customer level or the electricity distribution-customer level. At a minimum, this requires a tightly coupled connection to the power-generation operations of the nuclear plant. The LWR hybrid plant may then apportion energy between the industrial user and the electricity grid to optimize the revenue of the nuclear plant, depending on specific day-ahead electricity-grid capacity commitments and reserve capacity agreement requirements. For this market arrangement to work, the non-grid user is sold electricity without paying grid service fees (i.e., being considered a house load). This mode of energy sharing may require approval of governing utility commissions, depending on whether the hybrid operations can affect grid supply and pricing, and in consideration of provisions for grid-capacity payments that may apply to a hybrid system.

This study has addressed the technical feasibility and economic viability of LWR hybrid system operations based on realistic market around a specific reactor site in the Midwest United States near an industrial center that could benefit from more direct use of nuclear energy. The diverse manufacturing, agriculture, and transportation systems in this region provides several advantages to converting a nuclear plant into a hybrid plant that produces hydrogen and other feedstock commodities, such as polyethylene or formic acid. Large-scale hydrogen production can essentially service several refineries within 20–30 miles of the nuclear plant. This would result in a measurable reduction of air-pollutant emissions reduction in the region. In addition, a large, consistent supply of hydrogen would draw new industries to the area—especially other steel-reduction and ammonia plants. For example, the nation's first synthetic-fuels plant could also be sited near this hydrogen plant to convert CO_2 collected from the several ethanol plants in the region into methanol-based chemical feedstock and biofuels. With these perspectives in mind, this study has evaluated the business case for the following hybrid plant options.

- Hydrogen production for use in fuel-cell vehicles, heavy-duty transportation depots, and shipping vessels
- Hydrogen production for ammonia production, iron-ore reduction, and petroleum refining
- Hydrogen production for biogenically derived CO_2 conversion to methanol and synfuels
- Formic acid production for feedstock to the chemicals industry and as a form of hydrogen delivery
- Polyethylene production for plastic products manufacturing.

This evaluation assumes that hydrogen and ethylene production will be supported with energy from the nuclear power plant throughout most of the year while the station sends electricity to the grid as a reserve capacity of less than about 2% of the year. This mode of hybrid operations makes the best use of the capital investments required for hydrogen and ethylene production. Other high-level conclusions from this study include:

1. *The existing fleet of nuclear reactors can reliably produce cost-competitive, moderately high-pressure steam (5.2 MPa, ~300°C) for the projected life of a hybrid plant large capital-investment project.* Engineering calculations indicate the cost of steam generation and delivery by an existing LWR is already lower than the cost of producing steam with a new industrial-scale natural-gas

package boiler. In addition, while the cost of natural-gas production could stay at historically low costs for many years, this is dependent on several factors. The price of natural gas could rise any time when the current surplus is no longer available. The cost of nuclear fuel, on the other hand, is projected to remain flat for decades to come, with little or no volatility in price up to 40–60 years of future LWR operations. This assumes LWR upgrades for license extension remain within plant maintenance and refurbishing activities. **In short, LWR hybrid plants can provide low-cost energy to U.S. energy-intensive manufacturing industries, which can help maintain American competitiveness.**

2. *Affordable clean hydrogen can be produced using energy from the nuclear power plant.* The DOE target for the levelized cost of hydrogen production ((i.e., LCOH <$2.00/kg H_2) can be met and exceeded. The analysis indicates an LWR electricity/hybrid plant can also outperform conventional natural-gas steam reforming under specific operating conditions and clean energy allowances. **The economic evaluation indicates H_2 can be produced for around $1.50/kg, based on the financial parameters invoked for a publically bonded capital project.**

3. *Projected growth in the hydrogen market for fuel-cell vehicles, petroleum refineries, iron-ore reduction, and biofuels and ammonia synthesis provide opportunities to scale-up hydrogen production to nuclear power plant proportions.* The transportation industry seeks to begin operating bus fleets. Iron-ore reduction can be completed with hydrogen produced by the power provided from the nuclear power plant to reduce emissions associated with natural-gas reforming. Similarly, hydrogen can be sent to refineries in the region to help reduce carbon dioxide emissions. New ammonia plants also can provide an outlet for hydrogen production. Finally, the CO_2 produced at ethanol plants can be converted into methanol and synthetic fuels using H_2.

4. *Ethylene production with an emerging electrochemical process can reduce the cost of polyethylene production by over 30%.* At an estimated process energy of 3.06 kwh/kg polyethylene, a nuclear power plant could produce on the order of 2.5 million tons per year of polyethylene using a new INL electrochemical process. The process, electrochemical nonoxidative de-protonation (NDP), demonstrates remarkable advantages compared to steam-ethane cracking in terms of capital cost (40% reduction), operating cost (50% decrease), process energy requirement (77% reduction), and carbon footprint (>70% saving), which indicate a promising future for ethylene production via the electrochemical NDP technology. **At the current polyethylene sales price of $1,521/tonne, annual gross sales of $3.8 billion can be realized.**

5. *Formic acid, HCOOH, which is a commodity chemical (for example, it is used as a biocide or, in the form of its akali salt, as a de-icer) can be synthesized by direct electrochemical reduction of carbon dioxide using electricity from the nuclear plant.* The formic acid can then be either sold as a chemical product, decomposed to release the hydrogen (4 wt %) or directly oxidized in a fuel cell to generate electricity. If approximately 15% of the nameplate capacity of a typical nuclear power plant was used to energize a commercial formic acid synthesis reactor, then the system could generate about 0.3 metric ton (Mt) per year of the acid, which is noticeable compared to the global demand (1.2 Mt/y). At the current market price (about $500/tonne-formic acid), that production rate would generate about $150 million/year. However, the analysis in this assessment indicate water and steam electrolysis are less-expensive routes for producing hydrogen for the industrial uses evaluated in this study. Hence, this hybrid option is viable for locations where formic acid is either produced or consumed as a chemical commodity. It may help raise the revenue of those nuclear power plants in these locations.

6. *Hybrid systems can be used for daily and seasonal energy storage.* **LWR hybrids are especially suitable for thermal- and chemical-energy storage, with the possibility of producing power that matches diurnal demand cycles or peak-season demands.**

7. *Nuclear energy has very low emissions and can be valued similar to other clean energy sources, such as wind and solar.* Hybrid LWR operations will allow nuclear plants to operate at their nameplate capacities while compensating for the variability of intermittent wind and solar energy additions to the electricity grid. **The synergy of nuclear and renewable energy sources can help reduce both U.S. Clean Air Act criteria air pollutants as well as carbon dioxide emissions.**

8. *Nuclear power generating stations provide important grid reliability, and hybrid systems can help maintain certain grid resiliency that is becoming increasingly important with the build-out of renewable energy.* **Hybrid LWR plants that mainly switch power production between large electrical loads and the electricity grid can be used to balance generation and demand on a short time scale (possibly minute by minute). This may help regulate frequency (f) and possible reactive power (var) at the transmission level of the grid.** The actual value of grid-scale LWR hybrid systems requires additional study and evaluation.

In summary, the outcomes of this first in-depth technical/economic assessment of LWR hybrid electricity/H_2 production indicates electrolysis can compete with the conventional process of producing of H_2 by natural gas reforming. However, four conditions likely need to be met before a viable business case can move forward.

Condition 1- A consistent, reliable, and low-cost energy is available throughout the life of the project. Many of the U.S. nuclear power plants meet this condition. The DOE target of producing hydrogen for less than $2/kg looks to be possible when the LWR can provide power for less than about $44/MWh (4.4¢/kWh). The breakeven LCOH for electrolysis, considering the DOE Energy Information Agency baseline natural gas price projection, is $1.56/kg H_2 with electricity provided to the electrolysis plant at around $30.1/MWh (3.1 ¢/kWh). In the worst-case scenario, should natural gas prices remain even drop below the current selling price for the next 30 years, the electricity price required to equate electrolysis performance to natural gas reforming decreases to $23/MWh (2.3¢/kWh) (at around $1.34/kg H_2). However, given the unlikelihood of natural gas prices remaining indefinitely at their historically low prices, it appears LWRs can provide low-cost electricity to a large hydrogen plant. Other conditions also favor the use of nuclear power plant energy for hydrogen production, including the benefits of clean hydrogen and potential grid regulation services that could be paid to the LWR plant owners.

Condition 2- The capital and operating costs of electrolysis stacks are reduced to around $100/kWe for high-temperature steam electrolysis solid-oxide stacks and less than $86/kWe for polymer-electrolyte membrane stacks (direct current power-input rating). Although these cost targets will require additional research and development, manufacturing projections indicate there is a likelihood this can be accomplished.

Condition 3- The market for hydrogen in industrial centers is large and can be supplied from a central hydrogen-production plant. This study indicates market opportunities already exist for high-value, low-volume hydrogen beginning immediately and growing exponentially while high-volume, lower-value hydrogen markets may emerge as soon as 3–7 years.

Condition 4- Policy and regulatory conditions spur the transition from electricity production to nuclear electricity/hydrogen hybrid operations. To optimize revenue for the nuclear power plant, or even to achieve revenue adequacy, it may be necessary to authorize capacity payments for the period of transitioning from day-ahead scheduling to a plant that responds to market signals for electricity production and non-electrical product manufacturing. In addition, policy incentives for clean energy can especially promote markets for LWR hybrid operations.

CONTENTS

FIGURES

Figure 1. Cost of high-pressure steam production using natural gas and nuclear energy. Arrows indicate U.S. DOE Energy Information Agency (EIA) cost projections for natural gas. 2

TABLES

ACRONYMS

AE	alkaline electrolysis
AEO	Annual Energy Outlook (report)
APEA	Aspen Process Economic Analyzer
BOP	balance of plant
BYU	Brigham Young University
CAGR	compound annual growth rate
CAPEX	capital expenditures
CFD	computational fluid dynamics
CSP	concentrated solar power plant
DC	direct current
DCC	direct capital cost
DIW	deionized water
DOE	Department of Energy
DRI	direct reduction of iron
EFORd	equivalent demand forced outage rate
EIA	Energy Information Agency
FT	Fischer-Tropsch
HBI	hot-briquetted iron
HHV	higher heating value
HDSAM	hydrogen delivery scenario analysis model
HTE	high-temperature (steam) electrolysis
HTSE	high-temperature steam electrolysis
HVAC	heating, ventilation, and air conditioning
IHX	intermediate heat exchanger
INL	Idaho National Laboratory
IRR	internal rate of return
LCOH	levelized cost of hydrogen
LHV	lower heating value
LMV	locational marginal prices
LDPE	low-density polyethylene resin
LTE	low-temperature electrolysis
LWR	light-water reactor
MACRS	modified accelerated cost recovery system
MMT	million metric-tonne
MSDS	material safety data sheet

NDP	Nonoxidative de-protonation
NG	natural gas
NHES	nuclear-renewable hybrid energy system
NPV	net present value
NRC	Nuclear Regulatory Commission
NREL	National Renewable Energy Laboratory
O&M	operating and maintenance
OCF	operating-capacity factor
OPEX	operating expenses
OSTG	once-through steam generators
PCM	phase-changed material
PE	polyethylene
PEM	polymer-electrolyte membrane
PFD	process-flow diagram
PJM	Pennsylvania, Jersey, Maryland (Interconnection)
PP	polypropylene
PWR	pressurized water reactor
RTO	regional transmission organization
SHS	sensible heat storage
SMR	steam-methane reforming
SOEC	solid-oxide electrolysis cell
synfuel	synthetic fuel
TBV	turbine bypass valve
TCI	total capital investment
TCV	turbine control valve
TDC	total depreciable capital
TEA	techno-economic assessment
TES	thermal-energy storage
tpd	tonnes per day
TRL	technology readiness level
UCAP	unforced capacity
UI	University of Idaho

1. INTRODUCTION

Light-water reactors (LWRs) are increasingly challenged to compete with natural gas (NG) combined-cycle power plants in wholesale electricity markets due to the historically low cost of natural gas. In addition, in areas where wind- and solar-power generation is being built, the minute-by-minute selling price of electricity is often less than the marginal cost of operating baseload coal and nuclear plants. Consequently, baseload nuclear plants are practically forced to operate at a loss during some periods of the year. This is unsustainable; thus, a new operating paradigm is needed to maintain the profitability of LWR nuclear power plants.

Under the Department of Energy (DOE) Nuclear Energy Light Water Reactor Sustainability Program, Idaho National Laboratory (INL) has completed an initial techno-economic assessment (TEA) of hybrid operations that can increase the revenue of existing nuclear power plants in the United States. This TEA is mainly focused on hydrogen generation for markets in the Midwest. In addition, the possibility of producing polyethylene, formic acid, and methanol were evaluated. Many nuclear reactors are located in similar areas that can support growth in the industrial-manufacturing sector.

This assessment did not consider steam arbitrage to an energy complex, although a wide variety of industrial users could take advantage of the low-cost steam produced by an LWR [1]. Such an energy park is possible, and its potential can be explored later. Rather, this report focuses on hybrid operations where the majority of energy used by the industrial offtake is electricity. This will have the least impact on LWR operations, while extracting of a large amount of thermal energy would require major modifications and would necessarily involve changes to the operating basis and Nuclear Regulatory Commission's (NRC's) operating license. In the current assessment, hydrogen, polyethylene, and formic acid are produced in an electrochemical process that requires minimal heat that can be supplied through the steam-bypass system that is already incorporated into most nuclear plant designs. For example, high-temperature steam electrolysis (HTE) requires less than 7% of the total thermal energy produced by an LWR. With electricity as the main source of energy provided to the electrolysis plant, the LWR power generation system and appurtenant unit operations on the secondary side of an LWR will not be significantly impacted.

Hydrogen and polyethylene markets are growing in the United States and in all other countries. Hydrogen is being recognized as an important energy carrier for energy storage and production of steel, fertilizers, and synthetic fuels. It is needed to refine petroleum crude and for direct use in fuel-cells for electricity generation and for small and heavy-duty transportation. As markets for clean hydrogen develop, water-splitting electrolysis processes powered by clean energy from LWRs provide a tremendous opportunity to change air pollution emissions.

1.1 Light-water Reactor Energy Costs Comparison

The cost of producing hydrogen using natural gas steam-methane reforming (SMR) is highly dependent on the cost of natural gas. Similarly, the cost of producing hydrogen by electrolysis is a strong function of the cost of electricity. Existing nuclear plants can provide a reliable and cost-competitive supply of steam and electricity for hydrogen production for decades to come [2,3]. A comparison of the cost of producing high-pressure steam using a natural gas-fired package boiler versus the cost of producing the same quality and quantity of steam using an LWR is shown in Figure 1. Existing LWR plants produce high-pressure steam for $4.00–5.25/1000-lb depending on the size of the nuclear plant and capital recovery for upgrades to the plant. This is currently 15–45% lower than the cost of producing steam using a natural gas package boiler even before any cost for CO_2 emissions is levied against SMR. The authors believe the cost of steam production by the existing U.S. fleet of LWRs will remain competitive, even with plant upgrades for future license extensions.

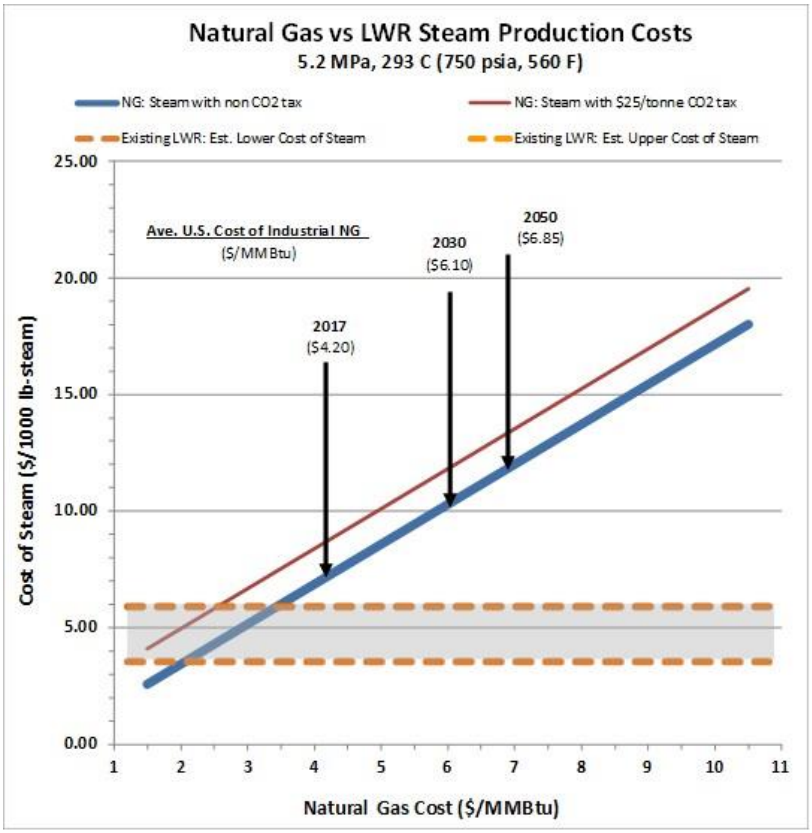

Figure 1. Cost of high-pressure steam production using natural gas and nuclear energy. Arrows indicate U.S. DOE Energy Information Agency (EIA) cost projections for natural gas.

Figure 1. Cost of high-pressure steam production using natural gas and nuclear energy. Arrows indicate U.S. DOE Energy Information Agency (EIA) cost projections for natural gas.

In 2018, the cost of producing electricity with an LWR ranged between about $30 and $40/MWh (the lower for multi-unit plants, the larger for single unit plant). These costs are trending down following capital and operating costs that were required to meet NRC guidance following the Fukushima accident. Electricity produced by single nuclear reactor plants are naturally more expensive than are dual-unit plants. For the purposes of this preliminary assessment, the costs of hydrogen production by low-temperature PEM (labeled low-temperature electrolysis [LTE]) and HTSE (also referred to and labeled high-temperature electrolysis [HTE] throughout this report and in pertinent references) are bracketed between $20 and $50/MWh (in 2018 dollars) to provide a common reference for LWR plant managers because several plant operators have indicated their operating costs can be reduced to less than $25/MWh withing 5 years. A few multi-unit plants have projected costs may be further reduced to just over $20/MWh.

1.2 Future Paradigms for LWRs

LWRs have five potential business cases:

1. *Traditional Baseload.* The nuclear plant operating as a baseload power station, at full capacity except during regular outages to refuel and perform maintenance or plant upgrades. (This mode of operation is not sustainable for many nuclear plants as baseload demand shrinks in deregulated markets, and as the selling price of electricity falls below the total production cost of nuclear stations.)

2. *Flexible Operation*. A nuclear power station dispatches power by ramping down and up to meet net generation demands. Besides selling less electricity throughout the year, this mode of operation could impact revenues due to higher maintenance costs.

3. *Dedicated Energy Park*. A traditional nuclear power generation station is dedicated to selling power and thermal energy (steam or a secondary heat-delivery loop) to one or more energy users according to the energy demands of the users. (This paradigm requires a coordinated buildup of energy users near the power plant where thermal energy is used in their processes.) A wide variety of industrial users could take advantage of the low-cost steam produced by an LWR [1].

4. *Hybrid Operations*. The nuclear plant participates in the electricity grid market while apportioning electricity or thermal energy to one or more energy users according to market signals, to maximize revenue for the nuclear plant. Hybrid operations will usually require energy or product storage to ensure a constant supply of energy is sent to the industrial manufacturing plant. (The business case for hybrid options depends on efficient use of energy and capital of the overall system.) Hybrid operations opens the potential of the systems to be used as spinning reserves when shifting power between the direct user of electricity and the grid. This is possible only when the electricity user can rapidly move from near-maximum capacity to near-minimum capacity within about 10 minutes or less in accordance with North American Electric Reliability Corporation (NERC) regulations [4]. If the electrical user involves large resistive loads, then it may also be possible to provide frequency regulation by taking up or giving up power to the grid in a matter of a few seconds.

5. *Power Revenue Optimization*. The nuclear plant produces and stores energy during periods of oversupply to dispatch additional electricity to the grid during periods of scarcity.

In the current market, some baseload suppliers are curtailed to some level during the night when load demand is at its lowest. Many utilities have structured electricity pricing to encourage more demand during off-peak schedules. As demand picks up in the morning, dispatchable operating reserves are added to grid generation. Because non-commercial renewables alone are not dispatchable, the added generation reduces the need for thermal-electric generation reserves. As renewable generation increases through the morning, traditional baseload plants are required to curtail output—that is, to operate flexibly. It is conceivable, and even projected, that traditional baseload nuclear plants could be shut off completely during seasonal periods of high renewable generation and low electric demand. This point is illustrated in Figure 2, showing a bulk electric grid, which has reached a solar-power penetration of 45% total capacity. This emphasizes the urgency to develop alternative markets for nuclear plants, in particular, unless regulations are in place to fairly compensate these plants for other benefits they may provide (specifically, grid reliability and resiliency, clean-energy generation, and regulation of reactive power and frequency on the grid).

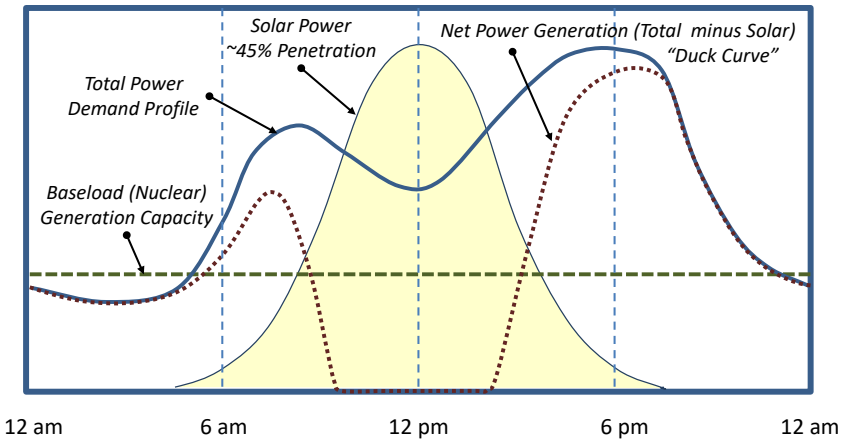

Figure 2. Representative power demand and supply curves for a typical August afternoon. Baseload capacity (including nuclear) = 60% of total annual demand; solar capacity = 45% of total annual demand.

1.3 LWR Hybrid Operations

A hybrid system provides an offtake for energy produced by an LWR power generation station when the price offered for committing electricity to the grid is lower than the cost of producing this electricity. A secondary user benefits by purchasing electrical power, steam, or thermal energy directly from the LWR site at a cost that is lower than can be purchased from the grid at either the electricity transmission-customer level or the electricity distribution-customer level. At a minimum, this requires a tightly coupled connection to the power-generation operations of the nuclear plant. The LWR hybrid plant may then apportion energy between the industrial user and the electricity grid to optimize the revenue of the nuclear plant, depending on specific day-ahead electricity-grid capacity commitments and reserve capacity agreement requirements. For this market arrangement to work, the non-grid user is sold electricity without paying grid service fees (i.e., being considered a house load). This mode of energy sharing may require approval of governing utility commissions, depending on whether the hybrid operations can affect grid supply and pricing, and in consideration of provisions for grid-capacity payments that may apply to a hybrid system. Some nuclear power plant hybrid energy systems may be capable of dispatching load to the grid by quickly shifting power from the industrial user to the grid. Under this mode of operation, the hybrid would be dispatchable as a non-spinning reserve. Then the load can be shifted back to the hybrid user once the grid demand has come down. Some hybrid nuclear plants could also regulate reactive power as well as frequency if the response time constants of the hybrid are sufficiently agile. Such ancillary grid services may someday be valorized by the regional reliability office or grid balancing authorities.

Figure 3 depicts how a hybrid system can will be implemented in an integrated energy system where electricity is provided to the grid when the selling price is high, or to a manufacturing plant that can rapidly absorb this electricity as grid demands rapidly change. In this illustration a portion of the available thermal energy is provided to the industrial user in a coordinated manner. In the case of HTE, the ratio of thermal energy delivered to the electrolysis plant is less than 7% of the total thermal energy produced by the nuclear plant. The remainder of the stream produced by the LWR is used to generate electricity needed by the electrolysis process. Because the temperature rise of the electrolysis system lags thermal energy and electricity delivery to the electrolysis plant, a thermal reservoir may be advantageous to achieve rapid response to the electric grid market signals. Therefore, this report discusses energy extraction and delivery options for LWRs and the types of energy storage that could be used to buffer thermal-energy supply transitions.

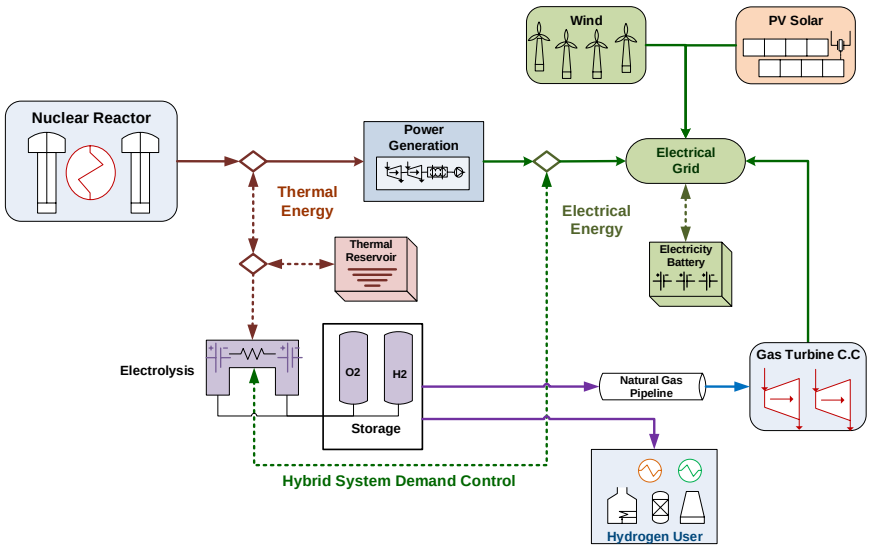

Figure 3. LWR hybrid electricity/hydrogen production-interface development and demonstration.

Four fundamental principles provide a driver for LWR hybrids:

1. The existing fleet of nuclear reactors can reliably produce cost-competitive, moderately high-pressure steam (5.2 MPa, ~300°C) for the projected life of a hybrid-plant large capital-investment project. Engineering calculations indicate the cost of steam generation and delivery by an existing LWR is already lower than the cost of producing steam with a new industry-scale natural gas package boiler. In addition, while the cost of natural-gas production could stay at historically low costs for many years, this is dependent on several factors, and the price of natural gas could rise any time before resource scarcity is realized. The cost of nuclear fuel, on the other hand, is projected to remain flat for decades to come, with little or no volatility in price up to 40–60 years of future LWR operations. This assumes LWR upgrades for license extension remain within plant maintenance and refurbishing activities. In short, LWR hybrid plants can provide low-cost energy to U.S. energy-intensive manufacturing industries, and this can help maintain American competitiveness.

2. Nuclear energy has very low emissions; therefore, it should be valued as a clean-energy, low-carbon, source with the same considerations as renewable energy. Hybrid LWR operations will allow nuclear plants to operate at their nameplate capacities while compensating for the variability of intermittent wind and solar energy additions to the electricity grid. The synergy of nuclear and renewable energy sources can help reduce both U.S. Clean Air Act criteria air pollutant emissions, as well as carbon dioxide (CO_2) emissions that are implicated as a major cause of global warming.

3. Hybrid systems can be used for daily and seasonal energy storage. LWR hybrids are especially suitable for thermal- and chemical-energy storage, with the possibility of producing power that matches diurnal-demand cycles or peak-season demands.

4. Nuclear power generating stations provide important reliability, and hybrid systems can help maintain grid resiliency that is becoming increasingly important with the build-out of renewable energy. Hybrid LWR plants that switch power production between large electrical loads and the electricity grid can be used not just to balance generation and demand as non-spinning reserves that are dispatched within minutes to the grid but possibly on shorter time scales (minute-by-minute) to help regulate reactive power (*var*) or (second-by-second) to help stabilize frequency (*f*) at the transmission level of the grid.

The focus of this study is on the first and second of these principles. The third principal will be studied in future DOE LWRS program studies. Attention to the fourth principle is being examined by various organizations, including the DOE Grid Modernization Initiative, and ongoing efforts are being made to understand the value of assets like large nuclear power generating stations beyond the traditional grid market. Recommendations for future analysis relative to all four of these principles are given in Section 8 of this report.

This TEA mainly focuses on hydrogen generation for associated markets at a site in the Midwest as a possible beginning for conversion of a nuclear power station into a hybrid facility or an industrial complex. Preliminary evaluations of polymer production—based on polyethylene feedstock production—and two important chemical commodities (methanol and formic acid) are also considered. In addition, because the value of utilizing heat produced by an LWR is compelling, a section of this report summarizes LWR heat extraction and thermal-energy storage to provide an initial understanding of pertinent technology development needs. Finally, interest is growing in utilizing biogenically produced CO_2 from any of the numerous ethanol plants in the Midwest as a feedstock to produce formic acid, methanol, and urea fertilizer. Therefore, a pipeline-transport-tradeoff analysis is included in this report to understand the value of a large-scale CO_2 utilization hybrid system located near an LWR versus a distributed plant that would not have access to the thermal energy that can be provided by the LWR.

1.4 Hydrogen as an Energy Network

The advent of cleaner and cheaper power has revived interest in hydrogen as an energy source. Hydrogen can be used for production of iron pellets, nitrogenous fertilizers, polymers, synthetic fuels, forest products, food products, and hydrogen for fuel-cell vehicles. Hydrogen generation is also being considered for large-scale and long-term energy storage when power-generation capacity exceeds the demand of the grid. It can also be injected into natural gas pipelines and burned as fuel for heating and power generation with a fuel cell or gas turbine. If hydrogen is produced from clean, low-emissions energy sources, this will have a significant impact on air quality and can significantly help reduce greenhouse-gas emissions in the United States and throughout the world. A U.S. DOE concept referred to as H_2@Scale (meaning hydrogen at scale, see Figure 4) explores the potential for wide-scale hydrogen production and utilization in the United States to enable resiliency of the power-generation and transmission sectors while also aligning diverse multibillion-dollar domestic industries, domestic competitiveness, and job creation.

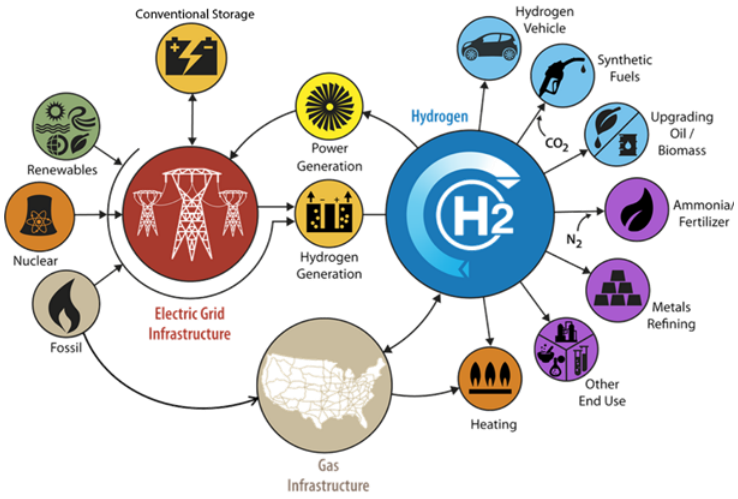

Figure 4. Visualization of DOE concept for H2@Scale [5].

The conventional process for producing hydrogen is steam-methane reforming (SMR), which uses steam and high-temperature heat to convert natural gas into H_2 and CO_2. SMR is mature, and plants have been built by gas-product supply companies such as Air Products, Praxair, Air Liquide, and Linde (among others). Alternatively, electrolysis can be used to split water into hydrogen and oxygen using electricity or pure thermal energy. Low-temperature alkaline electrolysis (AE) technology is fully commercial, but is more expensive than SMR, except on a small scale where pure hydrogen is needed or in regions where the cost of natural gas is high (unlike the U.S.). With assistance from DOE [6], advanced water-splitting materials and technologies are rapidly being advanced by electrolysis-technology-development companies. This includes the use of polymer-electrolyte membrane (PEM) electrolysis and high-temperature steam electrolysis (HTE). These two processes improve the overall efficiency of water splitting, and when nuclear or renewable electricity and heat are used, environmental emissions are near zero.

$$H_2O\ (\text{steam}) + CH_4\ (\text{natural gas}) + (O_2) \xrightarrow{\textbf{\textit{Combustion Process}}} H_2 + CO_2 \qquad \text{[SMR Reaction]}$$

$$H_2O\ (\text{alkaline solution}) + \text{electricity} \xrightarrow{\textbf{\textit{Electrochemical Cell}}} H_2 + O_2 \qquad \text{[AE]}$$

$$H_2O\ (\text{distilled water}) + \text{electricity} \xrightarrow{\textbf{\textit{Polymer Electrolyte Membrane Cell}}} H_2 + O_2 \qquad \text{[PEM Electrolysis]}$$

$$H_2O\ (\text{steam}) + \text{electricity} \xrightarrow{\textbf{\textit{Solid Oxide Electrolyte Cell}}} H_2 + O_2 \qquad \text{[HTE]}$$

1.5 Potential Industrial Markets

The diverse manufacturing, agriculture, and transportation systems around the Midwest provide several advantages in converting a nuclear power plant to a hybrid plant that produces hydrogen and other feedstock commodities, such as polyethylene. Large-scale hydrogen production can essentially service several of these industries, as explained in Section 4. This would have significant impact on air-pollution emissions in the region. In addition, a large, consistent supply of hydrogen would draw new industries to the area, especially other steel-reduction and ammonia plants. The nation's first synthetic-fuels (synfuels) plant could also be sited near this hydrogen plant to convert CO_2 collected from the several ethanol plants in the region into methanol-based chemical feedstocks and biofuels. With these perspectives in mind, this study intentionally evaluates the business case for the following hybrid plant operations.

- Hydrogen production for use in fuel-cell vehicles, heavy-duty transportation depots, and shipping vessels
- Hydrogen production of ammonia production, iron-ore reduction, electronics production, glass manufacturing, and petroleum refining
- Hydrogen production for biogenically derived CO_2 conversion to methanol, formic acid, and synfuels
- Polyethylene production for plastics industries.

References

[1] C. McMillian, R. Boardman, et al., *Generation and Use of Thermal Energy in the United States Industrial Sector and Opportunities to Reduce its Carbon Emissions*, NREL/TP-6A50-66763, INL/EXT-16-39689, October 2016, https://www.osti.gov/search/semantic:1334495.

[2] L. Davis and C. Hausman, "Market Impact of a Nuclear Power Plant Closure," *American Economic Journal: Applied Economics*, 2016, Vol. 8, No. 2, pp. 92–122.

[3] EIA, *2016 Outlook for Natural Gas Prices—U.S. Average*, U.S. Energy Information Agency, 2016.

[4] https://www.nerc.com/docs/pc/ivgtf/NERC_ancillary_services%20ERCOT%20IESO%20NYISO%20MISO%20PJM%20SPP%20WECC%2012%2014.pdf

[5] Bryan Pivovar, "H2@Scale figure produced by National Renewable Energy Laboratory," Department of Energy, 2017.

[6] Hydrogen production technology development falls under the DOE Energy Efficiency/Renewable Energy Fuel Cell Technology Office (or FCTO). https://www.energy.gov/eere/fuelcells/fuel-cell-technologies-office

2. HYDROGEN PRODUCTION

Hydrogen can be produced from a number of different technology pathways and diverse resources. Today, 95% of the hydrogen produced in the United States is made by natural gas SMR in large central plants [1]. SMR is the most economic technology available in most cases, primarily owing to an abundance of low-cost NG. However, alternative hydrogen production technologies with differing costs and levels of maturity are available or under development. For example, interest in electrolysis—the splitting of water into H_2 and O_2 using electricity—has grown in recent years. Electrolysis offers distinct advantages over SMR, and although current electrolytic production costs are a challenge, further research and development is expected to reduce costs. Hydrogen production by electrolysis includes the use of low-temperature PEM electrolysis, which uses only electric power for H_2 production, and high-temperature solid-oxide electrolysis, which uses electricity and heat. These two processes could generate H_2 without carbon emissions when nuclear or renewable electricity and heat are used for electrolysis.

This section, evaluates and summarizes the market potential for a smaller, single-unit pressurized water reactor (PWR) power plant to produce H_2 via PEM-based LTE and nuclear-integrated HTE (or HTE). For comparison, an economic potential for the conventional H_2 production technology (i.e., natural gas SMR) is also included in this TEA. In this case, the capacity of a centralized hydrogen plant is scaled to the nominal energy output or online operating capacity of the nuclear plant. Larger nuclear plants, including most boiling water reactors (BWRs) and multiple unit power plants could produce hydrogen at a lower cost than shown in this assessment based on larger scales of economies.

2.1 Cases Considered

The cost of producing H_2 using SMR is highly dependent on the cost of natural gas. Similarly, the cost of producing H_2 by electrolysis (LTE and HTE) is a strong function of the cost of electricity. Several case studies were conducted to parametrically analyze the effect of such variable operating costs, as well as capital costs (i.e., electrolysis stack costs), on the economic performance of the three hydrogen-production technologies considered.

The study of hydrogen production via SMR process was based on three NG-price scenarios, which utilized pricing data from the U.S. Energy Information Administration's Annual Energy Outlook (AEO) 2018 report [2]: low oil and gas resources and technology (high natural-gas prices), high oil and gas resources and technology (low natural gas prices), and reference natural gas price scenarios. The cases considering a reference natural gas price scenario served as SMR baseline cases throughout this assessment. Figure 5 shows natural gas prices in the Midwest (East North Central region) as projected by the AEO for 2018.

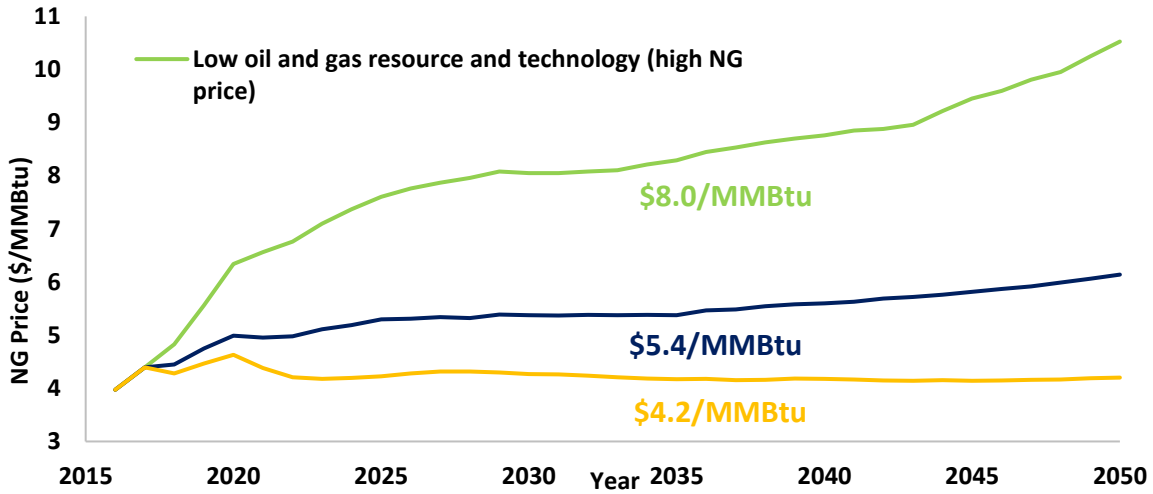

Figure 5. Natural gas prices (2017$) projected by the AEO for 2018. Mean natural gas prices are $8.0/MMBtu (million British thermal units), $5.4/MMBtu and $4.2/MMBtu for high, baseline and low natural gas price scenarios, respectively.

In this assessment, capital expenditures (CAPEX) and operating expenses (OPEX) for the nuclear system were not separately estimated because of the complexity and uncertainty of such a direct approach. Instead, the purchase price of electricity was used parametrically to account for all CAPEX and OPEX of the nuclear system. The wholesale prices of electricity considered ranged from $25–40/MWh. Steam purchased from the nuclear facility (also referred to as "nuclear process heat") was priced at the parametric cost of electricity times the 32.3% thermal efficiency expected for the power conversion system at a typical single-unit nuclear power plant. This effectively equates the cost of heat to the cost of electricity that could otherwise be produced and sold using this heat.

The hydrogen production cost sensitivities to variations in the PEM and solid-oxide electrolysis cell (SOEC) stack capital costs were also assessed. Varying only the stack cost was an adequate assumption as the stacks account for a large percentage of the overall cost for electrolytic H_2 production systems [3]. For the HTE plant, the baseline SOEC stack cost considered was $50/kWe (direct current [DC] power input to SOEC); this stack cost is based on input from Dominion Engineering [3] and is also recommended by the Pacific Northwest National Laboratory based on relevant experience in solid-oxide fuel-cell development.[1] The stack costs of $75/kWe (+50% baseline) and $35/kWe (-30% baseline) were also considered to reflect an expected spread in the cost of SOEC (with all other techno-economic inputs the same as in the baseline case). For the LTE plant, a PEM stack cost of $172/kWe (DC power input to PEM) (or equivalently a total uninstalled capital cost of $400/kWe [total system power usage]) corresponds to a *Projected Future* case[2] defined in James, et al.'s 2016 report [4]. However, this stack cost seems too conservative based on conversations with industry researchers; therefore, the baseline PEM stack cost considered in this analysis was halved to $86/kWe. As in the HTE cases, the stack costs of $300/kWe (+50% baseline) and $140/kWe (-30% baseline) were considered for the LTE cases to reflect an expected spread in the cost of PEM cells.

For LTE H_2 production analysis, this report considered a 24 tonnes per day (tpd) plant (or 23 tpd with a 97.0% operating-capacity factor [OCF]), which requires a total system power input of 50 MWe. It is

[1] HTE builds on the same technology used in solid-oxide fuel cells; hence, the manufacturing costs should rapidly decline as a market for fuel cells used for distributed power generation and heavy-duty transportation vehicles rises.

[2] A *Projected Future* case forecasts improved process parameters with normal improvements in technology as times passes and reduced costs, which are likely attributed to the new materials and systems with higher H_2 production efficiency, longer plant lifetime, and improved replacement cost schedule.

assumed that system power could be supported via a dedicated transmission line connecting the nuclear plant to an industrial plant. Such a scale is typical of a merchant H_2 supply to, for example, an average oil refinery and is defined as a "small-scale" (or low-volume) production case in this analysis.

For HTE H_2 production analysis, the report considered a 578-tpd plant (or 534 tpd with a 92.4% OCF), which requires the electrical and thermal energy of 846 MWe and 192 MWt, respectively. In this case, the report considered HTE integrated with the LWR at the nuclear power plant site as the source of heat and electricity. Such a world-class scale would provide H_2 to multiple industries and is defined as a "large-scale" (or high-volume) production case in this analysis.

For comparison to both the small- and large-scale cases, an economic potential for the SMR H_2 production plant (with a 90% OCF) was assessed. The capacity of an SMR plant was scaled to match the capacity of a given electrolytic H_2 production system.

2.2 Low-temperature Electrolysis

Low-temperature PEM electrolysis (i.e., at less than 100°C) is the process of separating water's elemental constituents by supplying an electrical current to a cell in which the anode and cathode are separated by a solid polymer electrolyte [4]. Water is passed over the anode while the anode is being supplied with an electrical current. The current splits the water into protons (H^+) and oxygen (O_2). The protons pass through the polymer electrolyte to the cathode. At the cathode, the protons reform into diatomic hydrogen, H_2, and leave the system to be further purified, as needed [4]. The hydrogen outlet pressure is 6.9 MPa. Once desired purity is reached, the H_2 can then be used as fuel. Oxygen likewise leaves the electrolysis cell from the anode side of the system where it may have been diluted with air (if a sweep gas is used). For this reason, no practical use for the O_2 is considered for LTE H_2-production analysis. Fgiure 6 depicts a generalized PEM electrolyzer system.

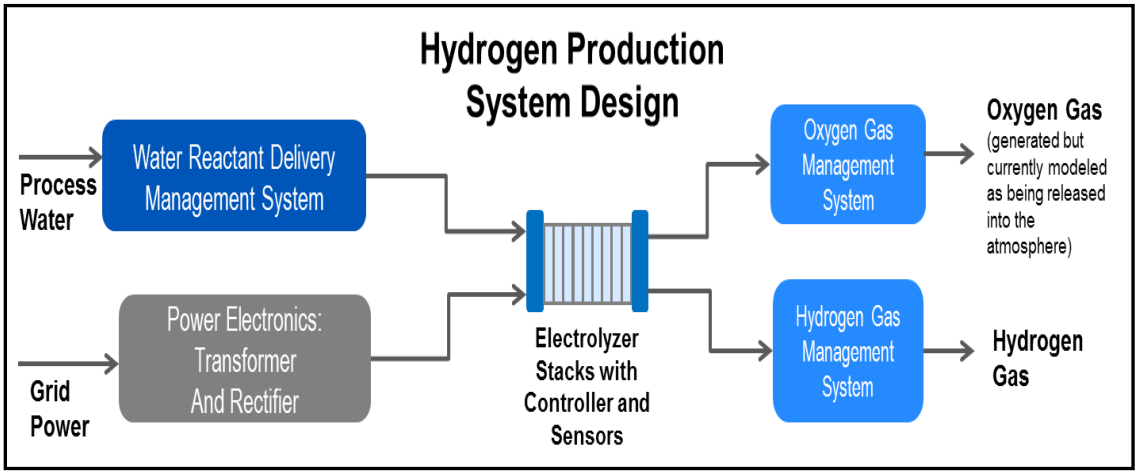

Figure 6. Generalized PEM electrolyzer system [4].

PEM electrolysis accounts for a small amount of current H_2 production, but it has inherent advantages over SMR. For example, if the electrical energy used for electrolysis is sourced from nuclear energy or renewable resources, such as photovoltaics or wind, H_2 can be produced without fossil fuels. Furthermore, electrolyzers can act as a responsive load on power grids, owing to their ability to turn on and off within minutes, and cycle output within subseconds [5]. This capability will become increasingly valuable as the grid incorporates higher levels of variable renewable energy. In addition, PEM-based LTE allows H_2 production on location, thus avoiding significant infrastructure costs for deliveryof H_2.

The economic potential estimates (Section 2.5.1) assumed 50.2 kWh of electricity are required to produce 1 kg of hydrogen (46.7 kWh from electrolyzer stack use, 3.5 kWh from balance of plant use) [6].

2.3 High-temperature Electrolysis Using Nuclear Energy

High-temperature electrolysis (also referred to as high-temperature steam electrolysis [or HTE] to reduce ambiguity in this report) has an operating range of over 600°C and uses electricity and heat to produce hydrogen. Low-cost steam is fed to the cathode where it is split into H_2 and oxygen ions (O^{2-}). The oxygen ions travel across the solid electrolyte to the anode where it is reformed into diatomic oxygen (O_2). As with a PEM electrolyzer, a sweep gas is generally used; therefore, there is no general use for the product oxygen. Electrolysis efficiency increases at higher operating temperatures, requiring less electrical energy. This increased efficiency can lower production costs compared with LTE, because the thermal energy required is generally less expensive than electrical energy. This assessment focuses on (oxygen-conducting) SOEC-based HTE, which is driven with steam and electricity from the pressurized LWR at the nuclear power plant site.

INL has spent several years developing detailed process simulations of the HTE process, mainly for nuclear-integrated cases. These simulations have been developed using Aspen HYSYS, a state-of-the-art, steady-state chemical process simulator [7]. This study makes extensive use of these models and modeling capability at INL to evaluate integration of a nuclear reactor with a Rankine power cycle and an HTE plant located near the reactor site. This report assumes familiarity with Aspen HYSYS; hence, a detailed explanation of the software capabilities, thermodynamic packages, unit operation models, and solver routines is beyond the scope of this work. Process modeling results are subsequently used as inputs for the TEA.

2.3.1 Model Development

The energy duty of the HTE process is approximately 85–90% electricity input. Thermal energy is used to produce and supply superheated steam combined with a gas recycle stream. With custom design of the hydrogen and oxygen separation processes, heat recuperation can be used to superheat steam that is supplied to the HTE process from intermediate-temperature steam generators.

Hydrogen can be efficiently produced using HTE with steam temperatures up to approximately 800°C in SOECs. The steam and associated electricity would be produced by the associated reactor and provide the required input to the HTE unit operations. Heat recuperation from the product streams is used to amplify the temperature of the steam generated in the steam generator to the temperatures required for HTE. Electricity is simultaneously directed to the HTE plant [8].

Figure 7 shows the detail of the overall custom HYSYS process model developed for the thermal and electrical integration of the HTE plant with the pressurized LWR. The model utilizes the steam-generator conditions and electricity produced by the power plant for the integration. Electricity is produced by a subcritical Rankine cycle at the plant. The HTE process draws steam from the steam generator for use in the electrolysis process, which takes place at thermally neutral conditions, defined as isothermal at 800°C and adiabatic. The SOEC operating pressure is 2.3 MPa, producing H_2 at 2.2 MPa. The LWR/HTE integration case consumes all thermal and electrical energy generated internally and supports a nominal H_2 production of 578 tpd, leaving no excess energy in the system.

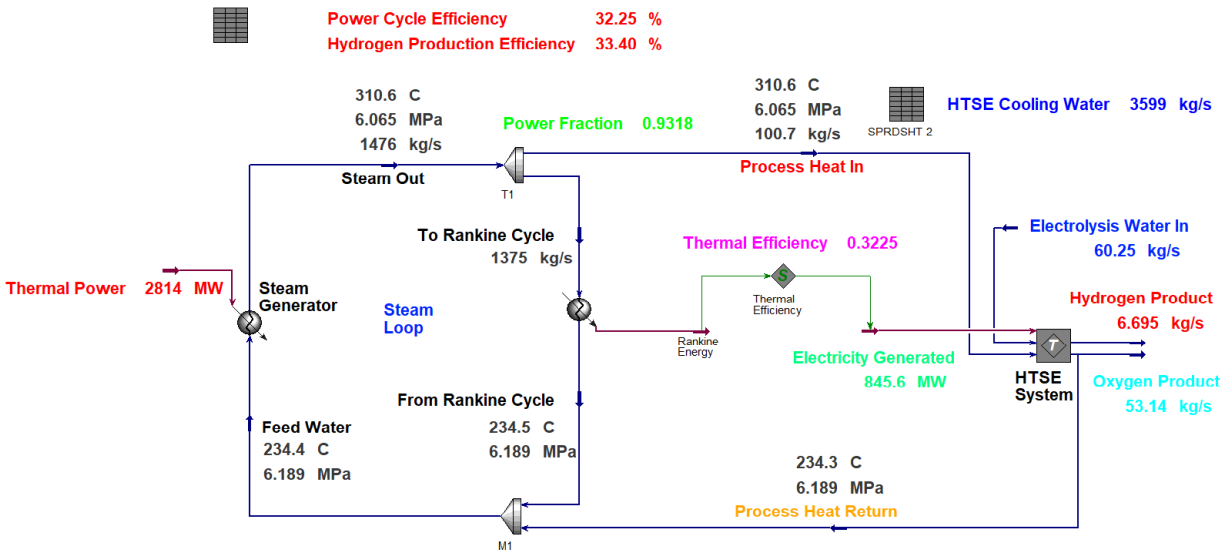

Figure 7. Process-flow diagram of the LWR/HTE integration.

The thermal loop providing heat integration is a closed loop. Steam is used to transfer thermal energy from the nuclear reactor to the HTE plant at a distance of 1000 m. The condensate is pumped from the HTE plant back to the steam generator. A separate water source is required for the electrolysis process. This is mostly a safety consideration. Because the steam generator is rated for a specified steam flow, the reactor system would not respond well to a decrease in steam should there be a situation at the HTE plant, even if it were only a 10% decrease in steam flow. Future work will explore the use of different thermal integration techniques to determine the best options.

Figure 8 shows the nuclear heat integration and recuperation for the HTE process with highlights showing low- and high-temperature heat recuperation, nuclear process heat integration, and electric topping heat. Table 1 summarizes the electrolysis-cell conditions applied in the analysis.

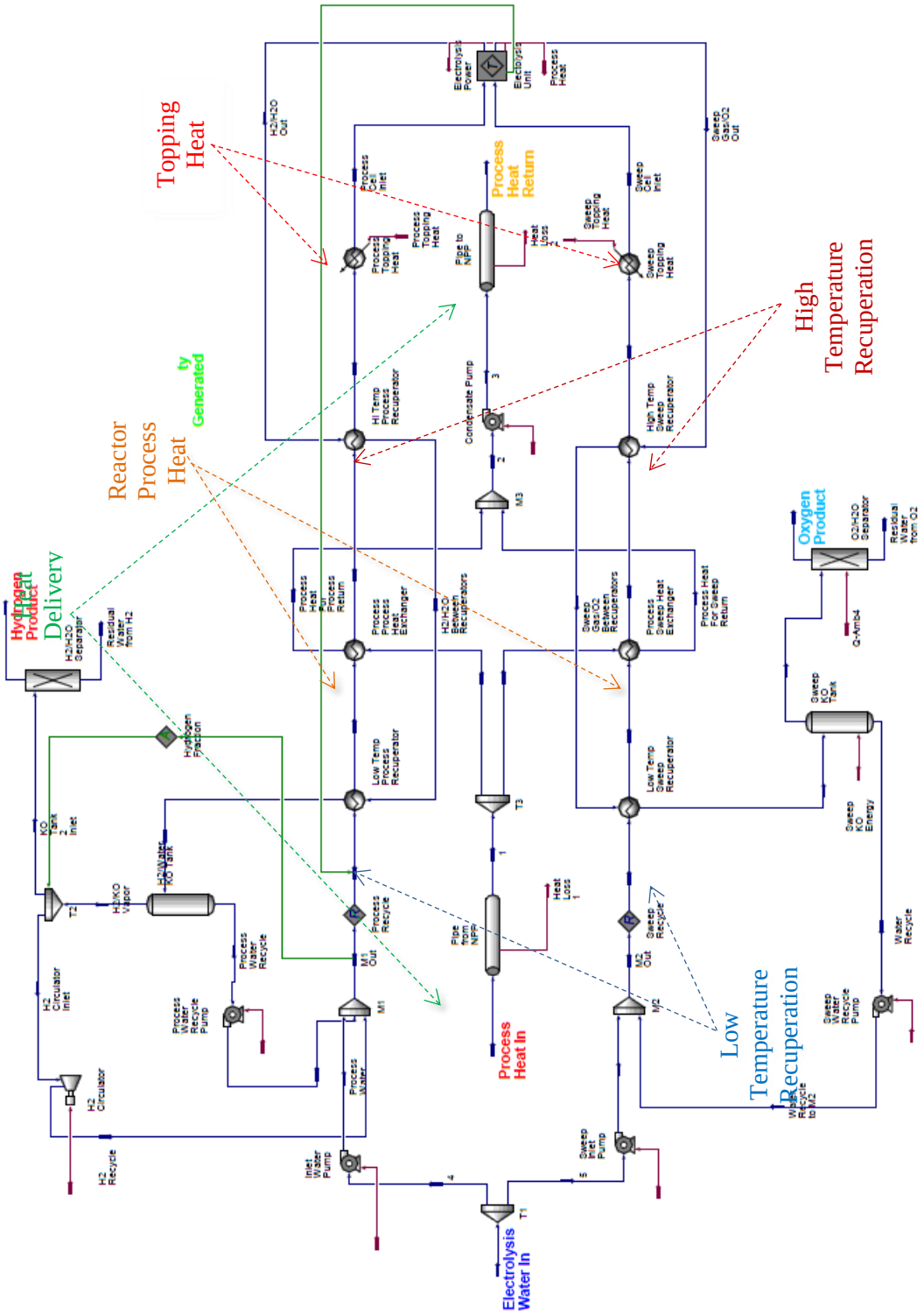

Figure 8. HTE heat-integration process-flow diagram.

Table 1. HTE electrolysis-cell parameters.

Parameter	Unit	Value
Number of Cells	–	1,307,924
Cell Area	cm^2	1000
Cell Active Area	%	70
Current Density	amperes/cm^2	0.7
Area Specific Resistance	Ohms × cm^2	0.4
Operating Voltage	Volts	1.29
Current (per cell)	Amperes	490
Hydrogen Inlet Mole Fraction	%	10
Operating Temperature	°C	800
Operating Pressure	MPa	2.3

2.3.2 Results of the Process Model

Figure 9 graphically presents a high-level material and energy balance summary for the LWR/HTE-integration case at nominal operating conditions. The breakdowns of electricity and thermal-energy consumptions, as well as cooling water use, are summarized in Table 2. A secondary steam loop transfers ~311°C steam from the LWR to the HTE facility, where feedwater is converted to low-temperature steam. High- and low-temperature recuperators are subsequently used to superheat the steam used in the electrolyzers. A total of about 192 MWt of thermal energy is needed for this purpose.

The HTE process requires both the feed and sweep streams to be heated to 800°C, which necessitates additional topping heat from an auxiliary heat source. This heat source could come from a combustor, electric heating, or waste heat from a neighboring process. In this assessment, this topping heat is provided by electrical heaters at the power rating shown in Table 2.

The hydrogen production efficiency for the HTE process is defined as the higher heating value (HHV) of the product hydrogen, divided by the HHV of feed gas and other thermal-energy input into the process [9]. As shown in Table 2, the production efficiency of hydrogen (33.4%) is very close to the thermal-to-electrical conversion efficiency (32.3%). Standard electrolysis of water typically is less than around 25% efficient.

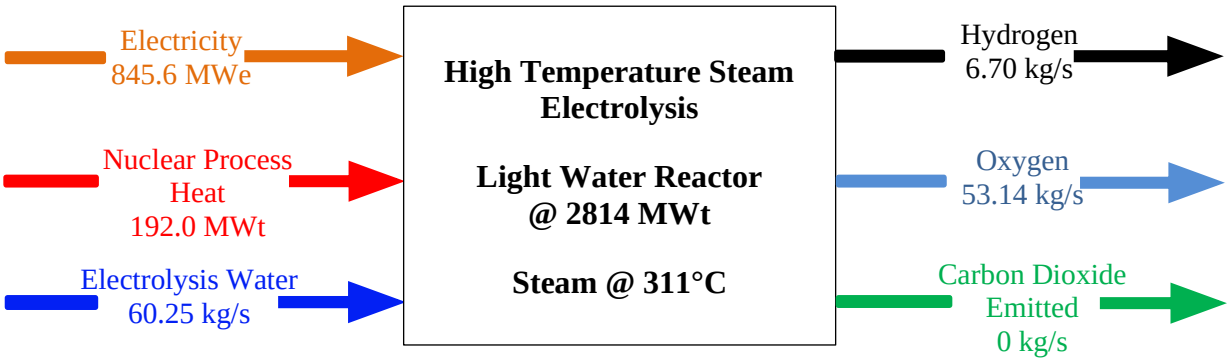

Figure 9. General energy and product flows for the LWR/HTE integration case.

Table 2. Hydrogen production summary.

Description	Unit	Value
Input		
Reactor Thermal Power	MWt	2814
Outputs		
Hydrogen	kg/s [tpd]	6.70 [578]
Hydrogen Production Efficiency	%	33.4
Power Cycle Thermal Efficiency	%	32.3
Oxygen	kg/s [tpd]	53.14 [4591]
Utility Summary		
Total Power Consumed	MWe	845.6
Electrolyzer	MWe	825.4
Pumps	MWe	0.272
Circulator	MWe	0.177
Topping Heaters	MWe	19.73
Nuclear Process Heat		
Total Nuclear Process Heat	MWt	192.0
Water Consumption		
Cooling Water for HTE Process	kg/s	3599
Water Consumed by Electrolysis	kg/s	60.25
Carbon Dioxide (CO_2) Emissions		
Emitted	tpd CO_2	0

Note: The reported values are based on the plant's nominal design capacity (i.e., an OCF of 100%). The actual values depend on the OCF, which in this report is set to 92.4%.

2.4 Economic Modeling Overview

The TEA was performed for each case (described in Section 2.1) using a standard discounted-cash-flow rate-of-return technology. In particular, DOE's H2A Production tool, Version 3.1 [6], was used to determine the levelized cost of hydrogen (LCOH) (i.e., minimum selling price) needed to achieve a net present value of zero, including a specified internal rate of return (IRR) on investments. This tool invokes typical plant economic cost estimates using scaled and factored analysis that include contingencies for engineering, piping, instrumentation and controls, etc. The cost calculation was based on a wide variety of inputs that characterize financial assumptions as well as capital, operating, maintenance, feedstock, utility, and replacement costs.

In this report, all costs are presented in 2019 dollars, unless otherwise stated. The following sections present the economic results.

2.4.1 Basis of Calculations

For all cases considered, the LCOH that achieves a 12% IRR for the given CAPEX and OPEX was calculated. This value is typically reported in the open literature as it serves as a common reference for investor decisions. Table 3 summarizes the economic parameter specifications for the current assessment.

Table 3. Summary of financial model input parameters.

Description	Value	Comments
Oxygen selling price	$0.0317/kg [$31.7/tonne] λ	Fixed selling price at plant gate for only HTE cases
Nominal IRR	12%	Selling price of hydrogen computed for each case
Electricity price ($/MWh-e)	20, 25, 30, 40, 50	
Thermal-energy (steam) cost ($/MWh-t)	Varies	Multiple of an electricity price and the thermal-to-electrical conversion efficiency of 32.3%
Capacity market payment ($/MWh-day)	132.4	See Section 2.4.3 for detailed calculation; only for HTE cases
Debt to equity ratio	80% debt, 20% equity α	80%/20% debt-to-equity ratio for a first-of-a-kind private/public project
Debt interest rate	5% α	Debt backed under Federal Loan Guarantee Program
Debt period	20 years	Debt backed under Federal Loan Guarantee Program
Annual inflation rate	1.9%	
Overall tax rate	24.8%	20% federal; 6% state
Capital depreciation schedule	Standard modified accelerated cost recovery system (MACRS) depreciation method	Depreciation method, with a property class of 15 years
Decommissioning	10% of total depreciable capital	
Salvage value	10% of TCI	
Working capital	10% of the annual change in total operating costs	
Plant construction period	1 year for the LTE and HTE cases, 3 years for the SMR cases	Percent capital invested for the SMR plant is 8, 60, and 32 for the 1st, 2nd, and 3rd years, respectively
Start-up year	2025	
Start-up time	1 year	Operating costs and revenues during start-up are 75% and 50% of the total values, respectively
Plant life and analysis period	20 years	Excluding construction time
OCF	97, 92.4, and 90% for the LTE, HTE, and SMR cases, respectively δ	LWR-integrated HTE system assumed to undergo coordinated outages/maintenance

Notes: α - A debt interest rate of 5% reflects the concept that State or Public Utilities Commissions will approve municipal bonds or the Project will qualify for Federal Loan Guarantees to help encourage continued operations of a Nuclear Power Plant.
λ - Oxygen sales are included in this case study because a variety of industries and medical services are possible in the Midwest Region.
δ - Capacity factors have been selected based on actual histories for SMR and LTE. HTE capacity factors assume solid oxide cell replacements are more frequent.

2.4.2 Capital-cost Estimation

Depreciable capital costs consist of the direct and indirect costs. Direct capital costs (DCCs) (or bare-module costs) for the HTE cases were estimated based on scaled costs (based on unit operations and equipment that is sized for the simulated application) from the preliminary plant engineering and economics completed by Dominion Engineering (under subcontract to DOE's Office of Nuclear Energy) [3]. In addition, for some equipment items, the Aspen Process Economic Analyzer (APEA) [10] was used to estimate the DCCs directly based on the engineering design estimates generated by HYSYS process models (i.e., economy of scale was not used). For the LWR/HTE integration cases, the DCC estimates were generated for the HTE system, balancing-gas system, feed and utility system, sweep-gas system, hydrogen/steam system, hydrogen-purification system, and nuclear steam-delivery system. The DCCs for the LTE and SMR H_2 production systems were adapted from the standard H2A v3.1 default values [6].

After the DCCs were obtained, the site preparation cost (10%), engineering fee (10%), project contingency (15%), contractor's fee (3%), and legal fee (2%), which make up the indirect costs, were assumed for all cases.

The cost of land is non-depreciable and was taken as 1.5% of the total depreciable capital (TDC) [11]. Finally, the TCI was calculated by summing the total depreciable and non-depreciable capital costs. Table 4, Table 5 and Table 6 present the capital-cost breakdown for the LTE (baseline), HTE (baseline) and SMR cases, respectively. Note that the capital costs presented are for inside the battery limits and exclude costs for administrative offices, utilities, storage areas, and other essential and nonessential auxiliary facilities. The results show that the largest single component contributor to the TCI for the baseline LTE case is the power electronics (31%), followed by the PEM stacks (26%). In the case of baseline HTE, the largest single component contributor to the TCI is the HTE vessel (41.9%), followed by the balancing gas system (13.2%).

Figure 10 graphically compares, at different PEM stack costs, the TCIs of the LTE plant with that estimated for the SMR plant, considering the low-volume H_2 production. Figure 11 compares, at different SOEC stack costs, the TCIs of the HTE plant with that estimated for the SMR plant, considering the high-volume H_2 production. As can be seen in Figure 10, the TCIs for the LTE plant (at the considered stack costs) are lower than the SMR case. On the other hand, the TCIs for the HTE plant (at the considered stack costs) are higher than the SMR case (Figure 11). The results also indicate that a TCI for both the LTE and HTE cases, as expected, increases as a stack capital cost increases.

Table 4. TCI for the baseline LTE case (24-tpd capacity, PEM stack capital cost of $86/kWe).

Depreciable capital costs ($)		
Direct (bare-module) costs		
PEM stacks	3,984,219	[26.0]
H_2-management system (cathode system side)	107,682	[0.7]
O_2-management system (anode system side)	107,682	[0.7]
Water-reactant delivery-management system	107,682	[0.7]
Thermal-management system	753,771	[4.9]
Power electronics	4,737,990	[31.0]
Controls and sensors	107,682	[0.7]
Mechanical balance of plant	215,363	[1.4]
Assembly labor	323,045	[2.1]
Other	323,045	[2.1]
Total direct capital cost	10,768,159	[70.4]
Indirect costs		
Site preparation	1,076,816	[7.0]
Engineering and design	1,076,816	[7.0]
Contingencies and contractor's fee	1,938,269	[12.7]
Legal fee	215,363	[1.4]
Total indirect capital cost	4,307,264	[28.1]
Non-depreciable capital costs ($)		
Land	226,131	[1.5]
TCI ($)	**15,301,554**	**[100]**
Electrolyzer power consumption (MWe)	46	
TCI per DC power input to PEM stacks ($/kWe)	329	

Note: Values in the brackets are the breakdown of TCI expressed in terms of percentage.

Table 5. TCI for the baseline HTE case: 578-tpd capacity, SOEC stack capital cost of $50/kWe.

Depreciable capital costs ($)		
Direct (bare-module) costs		
HTE[a]	137,325,961	[41.9]
Balancing-gas system[a]	43,382,308	[13.2]
Feed and utility system[a,c]	6,611,238	[2.0]
Sweep-gas system[b]	6,104,701	[1.9]
Hydrogen/steam system[b]	18,014,752	[5.5]
Hydrogen-purification[a] system	17,685,504	[5.4]
Nuclear steam-delivery system[b]	1,578,569	[0.5]
Total direct capital cost	230,703,033	[70.4]
Indirect costs		
Site preparation	23,070,303	[7.0]
Engineering and design	23,070,303	[7.0]
Contingencies and contractor's fee	41,526,546	[12.7]
Legal fee	4,614,061	[1.4]
Total indirect capital cost	92,281,213	[28.1]
Non-depreciable capital costs ($)		
Land	4,844,764	[1.5]
TCI ($)	**327,829,009**	**[100]**
Electrolyzer power consumption (MWe)	825.4	
TCI per DC power input to SOEC stacks ($/kWe)	397	

Note: Values in the brackets are the breakdown of TCI expressed in terms of percentage.

[a] Scaled from Dominion's report.

[b] Estimated by APEA.

[c] Excludes a deionized water (DIW) system as it is expected to use the existing DIW facility installed at the Nuclear power plant site.

Table 6. TCI for the SMR cases.

	Small scale (26 tpd[a])		Large scale (594 tpd[b])	
Depreciable capital costs ($)				
Direct (bare-module) costs				
Process plant equipment	19,981,130	[50.1]	131,279,532	[50.1]
Balance of plant and offsites	7,983,150	[20.0]	52,450,693	[20.0]
Selective catalytic reduction nitrogen oxides (NOx) control on stack	118,620	[0.3]	779,354	[0.3]
Total direct capital cost	28,082,900	[70.4]	184,509,579	[70.4]
Indirect costs				
Site preparation	2,808,290	[7.0]	18,450,958	[7.0]
Engineering and design	2,808,290	[7.0]	18,450,958	[7.0]
Contingencies and contractor's fee	5,054,922	[12.7]	33,211,724	[12.7]
Legal fee	561,658	[1.4]	3,690,192	[1.4]
Total indirect capital cost	11,233,160	[28.1]	73,803,832	[28.1]
Non-depreciable capital costs ($)				
Land	589,741	[1.5]	3,874,701	[1.5]
TCI ($)	**39,905,801**	**[100]**	**262,188,112**	**[100]**

Note: Values in the brackets are the breakdown of TCI expressed in terms of percentage.
[a] Scaled to match an LTE H_2 production capacity (applying an OCF of 90%).
[b] Scaled to match an HTE H_2 production capacity (applying an OCF of 90%).

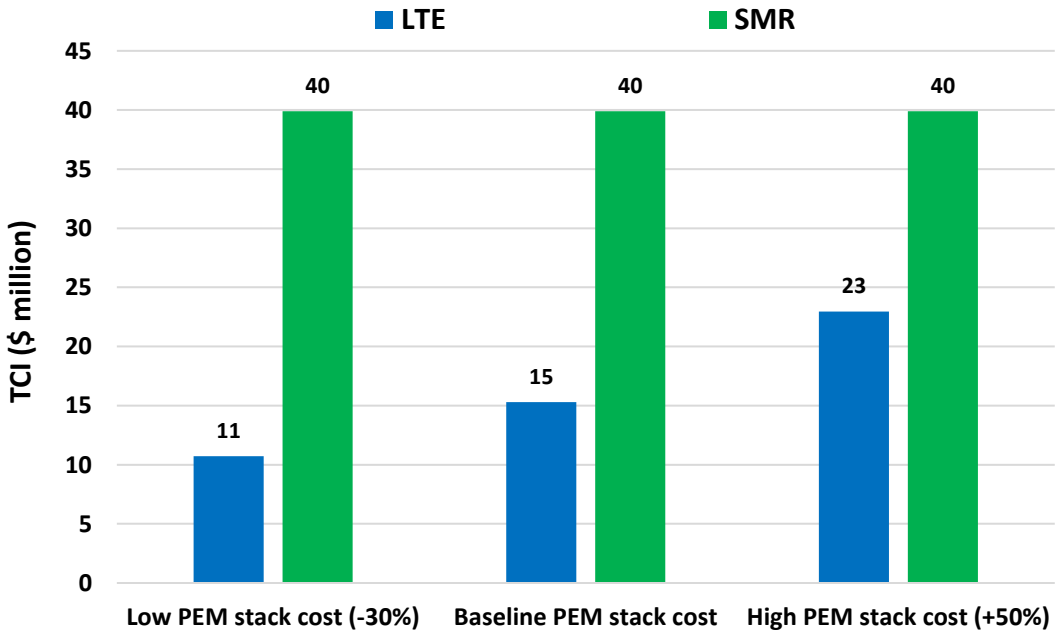

Figure 10. TCIs for the small-scale (23 tpd actual) H_2 production case (LTE versus SMR).

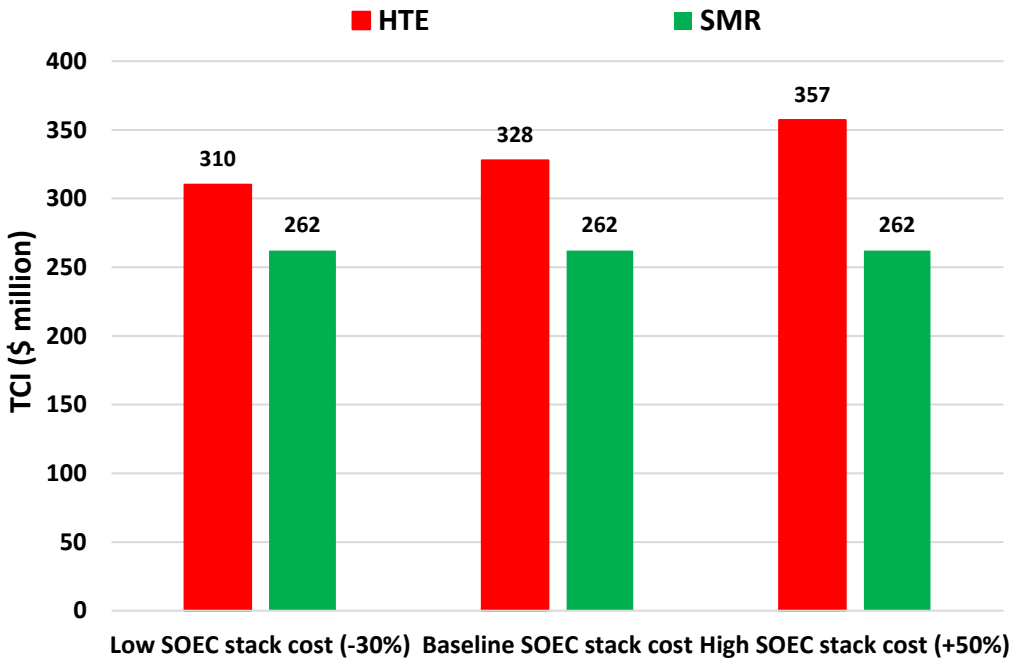

Figure 11. TCIs for the large-scale (534 tpd actual) H_2 production case (HTE versus SMR).

2.4.3 Estimation of Revenue

Yearly revenues were estimated for all cases based on the LCOH specific to each case. For the HTE case, additional revenues were considered: oxygen sales and *capacity (market) payments*.[3] An oxygen selling price of $31.7/tonne (i.e., a standard H2A v3.1 default value [6]) was considered in this analysis.

The capacity submitted to the capacity markets within a PJM regional transmission organization (RTO) is called unforced capacity (UCAP); it must be less than or equal to the generator's installed (nameplate) capacity, adjusted by the equivalent demand forced outage rate (EFORd) [12]. The EFORd is a measure of the probability that a unit will not be available due to forced outages or forced de-ratings when there is a demand on the unit to generate [12]. Therefore, *UCAP = Installed Capacity * (1 – EFORd)*.

The value of the Capacity Market relative to pertinent PJM was applied to the analysis. Table 7 summaries the 3-year forward capacity clearing prices from 2018 to 2021 and the corresponding EFORds specific to the region for this assessment [13]. In this TEA, these data were averaged (excluding the maximum and minimum values), yielding an average capacity market payment of $132.4/MWe-day and an average EFORd of 1.67%. The installed capacity was adjusted by subtracting the required thermal load of 192 MWt (or equivalently 61.9 MWe, applying a thermal efficiency of 32.3%) from the nominal design capacity of 894 MWe, so that the HTE plant is operated continuously, even when 100% of available power is bid into the capacity markets. This resulted in the UCAP of 818 MWe.

Table 8 and Table 9 present the revenues for the small- and large-scale baseline cases, respectively, for an electricity price of $30/MWh. Note that the revenues presented for each case are based on the

[3] *Capacity payments* are made to generators for the capacity they have available to produce electricity at key times, regardless of how much electricity they actually produce. Such capacity markets are run to ensure reliability of the power system by incentivizing entry of new generation and to provide payments to generation that may be critical for system reliability, but may not be profitable from selling electricity alone.

corresponding OCF (see Table 3). Also, these revenues did not consider the H_2 delivery and compression costs, which are discussed in detail in Section 2.4.5.

Table 7. Capacity market clearing prices and EFORds invoked for this study.

Capacity commit period start date [Delivery year]	Capacity market clearing price ($/MWe-day)	EFORd (%)
6/1/2018 [2018/2019]	164.8	1.03
6/1/2019 [2019/2020]	100.0	1.18
6/1/2020 [2020/2021]	76.5	5.44
6/1/2021 [2021/2022]	171.3	2.15

Table 8. Annual revenue for the small-scale baseline cases: electricity price of $30/MWh, mean natural gas price of $5.4/MMBtu.

		LTE	SMR
Hydrogen	Price ($/kg H_2)	2.69	2.79
	Produced (kg/day)	23,187	23,187
	Annual revenue ($)	22,806,550	23,611,680

Table 9. Annual revenue for the large-scale baseline cases: electricity price of $30/MWh, mean natural gas price of $5.4/MMBtu.

		HTE	SMR
Hydrogen	Price ($/kg H_2)	1.22	1.49
	Produced (kg/day)	534,414	534,414
	Annual revenue ($)	238,029,756	291,471,775
Oxygen	Price ($/kg O_2)	0.0317	
	Produced (kg/day)	4,241,784	
	Annual revenue ($)	49,093,845	
Capacity payments	Market clearing price ($/MWe-day)	132.4	
	Capacity submitted to the capacity markets (MWe)	818	
	Annual revenue ($)	39,536,586	
Total annual revenue ($)		326,024,311	291,471,775

2.4.4 Estimation of Manufacturing Costs

Manufacturing cost is the sum of direct and indirect manufacturing costs. Direct manufacturing costs for this project include the cost of raw materials, utilities, and operating labor and maintenance. Indirect manufacturing costs include estimates for the cost of overhead and insurance and taxes.

The stack cell replacement costs were calculated assuming stack replacement every 10 and 7 years for the PEM and SOEC stacks, respectively, based on the work (*Projected Future* cases) shown in [4]. Royalties were assumed to be 2% of the TDC [11]. Labor costs were estimated based on the number of operators per shift[4], shift frequency (5 shift for all cases), and labor cost[5] of $30.8/hr (2019$) for a total of 2,080 hr/yr. Maintenance costs were taken as 2% of the TDC then multiplied by 2.3 to take into account salaries and benefits for the engineers and supervisory personnel and materials and services for maintenance [11]. An overhead of 26% of the labor and maintenance costs was assumed. Annual property taxes and insurance were estimated at 2% of the TDC, which corresponds to a process of low risk, located away from a heavily populated area [11]. Table 10 and Table 11 provide the manufacturing costs for the baseline LTE and HTE cases, respectively, for an electricity price of $30/MWh. Again, operating availabilities of 97% and 92.4% for the LTE and HTE plants were assumed, respectively.

Table 10. Annual manufacturing costs for the baseline LTE case: 24-tpd capacity, PEM stack capital cost of $86/kWe, electricity price of $30/MWh.

Direct costs		
Materials		
PEM stack replacement ($)		207,377
Utilities		
Electricity	Price ($/MWh-e)	30
	Consumed (MWe)	50
	Annual cost ($)	12,745,800
Water	Price ($/k-gal)	2.64
	Consumed (k-gal/day)[b]	95
	Annual cost ($)	88,940
Royalties ($)		301,508
Labor and Maintenance ($)		5,186,240
Indirect costs		
Overhead ($)		1,823,312
Insurance and taxes ($)		306,031
Total manufacturing costs ($)		**20,659,208**

[4] The assumed numbers of operators per shift were 10, 14, and 12 for the LTE (24-tpd capacity), HTE (160-tpd capacity), and SMR (379-tpd capacity) cases, respectively. For each case scenario, they were scaled accordingly to match the target H_2 production capacities.

[5] In 2017, the average operator salary in the United States was $61,620 or $29.6/hr, for a total of 2,080 hrs per year. Applying an annual inflation rate of 1.9%, it is $30.8/hr in 2019 dollars.

Table 11. Annual manufacturing costs for the baseline HTE case: 578 tpd capacity, SOEC stack capital cost of $50/kWe, electricity price of $30/MWh.

Direct costs		
Materials		
SOEC stack replacement ($)		7,923,507
Utilities		
Electricity	Price ($/MWh-e)	30
	Consumed (MWe)	846
	Annual cost ($)	205,306,902
Nuclear process heat (steam)	Price ($/MWh-t)[a]	9.68
	Consumed (MWt)	192
	Annual cost ($)	15,033,826
Water	Price ($/k-gal)	2.64
	Consumed (k-gal/day)[b]	1,378
	Annual cost ($)	1,226,895
Royalties ($)		6,459,685
Labor and Maintenance ($)		22,953,801
Indirect costs		
Overhead ($)		5,080,056
Insurance and taxes ($)		6,556,580
Total manufacturing costs ($)		**270,541,253**

[a] Steam price is estimated by *steam price ($/MWh-t) = η*electricity price ($/MWh-e)*, where η is a thermal efficiency.

[b] Amount of water consumed only considers the process water for electrolysis, excluding the required cooling water amount, which is assumed to be available from nearby lakes.

2.4.5 Estimation of Delivery and Compression Costs

In addition to the H_2 production costs, the study calculated a delivery adder (i.e., the sum of delivery and compression costs) to account for the costs associated with transmitting H_2 from a central production facility to consumption areas. Delivery costs vary with location, quantity delivered, and delivery method (e.g., pipeline, gaseous truck, liquid truck), but estimating all potential delivery pathways and costs is outside the scope of this analysis. Instead, the hydrogen delivery scenario analysis model [6] (HDSAM) [14] was used to calculate pipeline delivery costs for the considered cases: small-scale LTE (short-distance transmission), small-scale SMR (short-distance transmission), large-scale HTE (long-distance transmission), and large-scale SMR (short-distance transmission) cases, shown in Table 12. The economic potentials for all cases presented in Section 2.5 include the delivery adder costs.

Table 12. Delivery adders for hydrogen production.

Cases		Distance (km)	Transmission {Compression} ($/kg H_2)	Adder total ($/kg H_2)	Pipeline inlet pressure (MPa)	Pipeline outline pressure (MPa)
Small-scale case	LTE	3.22	0.08 {0.00}	0.08	6.89	4.86
	SMR	3.22	0.08 {0.06}	0.14	2.39	4.86
Large-scale case	HTE	250	0.28 {0.06}	0.34	2.20	4.86
	SMR	3.22	0.01 {0.06}	0.07	2.39	4.86

2.5 Economic Modeling Results

2.5.1 Small-scale H_2 Production Cases (24 tpd)

Economic modeling results for the small-scale (24 tpd capacity) cases are presented in Table 13. Results are tabulated for three different PEM-stack capital costs. For each stack capital cost considered, the required hydrogen selling price (or LCOH) to achieve a 12% IRR at various electricity prices is listed. For comparison, the LCOH estimated for the conventional hydrogen-production technology (i.e., SMR process) is also included. These results are also graphically presented in Figure 12.

The results indicate that, in general, the LCOH increases linearly as the electricity price increases at a fixed PEM stack capital cost. At a fixed electricity price, an increase in the PEM stack cost of $25/kWe results in an LCOH increase of about $0.12/kg H_2. It is straight forward to observe that the LCOH resulted from the SMR cases increases as the natural gas price increases.

As shown in Figure 12, the economic performance of LTE process can compete with SMR process in a number of scenarios including: (1) a high natural gas price, (2) a low PEM stack capital cost, or (3) a low electricity price. In the best-case scenario (i.e., a high natural gas price and a low stack cost), for example, the LTE cases match (at around $3.45/kg H_2) or exceed the economic performance of the conventional SMR case when the price of electricity falls below $46/MWh. In the worst-case scenario (i.e., a low natural gas price and a high stack cost), the electricity price required to equate the performance of the SMR case in decreased to $25/MWh (at around $2.71/kg H_2), below which economics favor the LTE process over the conventional SMR process. The breakeven LCOH considering a baseline natural gas price and an average stack cost is $2.93/kg H_2 (at around $33.1/MWh).

Economic modeling results considering the baseline PEM stack cost of $172/kWe (DC power input to PEM or, equivalently, a total uninstalled capital cost of $400/kWe [total system power usage]) are presented in Appendix A.

Table 13. Required hydrogen selling price (LCOH) to achieve a 12% IRR for the small-scale cases.

	TCI ($), stack capital cost of $60/kWe [per DC power input ($/kWe)]		TCI ($), stack capital cost of $86/kWe [per DC power input ($/kWe)]		TCI ($), stack capital cost of $129/kWe [per DC power input ($/kWe)]	
	Electricity price ($/MWh)	LCOH ($/kg)	Electricity price ($/MWh)	LCOH ($/kg)	Electricity price ($/MWh)	LCOH ($/kg)
LTE	10,711,088 [230]		15,301,554 [329]		22,952,331 [494]	
	20	2.14	20	2.27	20	2.47
	25	2.40	25	2.52	25	2.73
	30	2.65	30	2.77	30	2.98
	40	3.16	40	3.28	40	3.49
	50	3.67	50	3.79	50	4.00

	TCI ($)	
	NG price (2017$/MMBtu)	LCOH ($/kg)
SMR	39,905,801	
	4.2	2.71
	5.4	2.93
	8.0	3.45

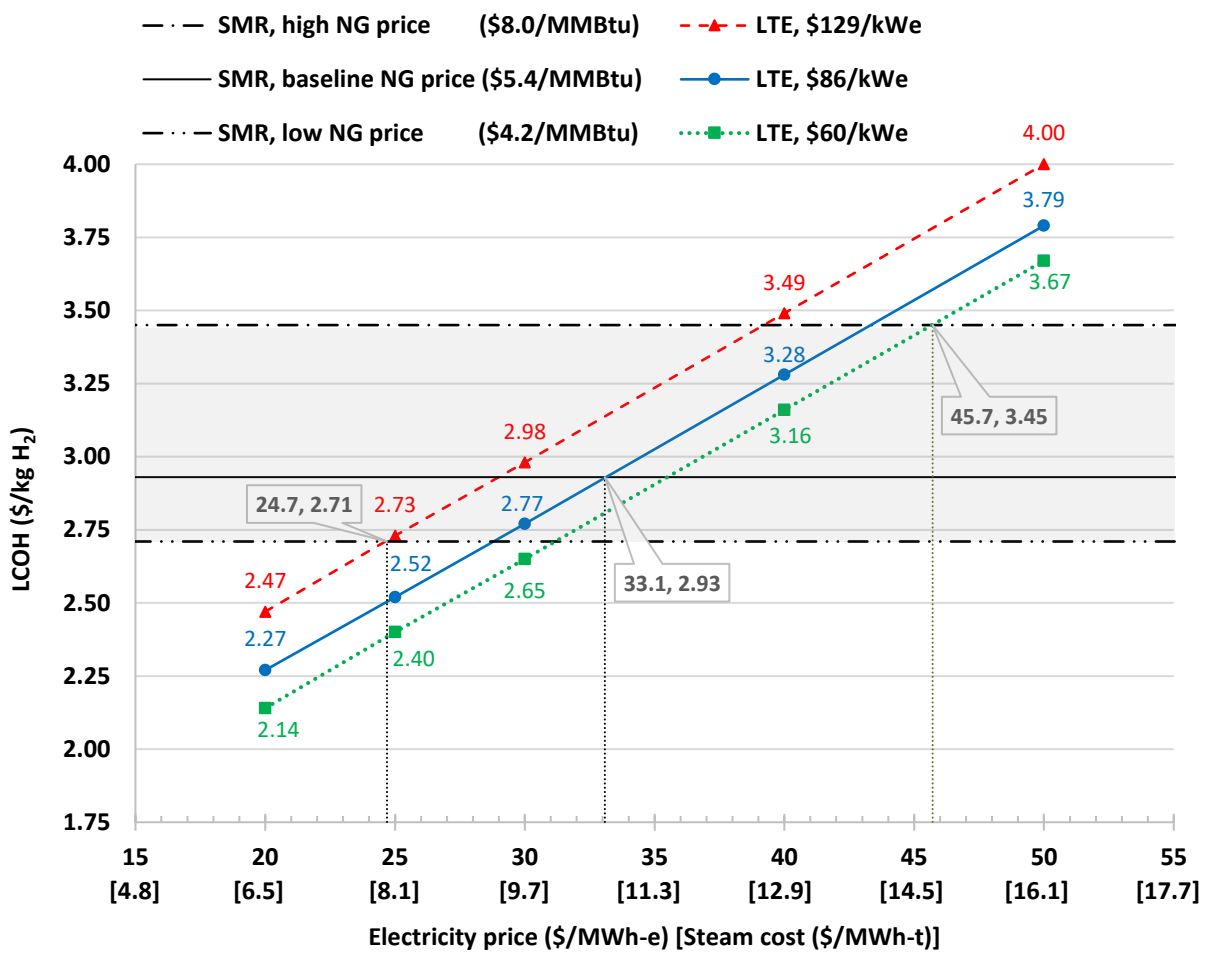

Figure 12. Small-scale cases results (24-tpd H_2 production). Bracketed values are the steam costs applying a thermal efficiency of 32.3%.

2.5.2 Large-scale H_2 Production Cases (578 Tpd)

Economic modeling results for the large-scale (578-tpd capacity) cases considering the capacity payment are presented in Table 14. Results are tabulated for three different SOEC-stack capital costs. For each stack capital cost considered, the required LCOH to achieve a 12% IRR at various electricity prices is listed. For comparison, the LCOH estimated for SMR process is also included. These results are also graphically presented in Figure 13.

The results indicate that, in general, the LCOH increases linearly as the electricity price increases at a fixed SOEC stack capital cost. At a fixed electricity price, an increase in the SOEC stack cost of $25/kWe results in an LCOH increase of about $0.05/kg H_2. It is straight forward to observe that the LCOH resulted from the SMR cases increases as the natural gas price increases. In comparison to the small-scale SMR cases, the LCOH resulted from the large-scale SMR cases is reduced at a given natural gas price due to the economy of scale.

As shown in Figure 13, the economic performance of the HTE process can compete with SMR process in a number of scenarios, including (1) a high natural gas price, (2) a low SOEC stack capital cost, or (3) a low electricity price. In the best-case scenario (i.e., a high natural gas price and a low stack cost), the HTE cases match (at around $2.08/kg H_2) or exceed the economic performance of the conventional SMR case when the price of electricity falls below $44/MWh. In the worst-case scenario

(i.e., a low natural gas price and a high stack cost), the electricity price required to equate the performance of the SMR case decreases to $23/MWh (at around $1.34/kg H_2), below which economics favor the HTE process over the conventional SMR process. The breakeven LCOH, considering a baseline natural gas price and an average stack cost, is $1.56/kg H_2 (at around $30.1/MWh).

Table 15 and Figure 14 present the same results for the large-scale cases without considering the capacity payment. In comparison to the cases with capacity payment, the hydrogen selling prices are increased by about $0.20/kg H_2 in all cases.

Table 14. Required hydrogen selling price (LCOH) to achieve a 12% IRR for the large-scale cases (with capacity payment).

	TCI ($), stack capital cost of $35/kWe [per DC power input ($/kWe)]		**TCI ($), stack capital cost of $50/kWe [per DC power input ($/kWe)]**		**TCI ($), stack capital cost of $75/kWe [per DC power input ($/kWe)]**	
HTE	Electricity price ($/MWh)	LCOH ($/kg)	Electricity price ($/MWh)	LCOH ($/kg)	Electricity price ($/MWh)	LCOH ($/kg)
	310,235,608 [376]		327,829,009 [397]		357,151,344 [433]	
	20	1.13	20	1.16	20	1.22
	25	1.33	25	1.36	25	1.41
	30	1.52	30	1.56	30	1.61
	40	1.92	40	1.95	40	2.00
	50	2.31	50	2.34	50	2.40
SMR	TCI ($)					
	NG price (2017$/MMBtu)		LCOH ($/kg)			
	262,188,112					
	4.2		1.34			
	5.4		1.56			
	8.0		2.08			

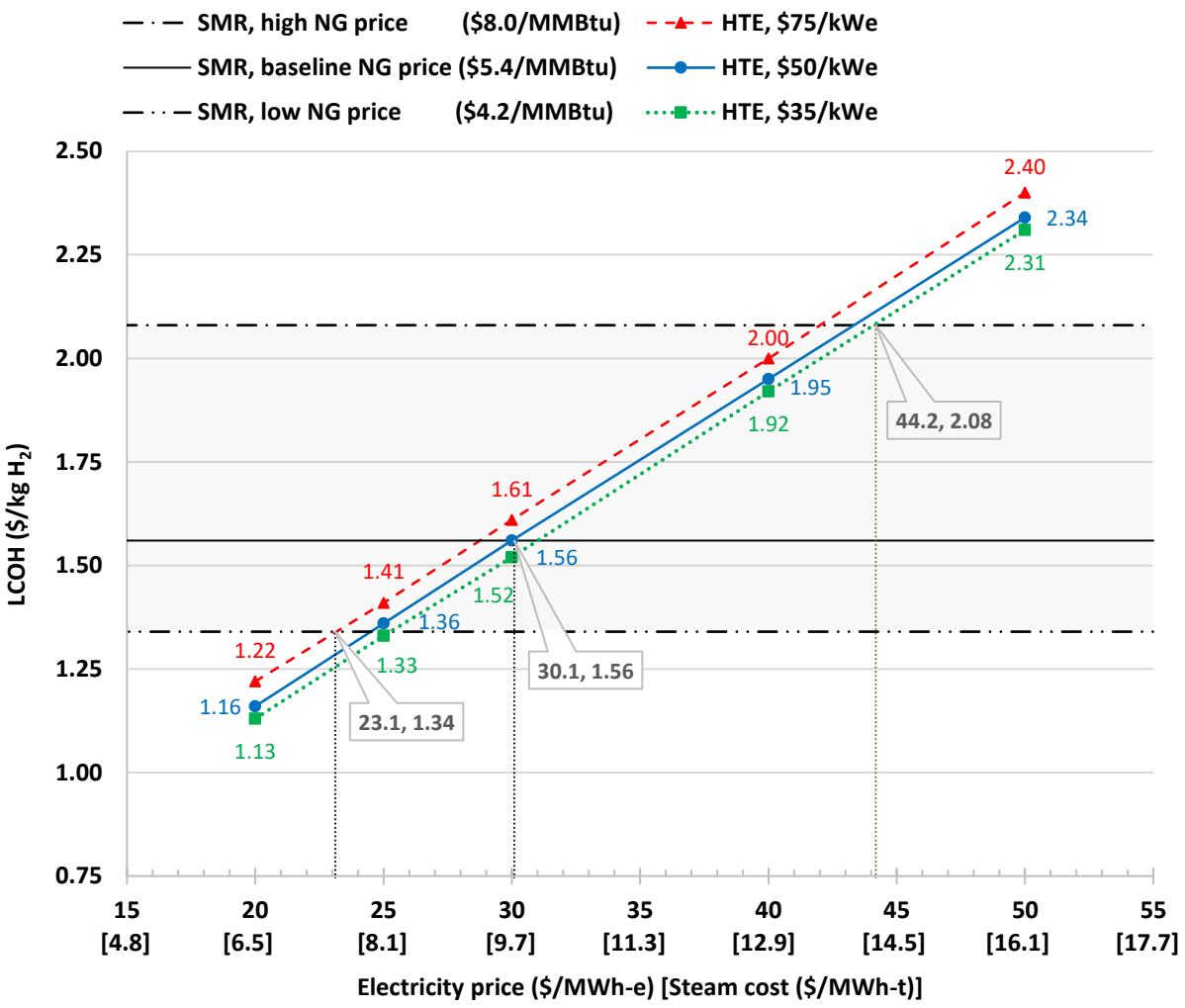

Figure 13. Large-scale case results (with capacity payment). Bracketed values are the steam costs applying a thermal efficiency of 32.3%. [Note: The selling cost of hydrogen is offset ~$0.25/kg-$H_2$ with oxygen sales).

Table 15. Required hydrogen selling price (LCOH) to achieve a 12% IRR for the large-scale cases (without capacity payment).

	TCI ($), stack capital cost of $35/kWe [per DC power input ($/kWe)]		**TCI ($), stack capital cost of $50/kWe [per DC power input ($/kWe)]**		**TCI ($), stack capital cost of $75/kWe [per DC power input ($/kWe)]**	
HTE	Electricity price ($/MWh)	LCOH ($/kg)	Electricity price ($/MWh)	LCOH ($/kg)	Electricity price ($/MWh)	LCOH ($/kg)
	310,235,608 [376]		327,829,009 [397]		357,151,344 [433]	
	20	1.33	20	1.36	20	1.41
	25	1.52	25	1.56	25	1.61
	30	1.72	30	1.75	30	1.81
	40	2.11	40	2.14	40	2.20
	50	2.50	50	2.54	50	2.59
SMR	TCI ($)					
	NG price (2017$/MMBtu)		LCOH ($/kg)			
	262,188,112					
	4.2		1.34			
	5.4		1.56			
	8.0		2.08			

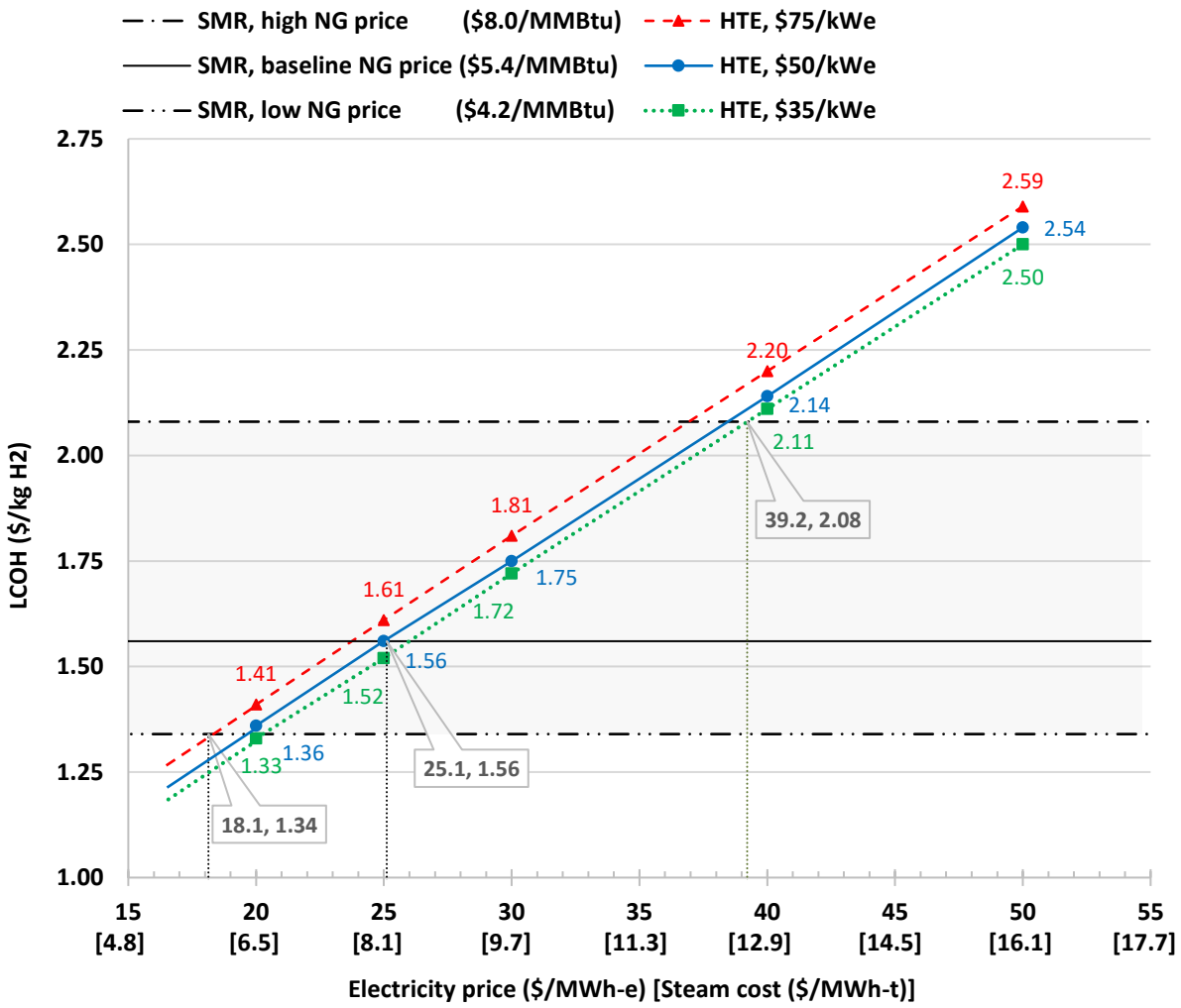

Figure 14. Large-scale case results (without capacity payment). Bracketed values are the steam costs applying a thermal efficiency of 32.3%. [Note: The selling cost of hydrogen is offset ~$0.25/kg-$H_2$ with oxygen sales).

2.5.3 Hydrogen Production Cost Breakdowns

Table 16 summarizes the H_2 production cost breakdowns for the four LTE cases, which are also graphically shown in Figure 15. From these results, it can be concluded that the primary cost driver for LTE H_2 production is the electricity cost for the electrolysis when the electricity price is high (>$40/MWh). However, the capital related costs would account for close to 50% of the total costs when the electricity price is low (<$20/MWh). In other words, a dramatic improvement in economic performance could be achieved when the variable operating and maintenance (O&M) costs (such as electricity price) can be reduced. In addition, if the PEM-stack capital cost can be reduced from $86/kWe to $60/kWe as a result of further development and commercialization of LTE technology, the LCOH (at a fixed electricity price) can be reduced by about $0.12/kg H_2.

Table 17 summarizes the H_2 production cost breakdowns for the four HTE cases with capacity payment, which are also graphically shown in Figure 16. Table 18 and Figure 17 present the same results for the HTE cases without capacity payment. The same trends are observed for all HTE cases as in the LTE H_2 production scenarios.

The H_2 production cost breakdowns for all cases are shown in Figure 18 (HTE cases with capacity payment) and Figure 19 (HTE cases without capacity payment).

Table 16. H_2 production cost breakdowns for LTE cases.

Component	$86/kWe, $40/MWh	$60/kWe, $40/MWh	$86/kWe, $25/MWh	$60/kWe, $25/MWh
Electricity	$2.01	$2.01	$1.25	$1.25
Steam	$0.00	$0.00	$0.00	$0.00
Other Variable O&M	$0.01	$0.01	$0.01	$0.01
Fixed O&M	$0.90	$0.85	$0.90	$0.85
Decommissioning Costs	$0.00	$0.00	$0.00	$0.00
PEM Stack Replacement Costs	$0.02	$0.01	$0.02	$0.01
Other Costs (including capital and taxes)	$0.27	$0.20	$0.26	$0.19
Compression & Delivery	$0.08	$0.08	$0.08	$0.08
LCOH ($/kg H_2)	**$3.28**	**$3.16**	**$2.52**	**$2.40**

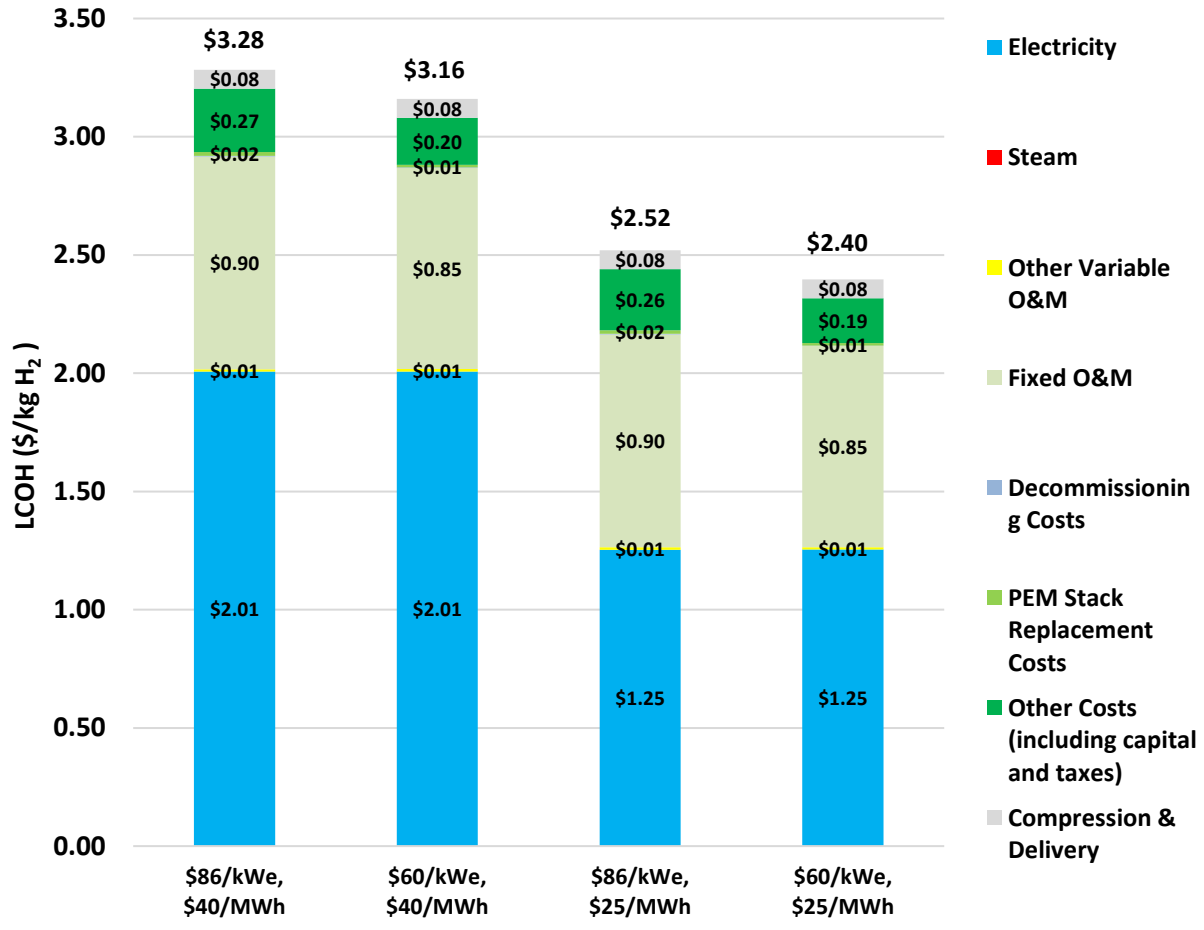

Figure 15. H_2 production cost contribution for four LTE cases (24-tpd H_2 production).

Table 17. H_2 production cost breakdowns for HTE cases (with capacity payment). [Note: The selling cost of hydrogen for HTE is offset ~$0.25/kg-$H_2$ with oxygen sales).

Component	$50/kWe, $40/MWh	$35/kWe, $40/MWh	$50/kWe, $25/MWh	$35/kWe, $25/MWh
Electricity	$1.13	$1.12	$0.62	$0.62
Steam	$0.08	$0.08	$0.05	$0.05
Other Variable O&M	$0.01	$0.01	$0.00	$0.00
Fixed O&M	$0.17	$0.16	$0.15	$0.14
Decommissioning Costs	$0.00	$0.00	$0.00	$0.00
SOEC Stack Replacement Costs	$0.03	$0.03	$0.03	$0.02
Other Costs (including capital and taxes)	$0.19	$0.18	$0.17	$0.15
Compression & Delivery	$0.34	$0.34	$0.34	$0.34
LCOH ($/kg H_2)	**$1.95**	**$1.92**	**$1.36**	**$1.33**

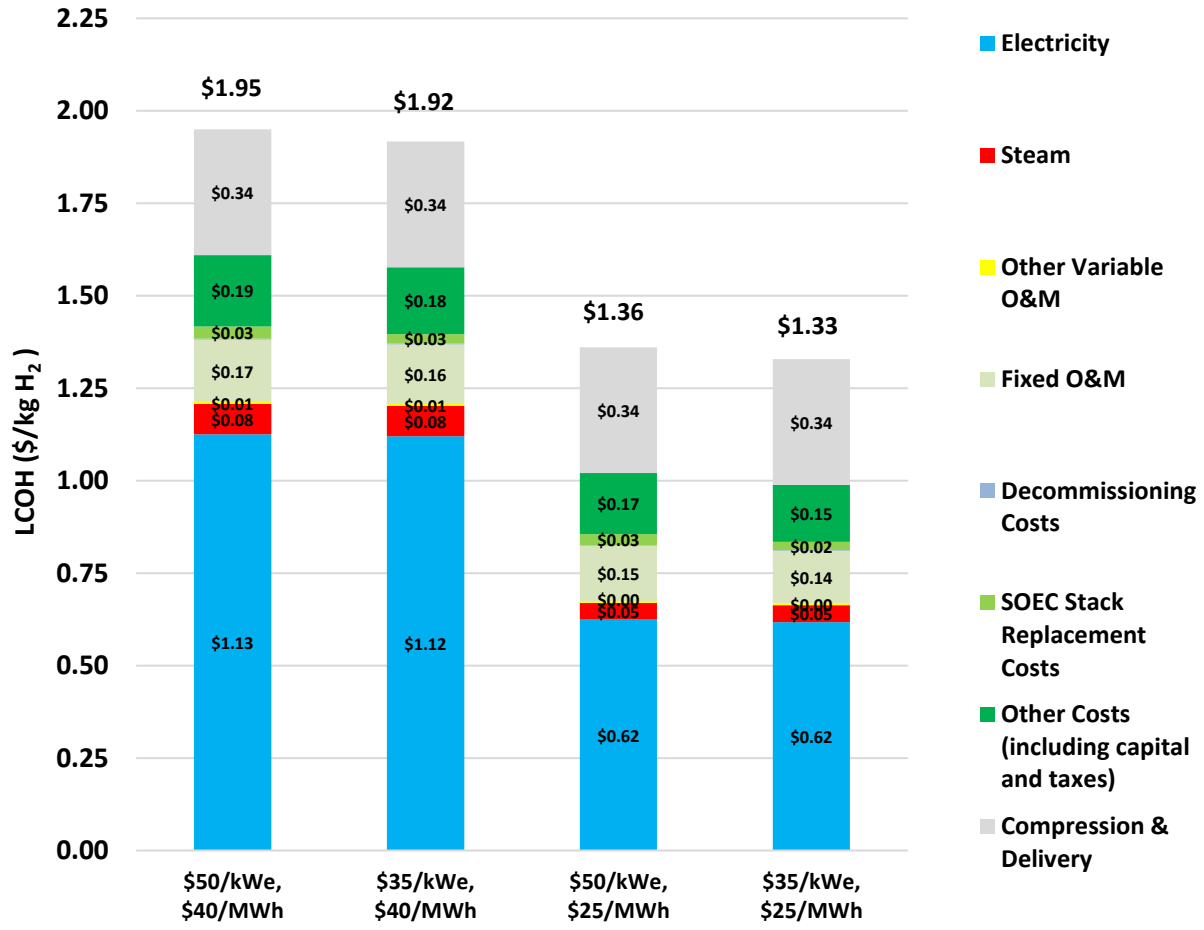

Figure 16. H_2 production cost contribution for four HTE cases (534-tpd H_2 production at 92.4% OCF with capacity payment). [Note: The selling cost of hydrogen for HTE is offset ~$0.25/kg-$H_2$ with oxygen sales).

Table 18. H_2 production cost breakdowns for HTE cases (without capacity payment).

Component	$50/kWe, $40/MWh	$35/kWe, $40/MWh	$50/kWe, $25/MWh	$35/kWe, $25/MWh
Electricity	$1.26	$1.26	$0.74	$0.74
Steam	$0.09	$0.09	$0.05	$0.05
Other Variable O&M	$0.01	$0.01	$0.01	$0.01
Fixed O&M	$0.19	$0.18	$0.18	$0.17
Decommissioning Costs	$0.00	$0.00	$0.00	$0.00
SOEC Stack Replacement Costs	$0.04	$0.03	$0.04	$0.03
Other Costs (including capital and taxes)	$0.22	$0.21	$0.20	$0.19
Compression & Delivery	$0.34	$0.34	$0.34	$0.34
LCOH ($/kg H_2)	**$2.14**	**$2.11**	**$1.56**	**$1.52**

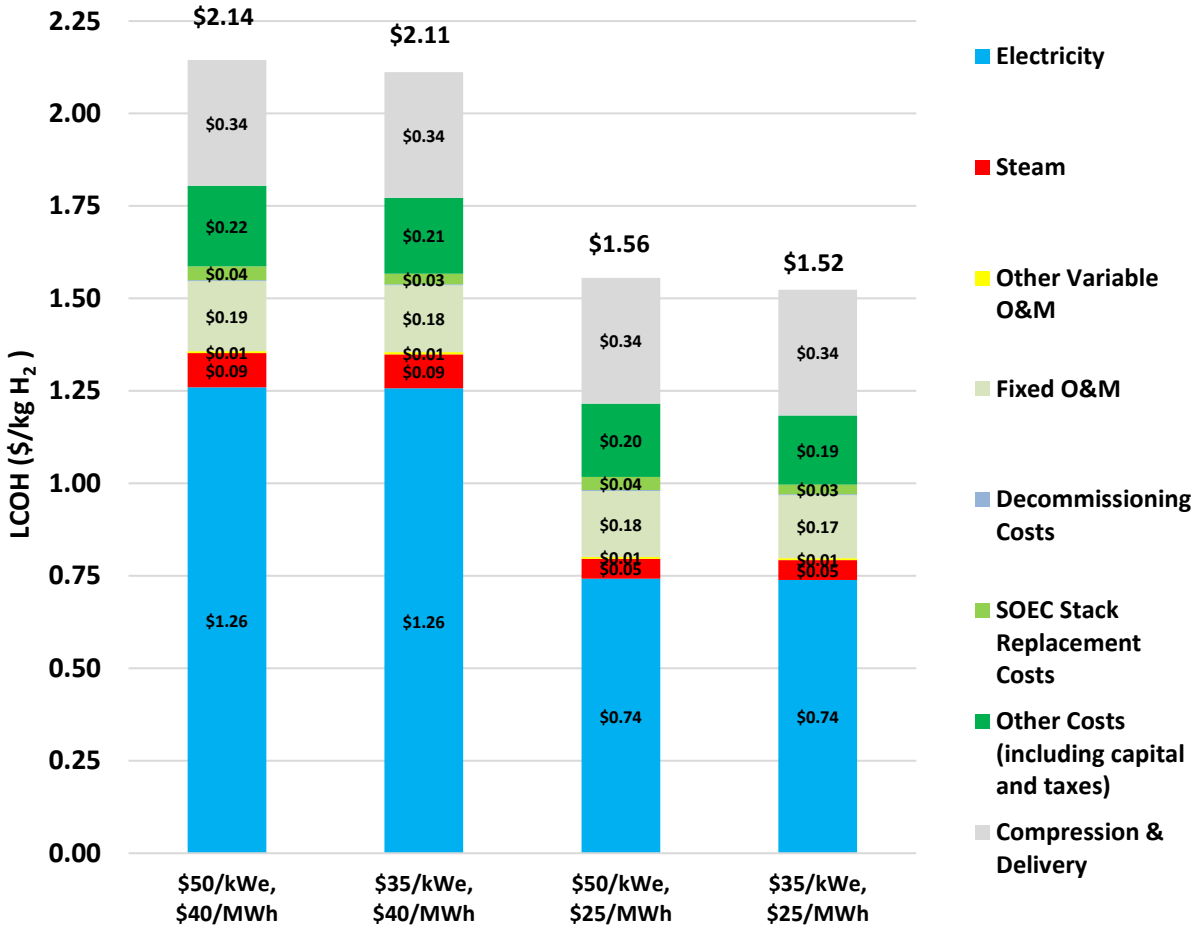

Figure 17. H_2 production cost contribution for four HTE cases (534-tpd H_2 production at 92.4 OCF without capacity payment).

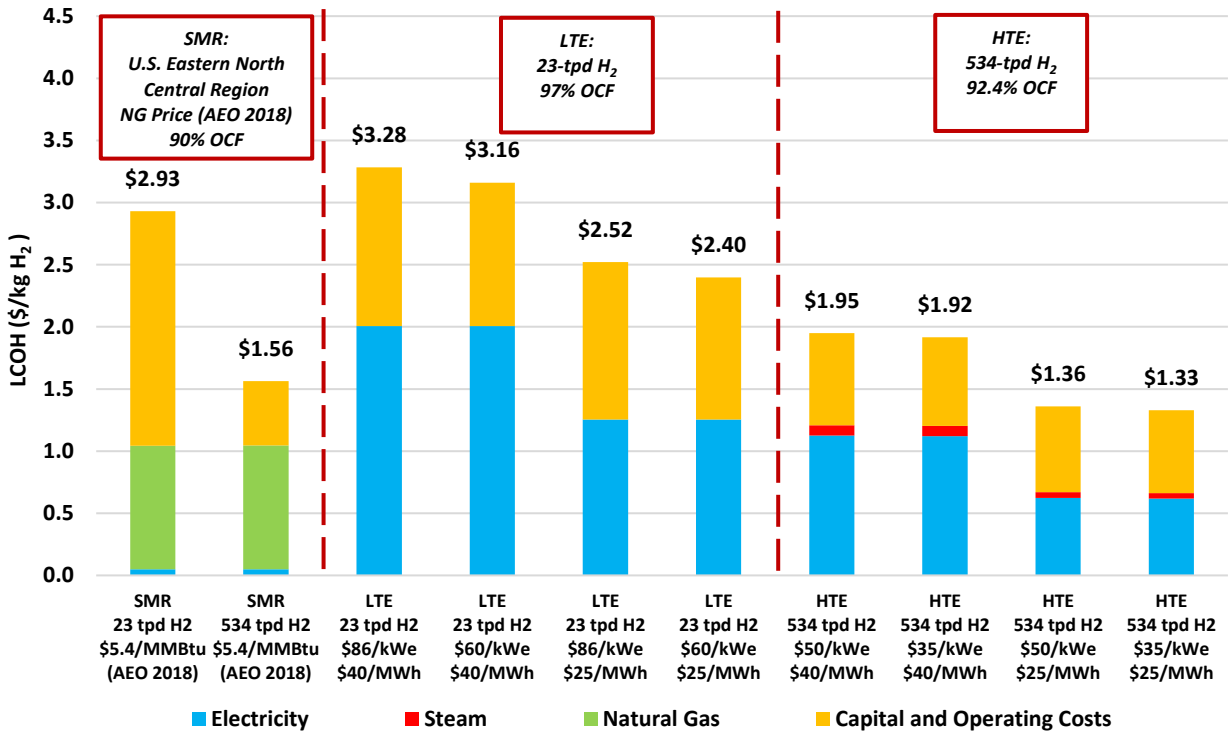

Figure 18. H_2 production cost contribution for all cases (HTE cases with capacity payment and oxygen sales).

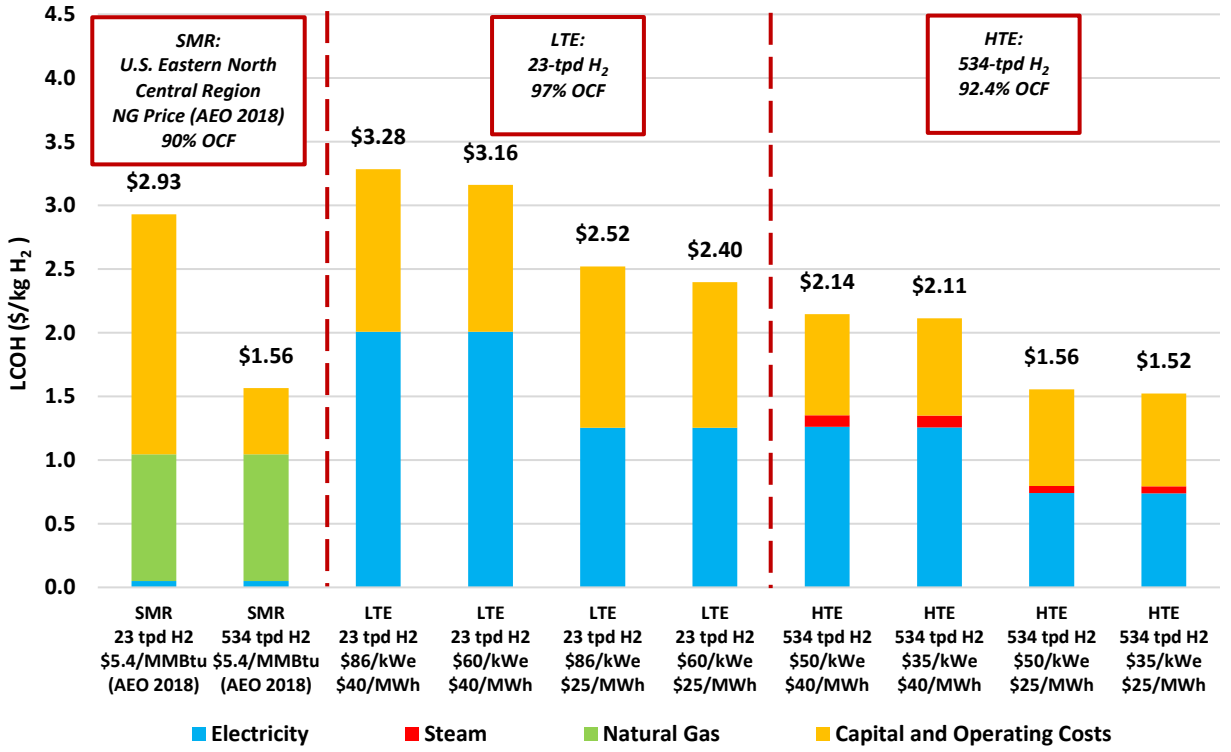

Figure 19. H_2 production cost contribution for all cases (HTE cases without capacity payment; with oxygen sales).

References

[1] U.S. DOE, "Hydrogen Production: Natural Gas Reforming," https://www.energy.gov/eere/fuelcells/hydrogen-production-natural-gas-reforming; 2018 [accessed February 18, 2019].

[2] U.S. EIA, "Annual Energy Outlook 2018," https://www.eia.gov/outlooks/aeo/tables_ref.php; 2019 [accessed January 26, 2019].

[3] P. Krull, J. Roll and R. D. Varrin, "HTSE Plant Cost Model for the INL HTSE Optimization Study," Reston (VA): Dominion Engineering, Inc.; March 2013, R-6828-00-01.

[4] B. D. James, D. A. DeSantis, amd G. Saur, Final Report: Hydrogen Production Pathways Cost Analysis (2013–2016), Arlington (VA): Strategic Analysis Inc., September 2016, DOE-StrategicAnalysis-6231-1.

[5] J. Eichman, K. Harrison and M. Peters, Novel Electrolyzer Applications: Providing More Than Just Hydrogen, Golden (CO): National Renewable Energy Laboratory; September 2014. NREL/TP-5400-61758. Contract No.: DE-AC36-08GO28308, Sponsored by the U.S. Department of Energy.

[6] U.S. DOE, DOE Hydrogen and Fuel Cells Program: DOE H2A Production Analysis, https://www.hydrogen.energy.gov/h2a_production.html; 2013 [accessed December 31, 2018].

[7] Aspentech, "Aspen HYSYS," https://www.aspentech.com/en/products/engineering/aspen-hysys; 2018 [accessed December 10, 2018].

[8] M. Bragg-Sitton, R. D. Boardman, R. S. Cherry, W. R. Deason, and M. G. McKellar, *An Analysis of Methanol and Hydrogen Production via High-Temperature Electrolysis Using the Sodium Cooled Advanced Fast Reactor*, Idaho Falls (ID): Idaho National Laboratory; March 2014, INL/EXT-14-31642, Contract No.: DE-AC07-05ID14517.

[9] J. S. Kim, R. D. Boardman, and S. M. Bragg-Sitton, "Dynamic performance analysis of a high-temperature steam electrolysis plant integrated within nuclear-renewable hybrid energy systems," *Applied Energy*, Vol. 228, 2018, pp. 2090–110.

[10] Aspentech, "Aspen Process Economic Analyzer," https://www.aspentech.com/en/products/pages/aspen-process-economic-analyzer; 2019 [accessed 12 February 2019].

[11] W. D. Seider, J. D. Seader, D. R. Lewin, *Product & Process Design Principles: Synthesis, Analysis and Evaluation*, (With CD): John Wiley & Sons, 2009.

[12] PJM, *PJM Manual 18*, https://www.pjm.com/-/media/documents/manuals/m18.ashx, 2019 [accessed March 12, 2019].

[13] PJM, "Capacity Market (RPRM)," https://www.pjm.com/markets-and-operations/rpm.aspx; 2019 [accessed March 12, 2019].

[14] Argonne National Laboratory, "Hydrogen Delivery Scenario Analysis Model (HDSAM)," https://hdsam.es.anl.gov/index.php?content=hdsam; 2019 [accessed January 30, 2019].

3. HYDROGEN MARKETS

This chapter discusses the case for producing hydrogen at the nuclear power station and selling it directly to potential markets in the area. Current hydrogen use in the area surrounding the nuclear power station is discussed in detail for specific uses of hydrogen and why producing and selling hydrogen directly has market potential.

Three scenarios are explored. The first scenario considers the existing industry in the area and compares hydrogen production prices for NG SMR production and clean hydrogen from the nuclear power plant. The second scenario suggests that the transformation of the power plant from electricity provider to hydrogen producer creates the supply for a new ammonia industry located within 15 miles of the nuclear plant. Hydrogen produced and delivered to this ammonia plant by the power plant is competitive with NG SMR production at the ammonia plant location. The third scenario argues that hydrogen can be produced and delivered to hydrogen vehicle fuel stations within a certain range of the power plant at a price comparable to distributed NG SMR production with a similar delivery system.

The results will show that hydrogen production using HTE is more economical than LTE for the large-scale production cases and that HTE can compete with NG SMR at a large scale. They will also show that at a small-scale LTE can also be competitive with NG SMR hydrogen production due to the relatively linear scaling of LTE compared to other industrial processes.

3.1 Cases Considered

Current and emerging hydrogen-production technologies utilize diverse energy sources, including natural gas reformation as well as solar and nuclear power for low-temperature and high-temperature water splitting. The produced H_2 also enables emerging domestic industries that value conventional and renewable H_2 to be an energy carrier for intermediate and end use. The success of this proposition depends, not only on H_2 demand from growing existing markets such as petroleum refining and ammonia (NH_3) production, but also on the development of new markets such as metal refining, synfuels and chemical production, and injection into natural gas pipelines or mixing with natural gas supplied to electric-power generators, all of which can significantly increase H_2 demand relative to current levels (~10 million metric-tonne (MMT) annually or 27,000 metric-tonne (MT) per day in the United States).

Petroleum refineries demand large quantities of hydrogen for hydrotreating refinery products (i.e., sulfur removal) and hydrocracking (i.e., converting heavy hydrocarbon molecules into lighter products). Hydrogen demands by petroleum refineries depend largely on the volume of crude processed, the ratio of gasoline to diesel production, and the heaviness (measured by American Petroleum Institute [API] gravity) and sulfur content of crude input. This study used DOE's EIA projections of crude input and gasoline, diesel, and jet-fuel production through 2050, along with projections of crude API gravity and S content from DOE's high-octane fuel study, to estimate growth in H_2 demand (other than reformer byproduct H_2) through 2050.

Blast furnaces and coke ovens are the dominant technology for producing pig iron from iron ore; pig iron, in turn, is fed into a basic oxygen furnace to produce steel. This process is energy intensive and generates large amounts of CO_2 emissions: approximately 1.6 MT CO_2 per MT of steel. Direct reduction of iron (DRI) using combinations of natural gas, syngas, and H_2 for iron production reduces energy consumption and CO_2 emissions compared to blast-furnace technology. Using a syngas mixture from natural gas for DRI reduces CO_2 emissions by approximately 35% compared to blast-furnace and coke-oven technology while using H_2 for DRI virtually eliminates CO_2 emissions in the iron-making process.

The U.S. produced 43.1 MMT, imported 4.5 MMT, and exported 8.2 MMT of iron ore in 2015, reflecting an apparent consumption of 39.5 MMT. The annual consumption of steel in the U.S. in 2017 was 106.2 MMT, while the annual production was 81.6 MMT, reflecting imports of 34.6 MMT (i.e., 32.6% of annual consumption). In 2017, 68% of the 81.6 MMT of steel production in the U.S. was produced in electric arc furnaces (i.e., only 32% was produced in basic oxygen furnaces). In general, the quality of steel produced in electric arc furnaces fed by scrap metal is lower compared to steel produced from a basic oxygen furnace or via DRI technology. DRI can provide up to 100% of the feed to an electric arc furnace to improve the quality of the produced steel.

The range of H_2 mass required to fully reduce 1 MT of iron ore is between 0.08 and 0.12 MT, depending on the technology employed, the reaction temperature, and the reaction off-gas available for H_2 preheating. Hydrogen price affects the economic feasibility more strongly than capital and operating costs of the DRI process. DRI can generate positive net present value (NPV) with an H_2 price of $2.8/kg and CO_2 emissions credits of $50/ton. Without CO_2 emissions credits, it is estimated that an H_2 price of $1.5/kg would generate positive NPV for DRI technology assuming an IRR of 12%. Although DRI via H_2 is possible, a mix of CO or syngas and H_2 is more favorable for DRI because the reduction process via H_2 alone is endothermic, while the reduction via CO + H_2 is exothermic, minimizes the use of H_2, and improves process economics at the expense of modest CO_2 emissions. Furthermore, the presence of carbon is favorable because it is a necessary element in steel making and reduces the melting temperature of iron.

A wide variety of synfuels and chemicals can be produced when H_2 reacts with CO_2. Assessing future H_2 demand requires identifying not only promising synfuels and their demand for H_2, but also the size and locations of CO_2 sources, especially those in the near-pure state, such as those produced at ethanol plants and SMRs used in NH_3 plants and petroleum refineries. The corresponding demand for input H_2 to produce liquid and gaseous hydrocarbon depends on the type of synfuels of interest. Synfuels such as Fischer-Tropsch (FT) diesel and FT jet fuel are of interest because they are compatible with existing infrastructure and can serve as a drop-in or as blending components to power the off-road transportation sector, which is difficult to directly electrify. Using H_2 to produce synfuels extends the life of CO_2 before releasing it into the atmosphere through the production of highly desired liquid hydrocarbon of very high volumetric energy density.

In 2016, the U.S. emitted 5 billion MT of CO_2. Since a large number of hydrocarbon synfuels and chemicals can be produced when H_2 reacts with CO_2, production of synfuels and chemicals represents another potential demand for H_2. Moreover, when CO_2 is captured for hydrocarbon synfuel production instead of being released to the atmosphere, the carbon in the produced fuel or chemical can be considered neutral. Because of their high volumetric and gravimetric energy density, liquid hydrocarbon fuels are of particular interest for aviation, marine, rail, and truck applications. There is also a projected growth of methanol production for domestic use and export markets.

Capturing CO_2 from diluted flue gases or from the atmosphere is costly and requires a significant amount of energy for capture and compression. However, approximately 100 MMT of U.S. annual CO_2 emissions already occur in concentrated form from ethanol plants and from SMRs producing H_2 for petroleum refining or NH_3. The bulk of these concentrated CO_2 sources are available for synfuel production using H_2. In the present study, a 3:1 H_2/CO_2 mole ratio was used to estimate H_2 demand for the production of synfuels, such as FT diesel or methanol, from CO_2. Converting all recoverable CO_2 from ethanol and SMR (refinery and NH_3) plants to carbon-neutral synfuels would require 14 MMT of input H_2 (6.0, 5.9, and 2.1 MMT, respectively, for synfuel production from ethanol plants, refinery SMRs, and NH_3 SMRs, respectively).

There are several CO_2 sources from ethanol and SMR plants within the Midwest. The CO_2 from these plants can be matched with approximately 450 MT per day of H_2 to produce FT diesel.

One possibility for rapidly expanding H_2-delivery infrastructure is to adapt part of the existing natural gas delivery infrastructure to accommodate H_2. Converting natural gas pipelines to carry a blend of natural gas and H_2 (up to about 20% H_2) may require only modest modifications, and the injected H_2 could permit blending and resale as natural gas with a "zero-carbon" component. The blended natural gas/H_2 mix could then be used as a combustion fuel in existing boilers and electric generators fueled with natural gas.

Adding H_2 to the natural gas supply can impact end-use equipment operations and emissions; thus, careful study is necessary. Further research and testing are needed to identify impacts to new and legacy customer end-use equipment (i.e., the set points on existing equipment, as related to Btu content and current fixed parameters of that equipment). Manufacturers design end-use equipment that is supplied via the natural gas network with fairly tight limits on Btu content, gas quality, etc., to promote safety and efficiency. Converting and redesigning that equipment for higher blends of H_2 in natural gas will be required.

The supply curve for each market is generated using the appropriate H2A production tool for either HTE or LTE and varying the OCF of the HTE from 0% to 95% to match the OCF of a typical nuclear power plant. An outage of 24 days every 18 months is typical of a nuclear power plant. This equates to an operating capacity of about 95.5%.

3.2 Hydrogen Market Opportunities

Table 19 lists the estimated hydrogen demand within a 100-mile radius from the representative nuclear plant selected for this study. The projected demand is broken up into current and future demand.

The current demand is for the near-term future and is expected to be met by NG SMR hydrogen production. The future demand will be targeted by this report for clean hydrogen such as HTE or LTE generated with the energy taken from a nuclear power plant. The table provides discrete demand values for existing customers located at different distances from the nuclear power plant and represents the demand for the existing market. The representative nuclear power plant has a hydrogen production capacity of about 578 tpd (or 534 tpd at 92.4% OCF), which is enough to supply the current hydrogen demand for the existing industries located within 100 miles of the representative plant. The development of clean hydrogen production also lends itself to producing new markets to supply.

Table 19. Current and future hydrogen demand within the representative nuclear plant site.

Demand Type	Potential Current Demand (kilotonnes/yr)	Potential Future Demand (kilotonnes/yr)
Refinery	47	59
Syngas: Hydrogen, SMR	0	72
Refinery	45	57
HBI Plant	0	160
Syngas: Ethanol	0	30
Syngas: Ethanol	0	20
DRI Plant	1	5
Refinery	39	49
Syngas: Hydrogen, SMR	0	57
DRI Plant	0	2
Syngas: Ethanol	0	20

DRI Plant	7	94
DRI Plant	5	74
Syngas: Ethanol	0	30
DRI Plant	0	1
DRI Plant	4	53
DRI Plant	0	2
DRI Plant	0	1
DRI Plant	3	44
Total Demand (tonnes/day)	413	2,274

3.3 Market Hydrogen Demand Curves

A demand curve is constructed by assuming the price that each market is willing to pay for hydrogen and its associated production cost via NG SMR. This assumes that each customer will build an SMR plant for their individual needs. Credit is not given to joint hydrogen-production ventures; instead, each customer is expected to be willing to pay the price of building and operating a SMR facility for their needs.

Using the H2A model for NG SMR production, the hydrogen-production price was generated for each of the markets based on their projected demand. For the existing hydrogen market, several demand values are used and compiled into a stepwise demand curve using the customers shown in Table 19. And their future demand [1]. A new ammonia plant market would have a hydrogen demand of 534-tpd H_2 which corresponds to about the same amount a single-reactor nuclear power plant nominally producing 900 MWe is capable of producing from a fully integrated HTE.

The demand is calculated using three different natural gas prices which represent the projection for high-, baseline-, and low-cost natural gas for the region [2]. The capacity factor used for SMR production in the H2A model is 90%, and compression and delivery over 2 miles is estimated using the equations shown in Table 20, which are used to calculate the CAPEX and OPEX associated with the compression and delivery of hydrogen through a pipeline. These assumptions were used for all three market demand curves. The hydrogen demand curve with the discrete values associated with the existing market is shown in a stepwise plot in Figure 20.

Table 20. Equations used for CAPEX and OPEX of hydrogen compression and delivery.

Pipeline		
Pipeline diameter (in.)	$D(V) \propto \sqrt{V}\ ;\ D(50\ tpd) = 4$	(1)
Pipeline material ($/mi):	$76550e^{0.0697D}$	(2)
Labor ($/mi):	$1.136(-51.393D^2 + 43523D + 16171)$	(3)
Right of way (ROW) ($/mi):	$1.04(-9 * 10^{-12}D^2 + 4417.1D + 164241)$	(4)
Miscellaneous ($/mi):	$1.134(303.13D^2 + 12908D + 123245)$	(5)
Compressor		
Power (kW):	$28(V)$	(6)
Compressor Cost ($):	$2.34(1962.2P^{0.8225})$	(7)

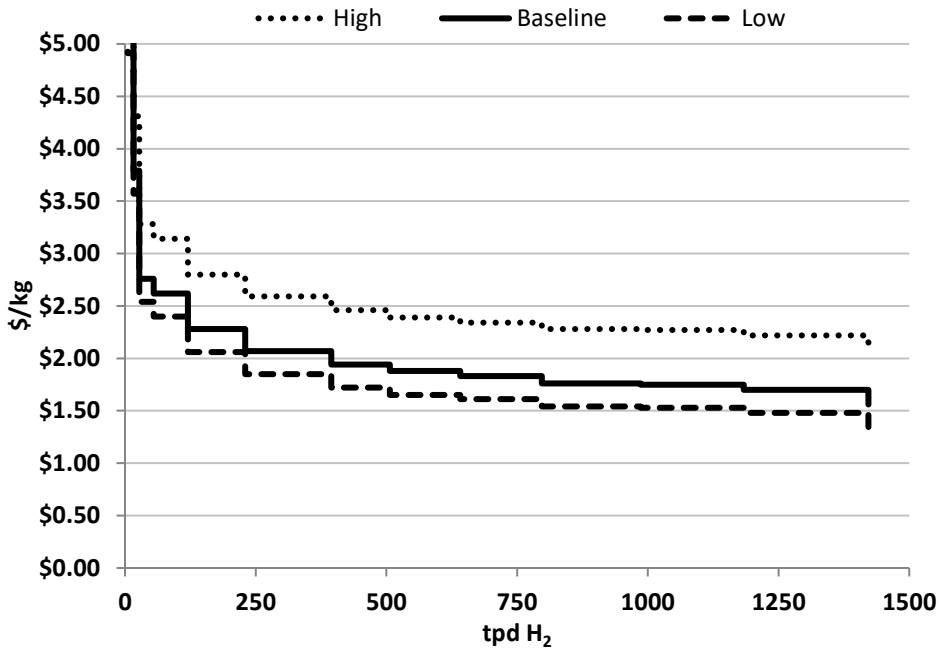

Figure 20. Hydrogen-demand estimation for existing market within 100 miles of the Modeled Nuclear Plant with high, low, and baseline natural gas prices.

3.4 Hydrogen Supply Costs

The approach to evaluating the cost of hydrogen delivered to the various customers in vicinity of the modeled plant reflects the hydrogen demand curve in Figure 20 where it is assumed the cost of hydrogen paid by the customer is set at the marginal cost of producing hydrogen with SMR and compression to service requirements within 2 miles of the point of consumption. We consider the feasibility of supplying the following customers with hydrogen:

- Case A. Fuel Cell Vehicle Fueling Deports within 25 miles of the nuclear plant. In this option, the hydrogen produced near the nuclear plant must be compressed and delivered to a holding tank at the filling station depot. We considered two options
  - Case A.1 is a small LTE plant producing 24-tpd H_2 and using compressed gas tube trailers to deliver the hydrogen to the filling stations
  - Case A.2 is a larger LTE plant producing 97-tpd H_2 using a small pipeline to deliver hydrogen to a larger distribution depot or filling station
- Case B. Single user or closely located cluster of hydrogen users within 15 miles of the nuclear plant site using about 100-tpd H_2 delivered by pipeline
- Case C. Single User within 15 miles of the nuclear plant site supplied hydrogen with a pipeline from a centralized LTE plant
- Case D. Single user within 15 miles of the nuclear plant site supplied hydrogen with a pipeline from a centralized HTE plant

Case B is representative of either one large petroleum refinery, or two refineries that are located within a reasonable distance to the 100-tpd H_2 plant. Cases C and D are representative of a single new large customer such as an ammonia plant or a DRI/HBI plant. Fuel Cell Vehicles Markets

There is currently an emerging fuel-cell vehicles market for light-duty and heavy-duty vehicles. Fuel-cell power locomotives and ships are already being tested in Europe. Nuclear power plants in the Midwest are conveniently positioned to supply compressed or liquefied hydrogen to filling stations that are located within a 25 to 100-mile radius of nuclear plant sites. For the purpose of this assessment, it is assumed that a market for at least 100-tpd H_2 can be reached within 5 years. This is based on the simple assumption that approximately 2% of personal vehicles and 5% of the heavy-duty trucking convert to on-board fuel cell electrically drive trains.

The current population estimate for the area within 100 miles of the representative reactor site is about 6 million people. Assuming a household size of 4 people per household and 2 cars per household, there are about 3 million personal vehicles in this area. With 2% of vehicles being fuel cell vehicles, there would be a total of 60,000 personal fuel cell vehicles in the area. The gasoline equivalence of hydrogen in fuel cell vehicles is about 1-kg H_2 per gallon of gasoline [3]. Hence, this corresponds to a hydrogen consumption of about 60-tpd H_2 from personal vehicles.

Since the demand level for the fuel cell vehicle market is significantly lower than the other markets suggested in this section, LTE is the only clean hydrogen option considered. LTE scales much more linearly by size than most other industrial processes; therefore, they are relatively similar in LCOH for several production plant sizes. The comparison between hydrogen production with LTE and NG SMR, including compression costs, is provided in Figure 21. Only compression need be considered for this comparison, since the delivery system would be similar for both SMR and LTE. Each would require a fleet of hydrogen tube-trailer trucks to deliver the compressed hydrogen to the several dispensing stations. This cost would be similar regardless of whether SMR is used to produce the hydrogen or LTE. The cost of compression does consider compressing hydrogen to the high pressures needed for fuel cell vehicle applications. The SMR production scenario considers that there would be four smaller SMR plants distributed around the area to localize the production and distribution of the hydrogen to the dispensing locations. These are sized at about 23 tpd each. The LTE is centralized at the nuclear power plant site making an equivalent amount of hydrogen as the four SMR H_2 production stations.

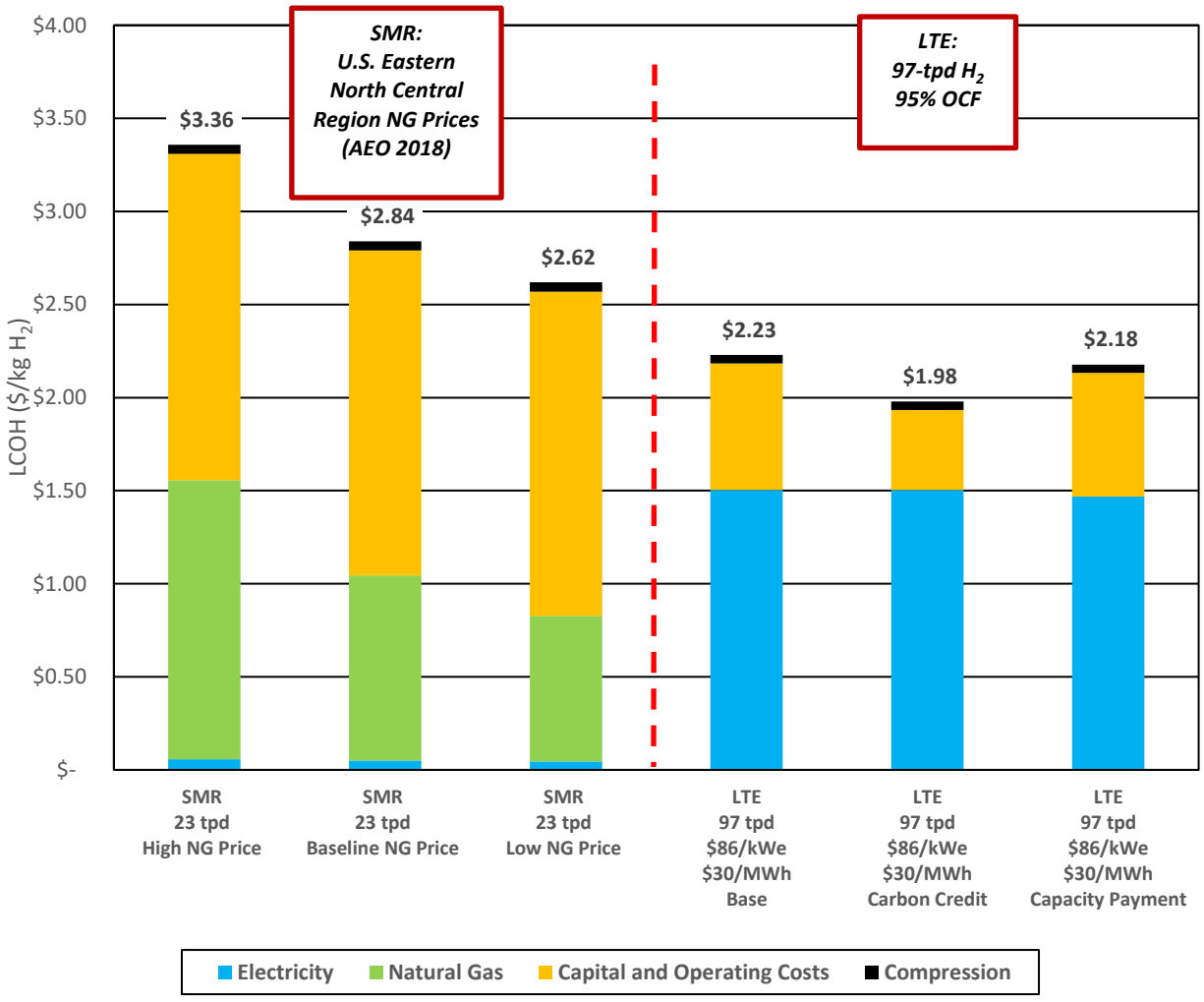

Figure 21. Comparison of hydrogen production and compression prices for use in the new fuel cell vehicle market.

This assessment shows LTE could be competitive to the distributed SMR production regardless of NG price. If an alternative were considered for SMR production at a centralized location, the comparison may be different. Although not plotted, a larger SMR plant producing 97-tpd H_2 would still cost more than the LTE plant at this scale. Any credit for CO_2 emissions avoidance would increase the value of the nuclear power plant electrolysis option.

3.5 New Ammonia Plant Opportunity

Whereas Table 20 projects markets for current hydrogen customers, it will be assumed that a new world-class ammonia plant can be drawn to a nuclear plant producing hydrogen. A large centralized hydrogen plant draws power and thermal energy to produce around 540-tpd H_2. The hydrogen produced at a nuclear power plant can be compressed and pumped to the ammonia plant via a pipeline. This plant will produce 2,940-tpd urea and 3,780-tpd ammonium nitrate per a detailed engineering process design basis for a fertilizer feedstock plant [4].

Ammonia capacity world-wide is increasing primarily in areas where the availability and cost of natural gas are lower, in particular the United States and the Middle East. Key players in market includes

BASF, Potash Corp., Yara International, CF Industries, Group DF, Togliatti, OCI Nitrogen, Agrium, Sabic, Koch Fertilizer and others [5]. The market is anticipated to grow at faster pace due to increased fertilizer need to reconstitute repetitive farming practices as world population continues to rise and increase in disposable income in various developing country such as India, Brazil, and Indonesia are shifting dietary consumption trends to crops that require fertilizer.

Urea, ammonium nitrate, ammonium phosphates, nitric acid, and ammonium sulfate were, in descending order of importance, the major derivatives of ammonia produced in the United States.

The domestic market for ammonia is stable and growing due to the prominence of the United States in the global agriculture market- both as producers of fertilizers and of food. Thus, there is still opportunity for additional domestic capacity to meet domestic needs. Further, if natural gas prices remain low, there is opportunity for the United States to become an exporter on the global market in a much bigger way than we have in the past. Nuclear hybrids that produce ammonia will be especially competitive for export to countries bracing climate change clean energy standards.

During 2011-16, world apparent consumption of ammonia increased at about 2% per year; growth is forecast to slow to about 1.8% annually during 2016–2021 (FAO 2017). The global ammonia supply/demand balance is expected to move toward a surplus, as future capacity additions will continue to outpace consumption, leading to declining utilization rates. Compound annual growth rate (CAGR) is the mean annual growth rate and is a useful measure of growth over multiple time periods. Globally, the market for ammonia is growing at a CAGR of 1.54% during the forecast period (2015–2020) as shown in Table 21.

Table 21. Total world ammonia demand, 2015–2020 (thousand tonnes) (Source: FAO 2017)

	2015	2016	2017	2018	2019	2020	CAGR (%)
NH_3 for fertilizer	110,027	111,575	113,607	115,376	117,116	118,763	1.54
NH_3 for non-fertilizer	33,616	34,506	35,308	36,207	36,786	37,521	
Total NH_3 demand	143,643	146,081	148,915	151,583	153,902	156,284	

Table 22 shows the total ammonia demand in North America is projected to reach 20.23 million tonnes in 2020 with a CAGR of 0.37% (FAO 2017). In the United States, large corn plantings increase the demand for nitrogen fertilizers.

Table 22. North America ammonia demand, 2015–2020 (thousand tonnes) (Source: FAO 2017)

	2015	2016	2017	2018	2019	2020	CAGR(%)
NH_3 for fertilizer	14,434	14,517	14,552	14,612	14,667	14,701	0.37
NH_3 for non-fertilizer	5,127	5,209	5,286	5,368	5,450	5,532	
Total NH_3 demand	19,561	19,726	19,838	19,980	20,117	20,233	

Data representing the three hydrogen production options for the new ammonia plant are presented in Figure 22. These show the LCOH for multiple cases of hydrogen production. These involve NG SMR at the three NG price projections. LTE production at the nuclear power plant includes compression and pipeline delivery to an ammonia plant that is approximately 15 miles away from the nuclear plant. A levelized cost of electricity of $30/MWh was assumed for these calculations. Additionally, the LCOH is shown for scenarios that would allow the nuclear hydrogen production to take advantage of a carbon credit of $25/tonne CO_2 as previously discussed or using capacity payments for the guaranteed electricity capacity that the nuclear reactor provides. The same cases are shown for HTE as for LTE. The production capacity of the large LTE plant is significantly lower than the HTE plant due to the higher electrical requirement for water-splitting at lower temperatures. Compression and delivery prices for HTE and LTE are higher than for NG SMR since the nuclear plant is assumed to be 15 miles from the ammonia and the NG SMR plant.

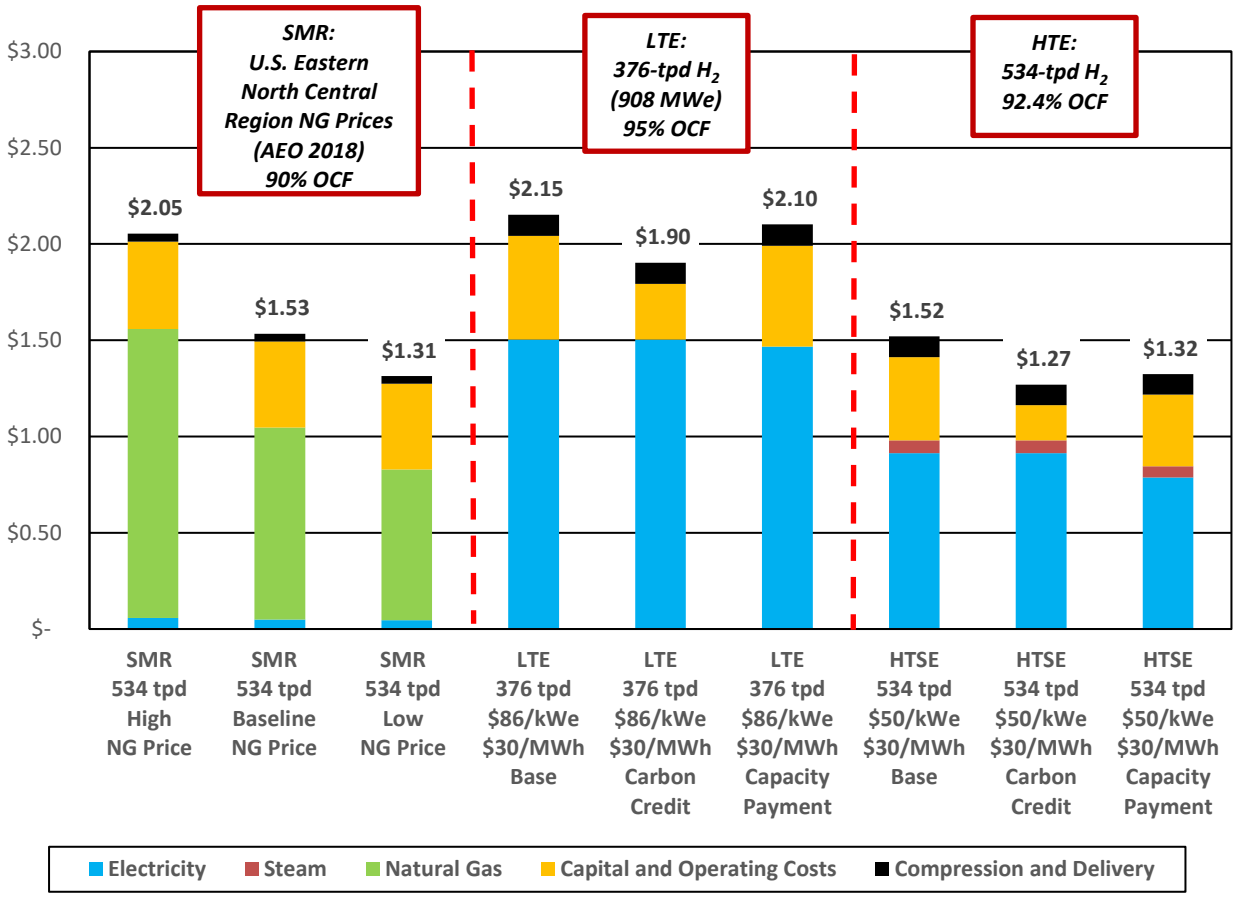

Figure 22. Comparison of hydrogen production, compression, and delivery prices by various methods for new ammonia plant demand (LCOH as $/kg•$H_2$). (Note: HTE cases assumes a capacity payment and oxygen sales).

Figure 22 shows that the price for producing hydrogen by HTE is competitive with the price of NG SMR if the NG prices follow the current projections. LTE hydrogen production is around the price of NG SMR production if the NG price is higher than the current baseline projection. Due to the lower thermal dynamic efficiency of LTE, the nuclear power plant can produce only 376 tpd versus the 534 tpd that can be produced by HTE at the same power plant. In addition, this study did not take credit for oxygen sales with LTE plants. This could decrease the cost of hydrogen about $0.25/kg-$H_2$.

3.6 Hydrogen Delivery Costs

The cost of compression and delivery of hydrogen through a pipeline is naturally a strong function of the pipeline capacity and distance. As a reference for expected compression and delivery costs through a pipeline, Figure 23 is provided which compares different production volumes and the associated LCOH that compression and delivery adds to the production cost of hydrogen using the equations specified in this chapter and the H2A production tool.

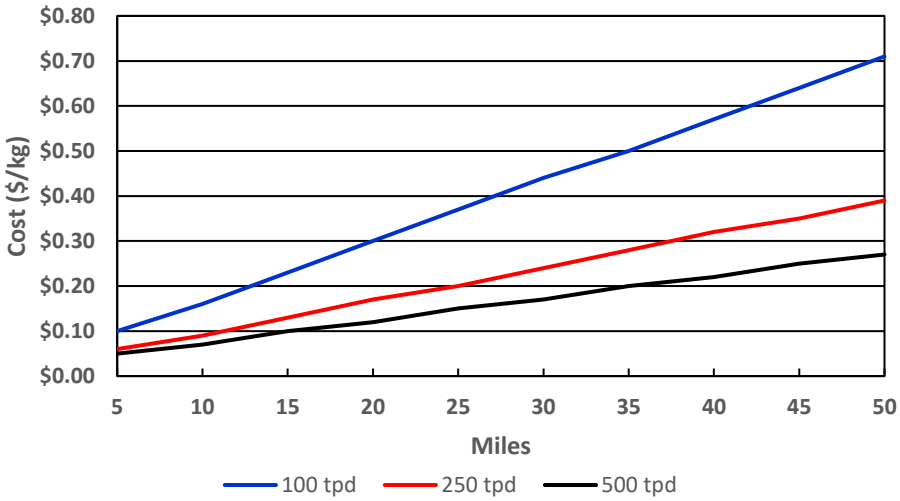

Figure 23. Compression and delivery costs for different production volumes over a range of distances.

As is expected, an increase in the delivery volume results in a decrease in LCOH increase associated with the pipeline. For this reason, other delivery methods should be investigated for smaller hydrogen production ventures such as the fuel cell vehicle market.

3.7 Hydrogen Storage

The LCOH in the supply curves does not take into account the costs associated with hydrogen storage and associated compression. Current hydrogen-storage techniques vary widely in capital and operating costs and can have a large effect on the LCOH, depending on the type of storage available and the storage technique used.

The Fuel Cell Technologies Office has set an ultimate target for hydrogen storage cost at $8/kWh based on lower heating value (LHV), where the LHV of hydrogen is assumed to be 33.3 kWh/kg [6]. This is an equivalent CAPEX of $226/kg of hydrogen stored. The current estimate for hydrogen storage CAPEX is $1000/kg stored without mass storage-tank production and $15/kWh, or $500/kg ($2007), based on an estimated 500,000 storage units produced per year [1]. This represent the physical storage of hydrogen as a compressed gas. This cost, with the cost of compression required for storage, is equivalent to $1/kg for one day of storage added to production and delivery costs. For an operating capacity of 95%, 19 days of storage would be required on average for refueling downtime, which would result in an LCOH increase of $19/kg. There are various options for decreasing or eliminating the storage cost of hydrogen.

Options to avoiding such high hydrogen storage costs simply include coordinating the refueling operations of the nuclear power plant with maintenance outage schedules of the large-scale industrial user. Otherwise, the electrolysis plant may switch to power from the grid that could be available during the shoulder months of the year when overall power demand by residential and commercial customers is at its lowest.

Hydrogen capacity may also be provided in the pipeline that supplies the hydrogen to the industrial customer. This would require higher pressures in the pipeline to provide the necessary surge capacity. The cost of higher-pressure lines should be evaluated in future studies.

Another option for hydrogen storage is material storage, which involves converting hydrogen to another compound or adding hydrogen to existing compounds to take advantage of the physical storage costs of these materials [6]. Each of these come with additional CAPEX and OPEX for balance-of-plant and other material costs. Geological storage is an even less-expensive option for hydrogen storage, but it relies on a geologic formation in the area capable of storing hydrogen. Additionally, this typically requires larger-scale hydrogen production to justify the investment.

3.8 Hydrogen Supply Market Summary

A comparison of the cost of producing hydrogen from a single nuclear plant is rolled into Figure 24 to illustrate the multiple markets that can be served by a combination of scalable LTE and HTE plants. For this analysis, we assume oxygen will not be captured for sales. Neither is any cost credit for CO_2 avoidance taken into account. We assume the customers will coordinate hydrogen use with the maintenance of the hydrogen plant and nuclear power plant re-fueling schedule. Otherwise, in the case of transportation deport, the tube trailers that delivery the hydrogen to the fueling stations or the delivery pipelines will need to provide stock-and-flow to the end user to avoid the significant costs of hydrogen storage unless this storage is factored into the filling stations regardless of the source of hydrogen supply.

With direct sale of electricity at the nuclear plant site for $30/MW-hr, the first market opportunity is to begin with an LTE electrical connection to the nuclear plant to service the highest value markets willing to pay between \$3.80–5.00/kg•H_2. Here the smaller 24-tpd LTE plant modeled in this study can meet this market need. The next set of customers are also relatively low volume users will to pay between \$2.65–2.75/kg•H_2. This price can be meet when scaling the LTE plant to around 100-tpd H_2.

Stepping up to large industrial users within some nominal distance (at least up to 15 miles), in order to be competitive with SMR, only the large-scale HTE plant is capable of competing. The large-scale LTE plant is less competitive at this scale due to the lower thermodynamic efficiency. However, the HTE hybrid plant could be competitive with a comparable SMR plant located near the industrial user located up to 100 miles from the nuclear plant.

Future studies should consider tradeoffs in H_2 delivery by pipeline versus industrial facilities with onsite LTE or HTE with dedicated electrical power lines that are tied directly to the nuclear plant. This may reduce the cost of hydrogen delivery if onsite LTE or HTE hydrogen production is possible at the same location where SMR plants are located. Oxygen sales may also be available if the electrolysis plant is located at the industrial user site; for example, for producing refined steel or for use in oxy-fired applications at a refinery plant.

The value of CO_2 in the United States depends on the product markets. Renewable energy credits may be possible with nuclear being recognized as a clean energy source that is comparable to wind and solar energy. Low-carbon products exported to other countries, particularly Europe, should be able to apply a credit for avoiding CO_2 and other air pollutant emissions.

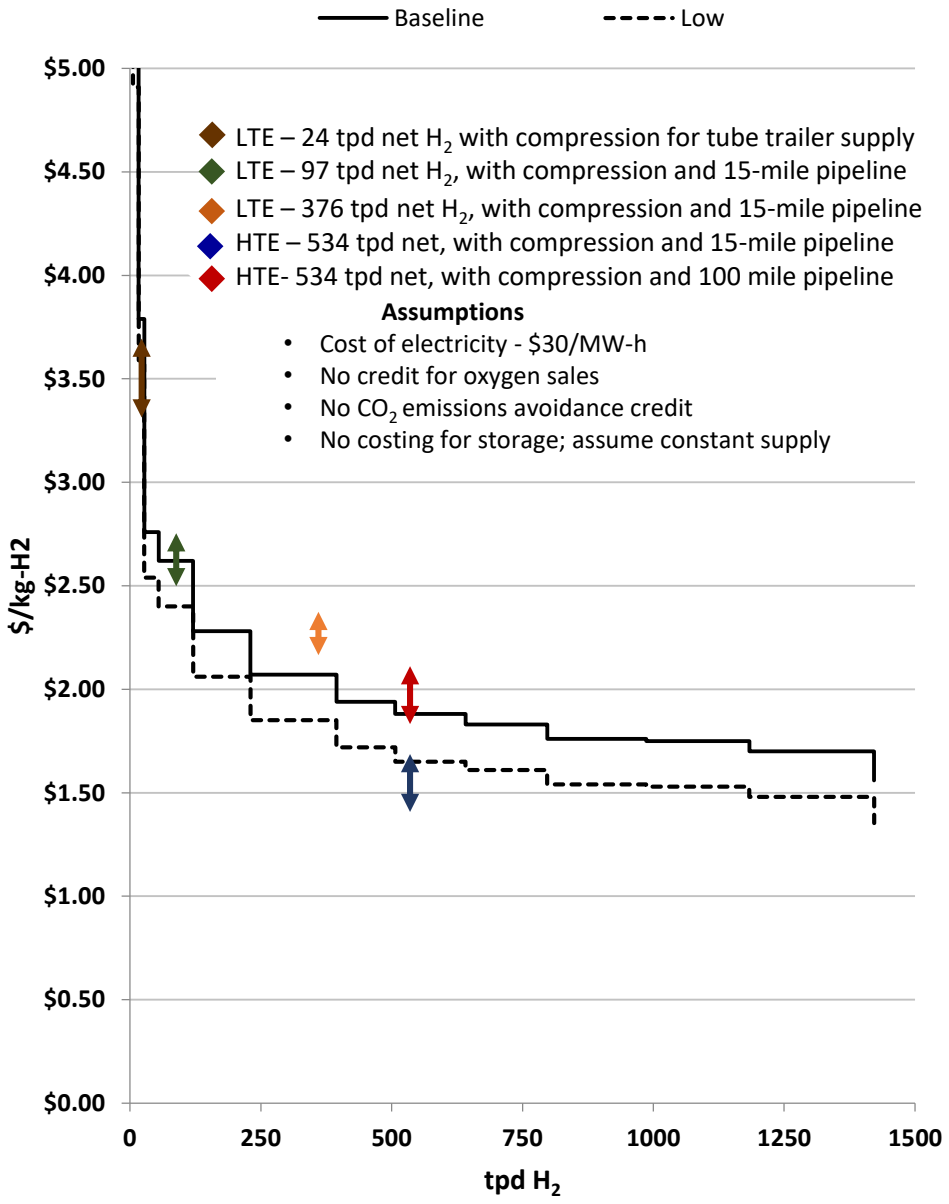

Figure 24. Comparison of hydrogen production and delivery cost options to user demand costs.

References

[1] U.S. DOE, "DOE Hydrogen and Fuel Cells Program: DOE H2A Production Analysis," https://www.hydrogen.energy.gov/h2a_production.html; 2013 [accessed 31 October 2018].

[2] U.S. EIA, "Annual Energy Outlook 2018," https://www.eia.gov/outlooks/aeo/tables_ref.php; 2018 [accessed 5 December 2018].

[3] U.S. DOE, "Measuring Fuels: Understanding and Using Gasoline Gallon Equivalents," https://cleancities.energy.gov/blog/measuring-fuels-understanding-and-using-gasoline-gallon-equivalents; 2017 [accessed March 27, 2019].

[4] R. Wood and R. Boardman, "Technical Evaluation Study: Nuclear-integrated Ammonia Production Analysis," INL TEV-666, Revision 2, May 2010.

[5] Yara 2018.

[6] Brian James, et al., *Final Report: Hydrogen Storage System Cost Analysis*, 2016.

4. POLYETHYLENE HYBRID PROCESS ASSESSMENT

Polyethylene (PE) is the largest-volume polymer worldwide, with a production of nearly 100 MMT in 2018 valued at $164 billion. World demand is strong with a forecasted compounded annual growth rate of 4% [1]. PE is formulated into low-density polyethylene resin (LDPE), linear low-density polyethylene resin, and high-density polyethylene resin. Overall PE demand in the U.S. is forecast to total 31.4 billion pounds in 2022, representing annual increases of 1.7% from 28.8 billion pounds in 2017. Positive macroeconomic conditions will increase shipments of manufactured goods, boosting demand for polyethylene packaging. The average U.S. high-density polyethylene resin, linear low-density polyethylene resin, and LDPE resin prices are forecast to rise 1.8, 1.5, and 1.7% per year, respectively, through 2022 (Figure 25).

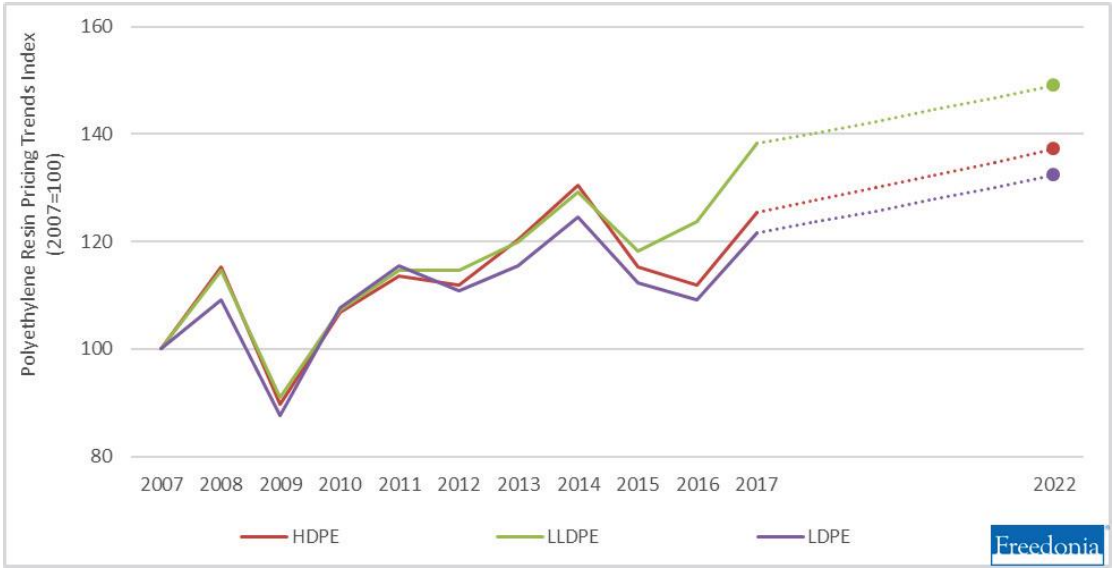

Figure 25. U.S. polyethylene prices by index, 2007–2022 (2007 = 100) [1].

4.1 Ethylene Feedstock Production

Polyethylene is produced through polymerization of ethylene ($CH_2 = CH_2$). With the shale gas boom, ethane (a common condensable compound of natural gas) has become the predominate feedstock used in the production of ethylene. The traditional ethylene production process employs steam cracking or thermal pyrolysis [2]. This process is extremely energy and capital intensive, yielding many byproducts, requiring extensive separations and purification steps to produce the final ethylene product [3].

Electrochemical nonoxidative de-protonation (NDP) is a newly developed technology for converting ethane to ethylene at a significant lower temperature (400–500°C). Compared to the traditional steam-ethane cracking process, it requires significant less energy and can essentially eliminate CO_2 and pollutant emissions [4]. Because NDP requires electricity and moderate heating, it is a prime candidate for coupling with an LWR, following the same principles as integration of high temperature steam electrolysis.

For the purposes of this assessment, an evaluation of the electrochemical NDP ethylene production process has been completed and compared to steam-ethane cracking and catalytic production of ethylene [5] to determine whether there is a business case for using the energy provided by the nuclear power plant.

A block diagram for the electrochemical NDP is shown as Figure 26. Nuclear power is integrated and utilized for ethylene production in this process. Nuclear heat might also be utilized to preheat feedstock. Heat recuperation is also employed to raise the feedstock to the operating temperature of 500°C. These

sections might be slightly changed during detailed engineering design and fabrication: heat exchangers may be adjusted, separation might be accomplished by membrane-based technology or traditional distillation-column process, and the compression system might be moved to an integrated PE-production process.

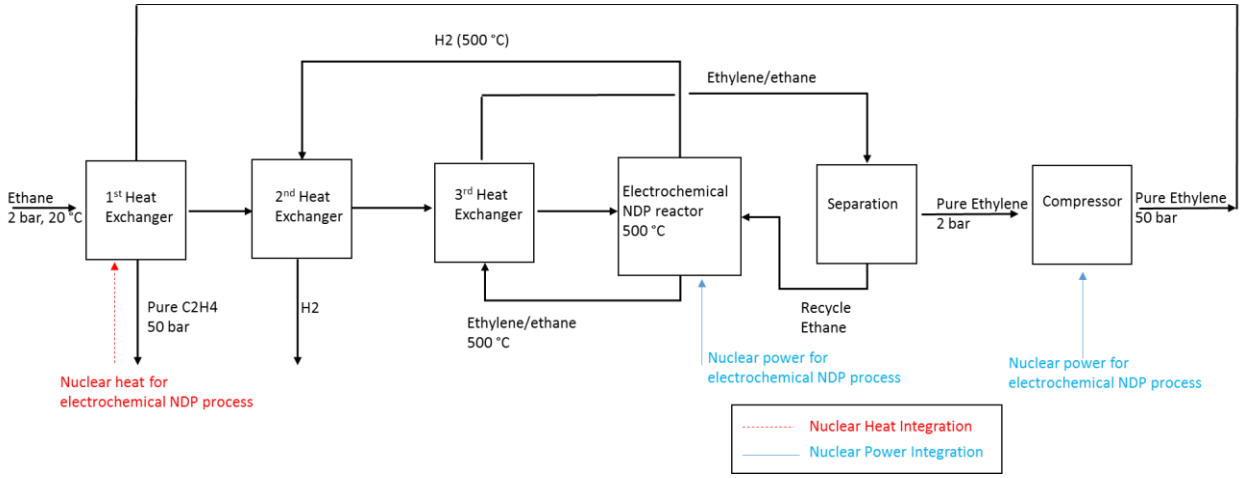

Figure 26. Process block diagram for ethylene production from ethane using electrochemical NDP.

4.1.1 NDP Process Modeling

In this study NDP was simulated using AspenPlus to complete a detailed energy and cost evaluation. When connected to the nuclear power plant, the electrochemical NDP processes produces 0.83 million metric ton per year (mtpa) ethylene, which is comparable to a medium-sized steam cracker [6].

The feedstock ethane is received at 20 psi (1.4 bar) and is compressed to 40 psi. The final ethylene product is not further compressed. The electrochemical reactor, referred to as ELECRTOR was modeled using an AspenPlus® RStoic reactor, coupled with Excel calculation for electricity usage. For the reaction $C_2H_6 = C_2H_4 + H_2$, the single-pass conversion efficiency is set to 60%, according to the laboratory results achieved at INL. The process-flow diagram (PFD) is shown as Figure 27. The process model provides an overall mass, and energy balance as well as an estimation of the capital and operating costs. Table 23 shows the mass balance for the NDP process. Table 24 gives a comparison of the two processes: NDP and steam cracker. Because an annual operation time of 8760 hours was used in the steam cracker reference plant [5], the same operating time was also used for the electrochemical NDP process for consistency.

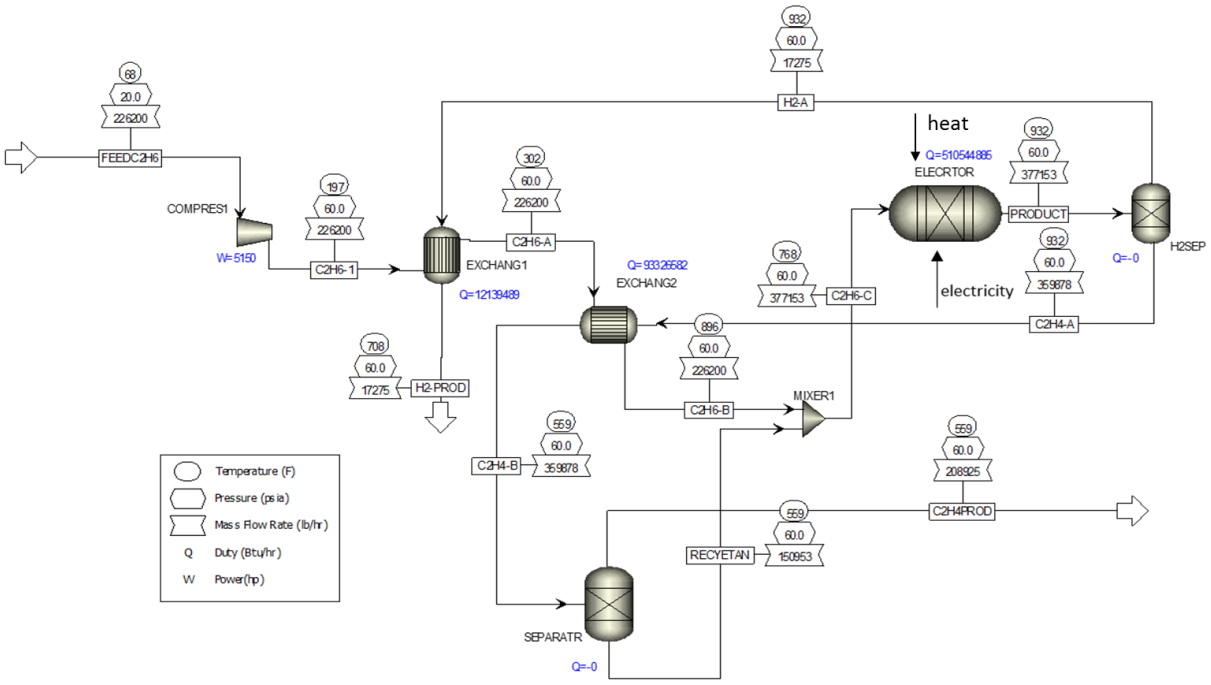

Figure 26. Process-flow diagram for ethylene production from an electrochemical NDP process with membrane separation.

Table 23. Mass balance for main streams for the electrochemical NDP process simulated by AspenPlus.

	FEEDC2H6	1	C2H6-1	C2H6-A	C2H6-B	C2H6-C	RECYETAN
Total flow, kg/hr	102,603	102,603	102,603	102,603	102,603	171,074	68,471
Total Flow lb/hr	226,200	226,200	226,200	226,200	226,200	377,153	150,953
Mole Flow lbmol/hr							
ETHANE	7,523	7,523	7,523	7,523	7,523	12,538	5,015
OXYGEN	0	0	0	0	0	0	0
ETHYLENE	0	0	0	0	0	0	0
HYDROGEN	0	0	0	0	0	76	76
Total Flow lbmol/hr	7,523	7,523	7,523	7,523	7,523	12,614	5,091
Temperature F	68	150	400	532	896	818	694
Pressure psia	20	40	40	40	40	40	40
Vapor Frac	1	1	1	1	1	1	1

	PRODUCT	C2H4-A	C2H4-B	C2H4-C	C2H4PROD	H_2-A	H2-PROD
Total flow, kg/hr	171,074	163,238	163,238	94,767	94,767	7,836	7,836
Total Flow lb/hr	377,153	359,878	359,878	208,925	208,925	17,275	17,275
Mole Flow lbmol/hr							
ETHANE	5,015	5,015	5,015	0	0	0	0
OXYGEN	0	0	0	0	0	0	0
ETHYLENE	7,523	7,447	7,447	7,447	7,447	75	75
HYDROGEN	7,599	76	76	0	0	7,523	7,523
Total Flow lbmol/hr	20,136	12,538	12,538	7,447	7,447	7,598	7,598
Temperature F	932	932	694	694	449	932	583
Pressure psia	40	40	40	40	40	40	40
Vapor Frac	1	1	1	1	1	1	1

Table 24. Process result summary for steam-ethane cracking and electrochemical NPD ethylene production.

Parameter	Unit	Steam Cracking	Electrochemical NDP
Annual Ethane Feed Rate	Metric Tonne/Yr	978,492	898,802
Annual Production Rate of Ethylene	Metric Tonne/Yr	830,132	830,159
Ethylene Product Purity	%	99.90	100
Annual Production Rate of H_2	Metric Tonne/Yr	*	68,643
H2 Product Purity	%	-	100
Ethane Single Pass Conversion	%	60%	60
Process Yield of Ethylene	%	85	92
Specific Thermal-energy Requirement	GJ/Metric Ton Ethylene	34	6
Specific Electricity Energy Requirement	GJ/Metric Ton Ethylene	5.5	2.8
Operation Hours Per Year	Hour	8760	8760
Plant Life Time	Year	30	30

* The off-gas generated from steam cracking process, including hydrogen, methane, acetylene, propylene, propane, and butadiene, are considered in the form of equivalent of natural gas for heating and are balanced in the final energy of fuel required

4.1.2 Capital Costs Projection

Currently, only an estimate of capital costs was possible. According to published data, the total capital investment (TCI) for a 1.5-mtpa steam-ethane cracker on the U.S. Gulf Coast was about at $2.13 billion in 2016 [7], and $1.43 billion for a 1-mtpa cracker [8,9,10]. A detailed cost breakdown for the main section of the plant is listed in Table 25. The major equipment (see Table 26) represents about 29% of TCI while indirect costs (containing 70 columns, 67 vessels, and several hundred other pieces of equipment) account for 43% of TCI [10]. By comparison, the electrochemical NDP process is much

simpler, consisting of one main electrolyzer and only various several auxiliary vessels and appurtenant equipment.

Considering the similarity of NDP and HTE, it is reasonable to estimate the NDP capital costs using DOE H2A for the high-temperature electrolysis model [11] and by including relevant estimates for the balance of plant (BOP) unit operations [12]. A power-generation cost of $1,500/kW for the electrolyzer specified in the H2A model in this study while $820/kW is commonly applied for steam splitting [11].

The TCI costs for both processes are listed in Table 25 and Table 27. For electrochemical NDP, BOP equipment costs are included with bulk materials. For comparison, the Lang-factor method was also used to estimate TCI based on major equipment [13]. An updated Lang factor of 3.28 [14] was used to double check the TCI for electrochemical NDP. The result obtained with the Lang-factor method is about 20% lower than that obtained from the H2A model (Table 27).

The results plotted in Figure 28 provide a visual comparison of the relative costs. The NDP TCI ($0.65 billion) is projected to be 40% less than that of the steam-ethane cracker ($1.1 billion).

Table 25. TCI for both steam-ethane cracking and electrochemical NPD processes.

	Unit	**Electrochemical**	**Steam Cracker**
Major Equipment	Million dollars	166	324
Bulk Materials/BOP		309	299
Indirect Cost		175	485
TCI		650	1,108
Ethylene,	tonne/yr	830,132	830,132
$/tonne ethylene		783	1,335
$/tonne ethylene over 30 years of plant life		26	45

Table 26. Detailed capital costs items for steam-ethane cracking [5].

Major Equipment	Bulk Materials	Indirect
Columns c/w trays	Removals/Demolition	Detail Design/Engineering
Drums/vessels	Site Earthmoving	Contingency
Pumps	Piling	EP fee
Compressors/Fans/Blowers	Buildings	Fringe benefits/Payroll Burdens
Heat Exchangers	Concrete	Consumables/Small tools
Tanks	Refractory/Fireproofing	Field supervision & Expenses
Material Handling	Structural Steel/Platforms	Support labor
Water Treatment	Piping system	Construction equipment rental/fuel
Miscellaneous Equipment	Insulation	Contractor fee
Electrical Equipment	Electrical/Instrumentation	Project management & Controls
Instrumentation devices (Tagged)	Painting/Coatings	Field establishment (trailer, toilets)
Freight	Other Misc. Costs	Other Misc. costs

Table 27. Electrochemical NDP capital-cost estimation.

	H2 rate, kg/hr	kwh/kg-H2	$/kW	%	Cost, M$	Installation factor	Installed Cost, M$
Electrolyzer	7835.752	36.8	1500	35	$151.4	1.1	$166.5
BOP	7835.752	36.8	1500	65	$281.1	1.1	$309.3
Indirect Cost							$175.8
TCI							$651.6
Lang Factor	3.282						
TCI Using Lang Factor							$546.5

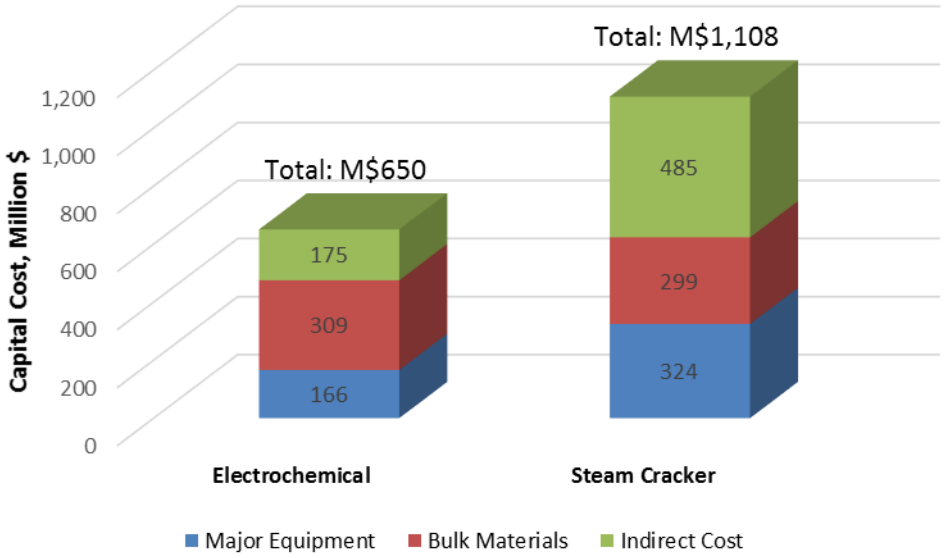

Figure 27. Capital costs for NDP and steam-ethane cracking.

4.2 Operating Costs Projections

Operating costs consist of feedstock (ethane), thermal energy, electricity, and labor cost for both the processes. A breakdown of the estimated operating costs (OPEX) for the steam-ethane cracking process were projected from published data [5]. A breakdown of these costs is tabulated in Table 28. Table 29 lists relative costs of raw materials which translate to the overall operating costs per tonne of product listed in Table 30.

Table 28. Detailed operation costs (OPEX) for steam cracking process

Section	**Unit Operation**	**Type of Utility Used**	**$/Tonne Ethylene**
Pyrolysis	Feedstock Preheater	CH4	30
	Cracker	CH4	32
	Transfer line exchanger	cooling water	8
Compression	Recirculation Heater	cooling water	6
	Interstage cooler	cooling water	4
Separation	Cool train	Refrigerant	21
	Reboiler	steam	38
	Condenser	Refrigerant	56
	Acetylene Preheater	steam	11
Total Thermal Energy			**205**
Compression	Compressor	power	21
Feedstock Ethane		NG liquid	235
	Labor		**36**
Total Operating Cost			**497**

Table 29. Summary of raw material costs for steam cracking and electrochemical NPD.

	Unit	**Value**
Electricity	$/kWh	0.014
Steam	$/tonne	20
	$/MMBTU	10.12
Natural gas	$/MMBTU	4
Cooling water	$/MMBTU	2
Refrigeration	$/MMBTU	20
Ethane	$/kg	0.2

Table 30. Relative operation costs summary for steam-ethane cracking and electrochemical NPD

	Electrochemical	**Steam Cracker**
	$/tonne ethylene	
Feedstock	217	235
Thermal Energy	23	205
Electricity	11	21
Labor	3	36
Total	253	497

Figure 29 graphically compares the total operating cost per metric tonne of ethylene produced. Electrochemical NDP is about one-half the cost of steam-ethane cracking. Feedstock cost accounts for 86% of the total operating cost for NDP process, whereas it accounts for just 47% for steam-ethane cracking. If feedstock cost is excluded, the operating costs would be $37/tonne versus $262/tonne for the two processes, mainly attributed to the much simpler process of NDP.

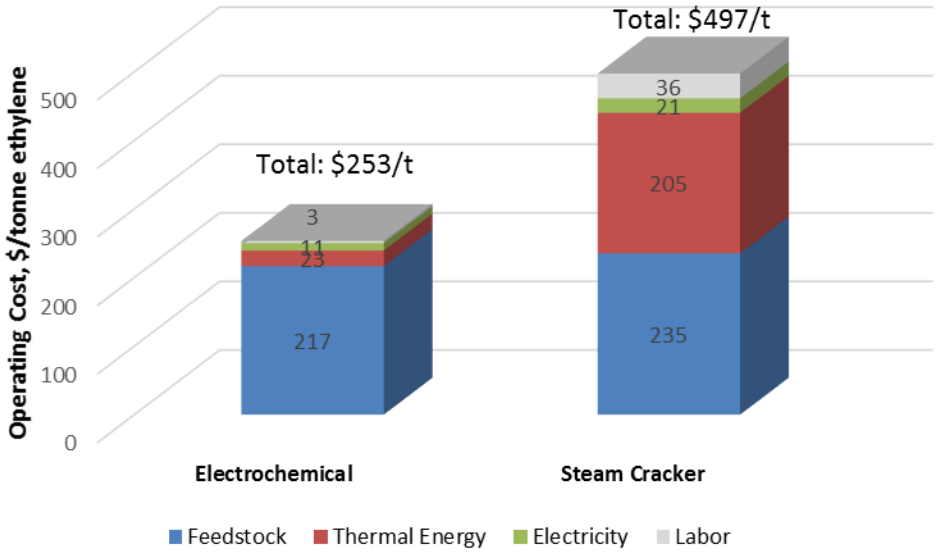

Figure 28. Relative operating costs for NDP and steam-ethane cracking

4.2.1 Energy Balance

The energy requirement for the two processes are summarized in Table 31. Detailed energy projections for steam-ethane cracking process were derived from the literature [5], as shown in Table 32. For each tonne of ethylene produced, a steam cracker requires thermal and electrical energy totaling 39.5 GJ compared to 8.8 GJ for electrochemical NDP Figure 30). It is worth noting that hydrogen generated in the electrochemical process is pure; no further separation is needed. The off-gas generated from the steam-cracking process include hydrogen, methane, acetylene, propylene, propane, and butadiene. This off-gas is generally burned to support process heating. No attempt is made to recover hydrogen.

Table 31. Energy consumption for steam-ethane cracking and electrochemical NPD processes.

	Electrochemical	**Steam Cracker**
	GJ/tonne ethylene	
Thermal Energy	6.0	34
Electricity	2.8	5.5
Total	8.8	39.5
H2 LHV	(10)	--
Feedstock C_2H6	56.3	61
Product C_2H_4	50.3	50.3

Table 32. Detailed energy consumption for steam-ethane cracking.

Section	Unit	Type of Utility Used	GJ/Tonne
Pyrolysis	Feedstock Preheater	CH_4	7.78
	Cracker	CH_4	7.76
Separation	Reboiler	Steam	3.96
	Acetylene Preheater	Steam	1.14
Fraction		Coolant/Refrigerant	13.38
Total Thermal Energy			34
Compression	Compressor	Power	5.54
Total Energy Consumption			39.5

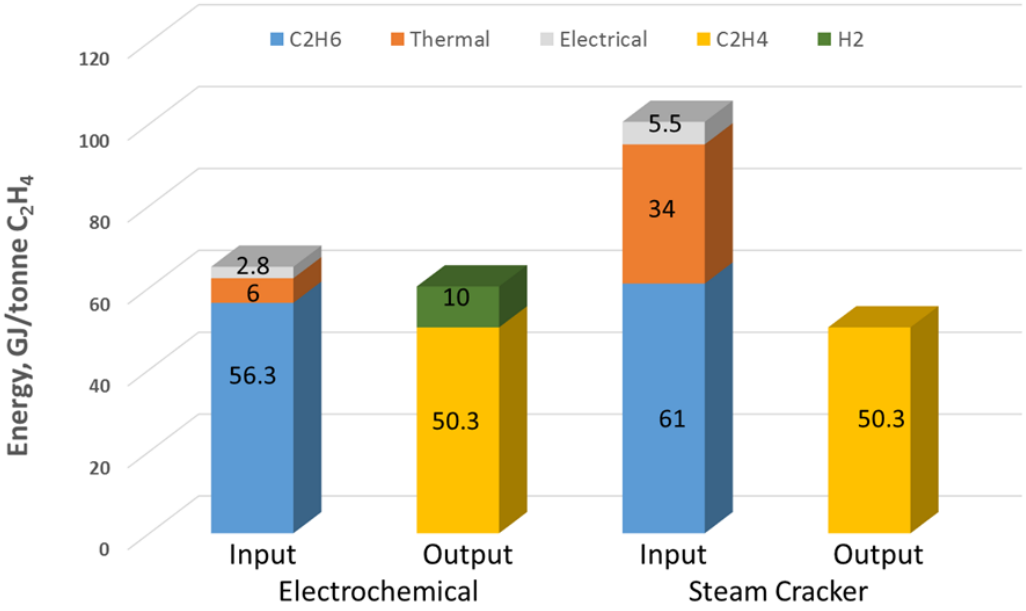

Figure 29. Energy requirements for NDP and steam-ethane cracking.

4.2.2 CO_2 emissions

Electrochemical NDP has a remarkable advantage relative to reducing CO_2 emissions. Figure 31 plots the output from the Aspen model for NDP with data obtained from the literature for steam-ethane cracking [4]. The steam-cracking process emits 1.47 tonne of CO_2 per tonne of ethylene, compared to 0.4 tonne of CO_2 released from the NDP process, resulting in a 72% reduce in CO_2 emission when grid electricity is used for NPD versus an 89% reduction when low-carbon electricity (e.g., nuclear, wind, or hydropower) is used. A 98% reduction in the carbon footprint can be achieved when low-carbon energy is used for both heat and electricity.

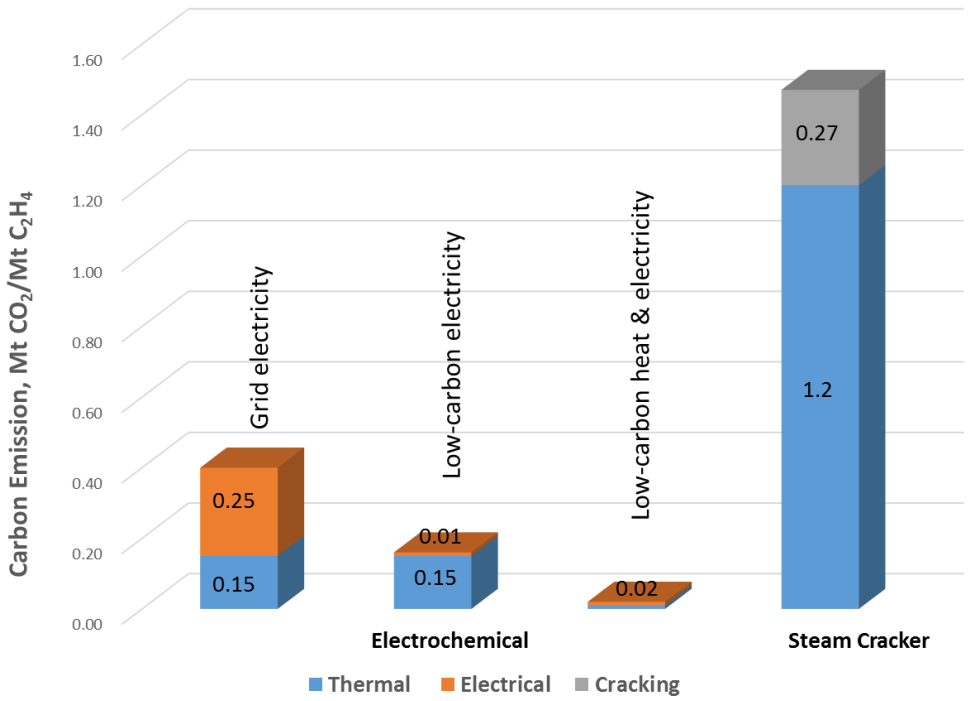

Figure 30. CO_2 emission for NDP and steam cracking.

In summary, electrochemical NDP exhibits several advantages compared to traditional steam cracking in terms of capital cost (40% reduction), operating cost (50% decrease), process-energy requirement (77% reduction) and carbon footprint (>70% saving). It presents an opportunity for a future LWR hybrid process integration.

4.3 LWR-Assisted LDPE Production from Ethylene

Capital and operating costs were analyzed following common assumptions for polymer industries [15], as summarized in Table 33. All costs presented are on a 2017 constant U.S. dollar basis. The Chemical Engineering Plant Cost Index is used to convert capital and operating costs to 2017 dollars. Capital costs are estimated from a variety of resources, but the study uses vendor quotes if available. Individual installation factors for equipment are calculated by Aspen Capital Cost Estimator.

Besides purchased equipment cost, bulk materials and indirect costs are required to complete the installation and make the plant ready for operation.

Table 33. Cost assumptions for LDPE production from ethylene.

Assumption Description	Assumed Value
Plant life	30 years
Plant financing debt/equity	60% / 40% of TCI
Interest rate for debt financing	8.0%
Term for debt financing	10 years
Construction period	3 year
On-stream factor	91% (8000 operating hours per year)
Labor	Based on plant capability
Maintenance	6% of fixed capital investment
Benefits and general overhead	50% of labor + maintenance
Administration	45% of labor
Quality control and laboratory	20% of labor
Insurance and taxes	1% of fixed capital investment
Electricity	$0.06/kWh

The LDPE processes details are based on a PE production rate of 0.83 mtpa (MMT per year), which is a medium size PE capacity for current PE plants [10] and matches the ethylene production rate from upstream. The capital and operation cost for a LDPE process are based on data from reference [15]. Cost estimates can be scaled to other capacities using the six-tenths factor rule [16], in which the cost of equipment scales to the 0.6 power of the capacity if the plant equipment is made larger rather than duplicated at the original scale to obtain more throughput:

cost of larger system = (original cost) × (larger capacity / original capacity)$^{0.6}$.

Costs were calculated based on 2017 prices. Polymerization-grade ethylene is compressed to 50 bar. The on-stream time is 8,000 h/a. The tubular reactors equipped with multiple feeds of ethylene and peroxide initiators are operated at 2000 bar. The initiators are a mix of dicyclohexyl peroxy dicarbonate, t-butylperoxy pivalate, t-butylperoxy 2-ethylhexanoate, and di(t-butyl)peroxide, which is fed in after the heating zone and at two further locations downstream. The pressure of the high-pressure separator is 25 bar. A twin-screw extruder with a side extruder to process LDPE of 0.918–0.939 g/ml density and 0.3–2.0 g/10 min melt-flow index is used [15]. The process block diagram is shown as Figure 32. Due to the high-pressure application of this process, nuclear power can be utilized for the compression system.

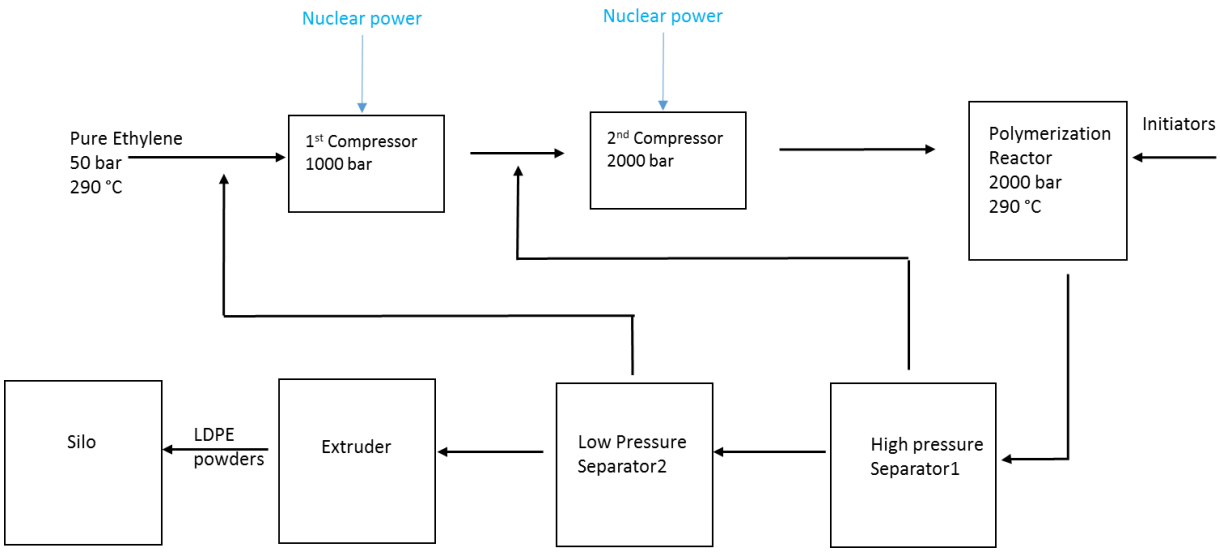

Figure 31. Process block diagram for LDPE at 830,000 tonne/year.

The capital costs of main purchased equipment are listed in Table 34 [15]. More than 80% of the total purchased equipment costs are for the compression system, extruder, and silos. Beside purchased equipment, bulk materials, and indirect costs are required for calculating the TCI for an installed plant. Bulk materials and indirect costs mainly include piping systems, control and instrumentation, installation, etc., as shown in Table 35. Then the TCI for this plant of 830,000 ton/year is about $344 million, which is four times higher than the costs of purchased equipment. This number is in agreement with the result obtained from the Lang-factor method. For liquid operation, a Lang factor of 4.74 is applied to the cost of purchased equipment for calculation of TCI [11]. Spreading the TCI over 30 years of plant life, the capital cost per year per ton of PE is about $14.

Table 34. Capital cost for LDPE process at 830,000 tonne of PE per year, based on 2017 U.S. prices.

Equipment	Million $
PE reactor	4.754
Polymer separation system (including high- and low-pressure separator, was separator, recycle gas coolers)	6.656
Compression system (including primary and secondary compressor, booster compressor)	27.336
Extruder	22.106
Silo	24.008
Purchased equipment cost	84.860
Bulk materials and indirect cost	259.335
TCI w/o interest	344.195
Lang factor	4.74
TCI using Lang factor	402.236
Capital cost per metric tonne (tonne)	$415/tonne
Capital cost per metric tonne (tonne) over 30 years	$14/tonne/year

Table 35. Bulk materials and indirect cost for LDPE process.

Piping	Control and instrumentation
Installation	Coating and insulation
Traffic zone	Electrical equipment
Buildings	Remaining costs

The overall operating cost can be divided into fixed-capital and variable costs. Fixed-capital costs must also be considered when a plant is out of operation whereas variable costs depend on the production rate. Fixed-capital costs include insurance, maintenance, labor, overheads, etc. Variable costs are feedstock (ethylene here), utilities, monomers, and other chemicals, such as initiators, modifiers, or stabilizers.

The specific costs were based on reference data [15] and were adjusted according to current situation. As presented in Table 36, the total operating costs are $896/tonne of LDPE for a plant capacity of 830,000 tonne/year. The production costs are dominated by the cost of feedstock (ethylene), accounting for 80% of the total operating costs (Figure 33). The price of ethylene as feedstock is taken as the average price of 2017 at $600/tonne [17]. Also, utilities (9%), labor (2.7%), overhead (2.5%), and maintenance (2.3%) contribute costs. It is worth noting that depreciation is not included here; if they had been, costs would be higher. Considering the onsite production of ethylene produced by the electrochemical process, the total operating costs for LDPE would be about $176/tonne if the cost of ethylene feedstock were taken out.

Table 36. Operating cost for LDPE process at 830,000 tonne of PE per year, on 2017 U.S. prices.

Items	$/tonne PE
Ethylene ($600/tonne)	720
Initiators (6–12 $/kg)	5
Other chemicals	5
Electricity ($0.06/kWh)	77
Other utilities (steam, water)	3
Insurance (1% of TCI)	3
Maintenance (6% of TCI)	21
Labor	24
Plant overhead (50% of labor and maintenance)	22
Administration (45% of labor)	11
Quality control and laboratory (20% of labor)	5
Total operation cost per metric tonne (tonne) of PE	$896/tonne PE
Total operation cost per metric tonne (tonne) of PE w/o ethylene cost	$176/tonne PE

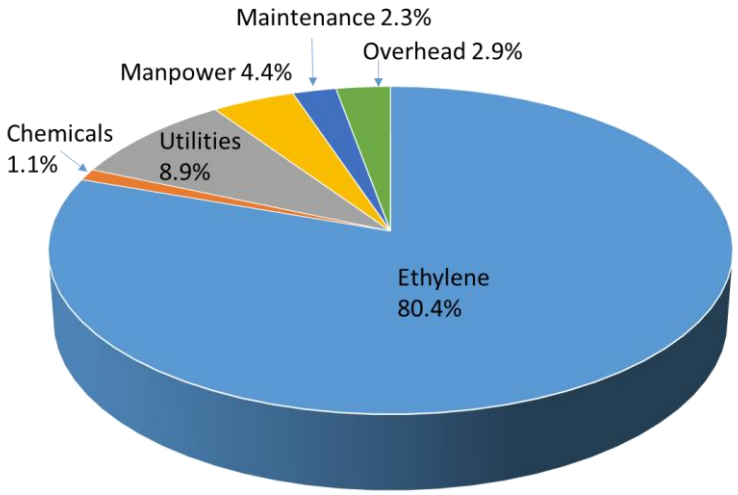

Figure 32. Composition of total operating costs (chemicals: initiators and other chemicals; utilities: electricity, steam and water; manpower: labor, administration and quality control; overhead: plant overhead and insurance).

4.3.1 Economics of LDPE Production from Ethane

The process applying an electrochemical NDP process exhibits notable advantages compared to a process using traditional steam-ethane cracking in terms of capital cost (45% reduction), operating cost (57% decrease), electricity requirement (36% reduction) (Table 37).

The TCI is about $996 million were the electrochemical NDP applied for ethylene production. This is about 69% of the cost of the process using steam cracking. It is worth noting that the TCI of NDP would be lowered to 54% of that of the process using steam cracking if a generation cost $820/kW is used for an electrolyzer. For operating cost, it is $429, compared to $673 for each tonne of PE produced for the two

processes. Only electricity is compared for energy requirement since electricity energy is dominant at PE production process. Each tonne of PE produced requires 7.4 and 10.1 GJ electricity, respectively, for the two processes.

Table 37. Economics for LDPE production from ethane via electrochemical NDP and steam cracking processes for 830,000 tonne of PE per year, based on 2017 U.S. prices.

	unit	**Electrochemical NDP**	**Cracking**
TCI	millions of dollars	996(784)*	1,452
TCI per tonne	$/tonne PE	1,200 (944)*	1,749
Total operating costs (TOCs)	$/tonne PE	429	673
electricity requirement	GJ/tonne PE	7.4	10.1

* When a generation cost of $1,500/kW is used for electrolyzer, the TCI is $996 million ; while it is $784 million when $820/kW is used, which is commonly applied in H2A models.

References

[1] Freedonia, 2018, "World polyethylene," https://www.freedoniagroup.com/industry-study/world-polyethylene-3210.htm

[2] G. J. Maffia, A. M. Gaffney, and O. M. Mason, "Techno-economic analysis of oxidative dehydrogenation options," *Top Catal*, Vol. 59 (2016), p1573–1579.

[3] A. M. Gaffney and O. M. Mason, "Ethylene production via oxidative dehydrogenation of ethane using M1 catalyst," *Catalysis Today* Vol. 285 (2017), p159–165.

[4] D. Ding, Y. Zhang, W. Wu, D. Chen, M. Liu, and T. He, "A novel low-thermal-budget approach for the co-production of ethylene and hydrogen via the electrochemical non-oxidative deprotonation of ethane," *Energy & Environmental Science* Vol. 11, 2018, pp. 1710–1716. doi: 10.1039/c8ee00645h.

[5] P. Thiruvenkataswamy, *Safety and techno-economic analysis of ethylene technologies*, M.S. Thesis: Texas A&M University, College Station, TX, 2015.

[6] L. Koottungal, "International survey of ethylene from steam crackers—2015," https://www.ogj.com/content/dam/ogj/print-articles/volume-113/jul-6/International-survey-of-ethylene-from-steam-crackers--2015.pdf

[7] Petrochemical Update, "U.S. ethylene complex construction costs data 2018–2020," http://analysis.petchem-update.com/content/us-ethylene-complex-construction-costs-data-analysis-2018-2020-0

[8] Petrochemical Update, 2016, "U.S. ethane cracker project costs rise 2.5% year to date," http://analysis.petchem-update.com/engineering-and-construction/us-ethane-cracker-project-costs-rise-25-year-date

[9] Petrochemical Update, 2017, U.S. ethane cracker construction costs rise a further 1% in Q4 2016, http://analysis.petchem-update.com/supply-chain-logistics/us-ethane-cracker-construction-costs-rise-further-1-q4-2016

[10] America's petrochemical outlook, (Jan. 2018), "Petrochemicals Special Report," https://www.platts.com/IM.Platts.Content/InsightAnalysis/IndustrySolutionPapers/americas-petrochemicals-outlook-h1-2018.pdf. Accessed at March 15, 2019.

[11] R. Turton, R. C. Bailie, W. B. Whiting, and J. A. Shaeiwitz, *Analysis, synthesis, and design of chemical processes*, 3rd Edition, 2010, Prentice Hall.

[12] Y. A. Wain, "Updating the Lang factor and testing its accuracy, reliability and precision as a stochastic cost estimating method," *PM World Journal* Vol. III, October 2014, https://pmworldjournal.net/wp-content/uploads/2014/10/pmwj27-oct2014-Wain-updating-the-lang-factor-Featured-Paper.pdf

[13] NREL, "H2A: Hydrogen analysis production models—H2A central hydrogen production model version 3.101," https://www.nrel.gov/hydrogen/h2a-production-models.html, and NREL, "H2A: Hydrogen analysis production models—H2A Central hydrogen production model version 3.2018," https://www.nrel.gov/hydrogen/h2a-production-models.html.

[14] E. A. Harvego, James E. O'Brien, and Michael G. McKellar, *System Evaluations and Life-Cycle Cost Analyses for High-Temperature Electrolysis Hydrogen Production Facilities,* INL/EXT-10-19726, http://www.osti.gov/scitech/servlets/purl/1047199, doi:10.2172/1047199.

[15] E. Lack, and F. Zanette, 2001, "High pressure process technology: fundamentals and applications – high pressure polymerization of ethylene," https://www.sciencedirect.com/topics/materials-science/high-pressure-polymerization.

[16] M. S. Peters, K. D. Timmerhaus, and R. E. West, *Plant design and economics for chemical engineers*, 5th ed. McGraw-Hill, New York, 2003, p. 242.

[17] The pH Report, 2018, "U.S. ethylene prices near all-time lows as over-capacity arrives," http://www.new-normal.com/chemical-companies/us-ethylene-prices-near-all-time-lows-as-over-capacity-arrives/, accessed March 2019.

5. FORMIC ACID

Formic acid, HCOOH, is a commodity chemical (global production ≈ 1.2 Mt/y, price ≈ 0.5 $/kg, compound annual growth rate ≈ 14%) [1, 2] that is used as chemical intermediate [3], as a biocide [4] and, in its potassium salt, as a component of environmentally friendlier deicing fluids [5]. It is included here as an option for base-loading nuclear power plants because it can be produced electrochemically [7] and can be directly sold as a commodity chemical or it could serve as an energy-dense hydrogen carrier [6] for energy storage and other applications. This section describes three approaches for its possible deployment to base load a nuclear reactor (Figure 34):

1. Production via electrochemical synthesis of formic acid or a formate salt, followed by sale of the product into the open market.
2. Electrochemical production followed by thermal decomposition into H_2 and CO_2 and then either sale of the hydrogen or for energy storage by its consumption in a fuel cell that feeds the same grid as the nuclear plant.
3. Electrochemical production followed by electrochemical oxidation in a fuel cell that, again, feeds the same grid as the nuclear power plant, thus serving as an energy storage medium. Two types of fuel cells should be considered: high temperature, which relies on a ceramic membrane and low temperature, which uses a polymeric membrane. The former promises much better energy efficiency but needs to be maintained near its operating temperature (>650°C) even when not in use to avoid thermomechanical issues.

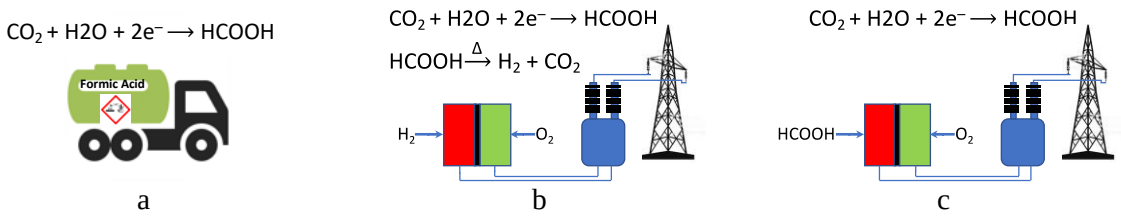

Figure 33. Approaches for storing base load energy in formic acid-derived carriers.

The preliminary techno-economic analyses presented below suggest that the first option is the closest to profitability and could be made economically viable through modest process improvements and by securing and using a frugal source of carbon dioxide. The second approach suffers from high costs for producing the product (either hydrogen or electrical power) thus necessitating R&D to reduce costs. The third approach compares favorably to other ways to satisfy peak power, but R&D would be needed to improve the roundtrip efficiency. Each approach benefits from the safety of storing the energy in a comparatively low-volatility liquid carrier that would be biodegraded should it escape from the storage vessel (Table 38).

Table 38. Safety characteristics of hydrogen storage compounds (from various web resources).

Compound	Vapor pressure at 20°C	Lower flammability Limit, Auto ignition Temperature	Health hazards
Potassium formate	Nonvolatile	nonflammable	Skin irritant
Formic acid, 85%	<4.4 kPa	18%, 520°C	Skin burns
Gasoline	~60 kPa	1.2% 247–280°C	Skin irritant, explosivity
Ammonia	122 kPa	15%, 651°C	Skin burns, explosivity
Hydrogen*	12.6 MPa	4% 536°C	Explosivity

* Extrapolated to 318 K from the boiling point for ammonia (264.8 K) and from the critical point for hydrogen (33.18 K, 13 bar)

5.1 Cases Considered

5.1.1 Assumptions

Each scenario contains an assumption that 135 MW of power is available at a cost of 30 $/MWh (8.3 n$/J). That amount of power is 15% of the recent nameplate capacity of a nominal power plant [8]; the cost is guided by recent power-purchasing agreements for renewable power [9]. In economic modeling, the sale prices of commodity products, formic acid, potassium formate, hydrogen[6], (respectively, $0.50 $/kg [1], $1.0 $/kg [10] and 1.5–16 $/kg[11] are reduced from their current market levels by 10% to account for substitution elasticity [12], the discount that induces customers to buy an ostensibly identical product from a new supplier.

5.2 Synthesis and Sale

In this approach, electrical energy that cannot be fed to the grid is diverted to manufacture formic acid or potassium formate produced by the electrochemical reduction of carbon dioxide. The product formic acid or potassium formate are sold as commodities.

The carbon dioxide could, in principle, be scrubbed from flue gas or air using conventional [13] or advanced sorbents [14, 15]; however, it would require the installation of several unit operations (blower, scrubbing tower, sorbent regeneration) that would add undue complications. Moreover, the technology for reducing CO_2 directly from such sorbents is still in early research [16, 17]. The study assumes, instead, that the carbon dioxide would be delivered by tanker-trailer, likely from a facility that fermented sugars to make ethanol, at a cost of 25 $/T, which is about the price of food grade CO_2 [18]. Note that the carbon dioxide would not be free in any case—even if it were vented by the supplier, the end customer would need to pay for its collection, purification, and delivery. Evidently, there are grades of CO_2, that cost less than 25 $/T, e.g., those that are used in enhanced oil recovery. However, here the study assumed that the CO_2 must be clean enough to be used in contact with the electrocatalysts. Possibly, purifying a cheaper grade using a guard bed would suffice, but in this preliminary survey, such approaches were not evaluated.

5.2.1 Model Development

The electrochemical reduction of CO_2 to HCOOH using water as the source of the protons requires the input of 2 mol electrons per mol of product at a potential ≥1.43 V [2]. The minimum voltage corresponds to the reversible thermodynamic change in free energy; a higher potential will be required to overcome kinetic barriers and transport resistances when the reaction is run at practicable rates. A direct electrolytic process that made 1 t/day (=1000 kg/day) of formic acid would require the input of 0.391 t/day of purified water, 0.957 t/day of CO_2 and at least 1.7 MWh of input energy:

$$1000\ kg_{HCOOH} \times \frac{1\ mol_{HCOOH}}{0.046\ kg_{HCOOH}} \times 2\frac{mol_{e^-}}{mol_{HCOOH}} \times 96485\frac{C}{mol_{e^-}} \times 1.43\ V = 6\ \text{GJ} = 1.67\text{MWh} \quad \text{(eq. 1)}$$

The difference between the thermodynamic potential and the potential required to achieve a given reaction rate is called the overpotential, η. Reference [19] suggests that η = 2.1 V is required to achieve rates of production corresponding to areal current densities of 0.15 A/cm^2, so a practicable energy input will be at least 4.1 MWh/t (=1.67 MWh × 3.44/1.43). For reference, modern electrolyzers [20] require the input of around 50 MWh/t_{H_2} at a current density of about 3 A/cm^2 and an overpotential of about 0.6 V. The minimum power input would be 6 GJ ÷ 86400 s/day = 69.4 kW; the practical power input, corresponding to an overpotential of 2.1 V would be 167 kW.

[6] Hydrogen costs vary greatly depending on the purity, state (liquid or gas), pressure for gaseous hydrogen, and quantity.

An electrolyzer that makes formic acid would be significantly less efficient and significantly larger than a water electrolyzer (Table 39). However, as suggested by Table 40, formic acid can represent a safer option than making hydrogen as well as a product that can be sold as a commodity chemical.

The most expensive unit operation in the process would be the electrolyzer. To approximately estimate its cost, we have extrapolated the techno-economic analysis that was compiled recently by researchers at the University of Delaware [21] to arrive at a CapEx of 65 $/kW for the formic acid electrolyzer, which it is assumed will be straight-line depreciated over 20 years. A low temperature water electrolyzer stack is considerably more expensive at >250 $/kW [21] for an alkaline electrolyzer with a PEM electrolyzer being several times higher.

Table 39. Comparison of electrolyzers.

Product	**Thermodynamic potential**	**Overpotential**	**Energy efficiency**	**Current density**
H_2	1.23 V	0.6 V	67%	3 A/cm^2
HCOOH	1.43 V	2.1 V	40%	0.3 A/cm^2

With those assumptions, formic acid would cost at least $0.3–0.7/kg (Table 40, the lower value corresponds to the thermodynamic limit and the use of industrial grade CO_2), which bracket the current commodity price (0.5 $/kg, suggesting that this approach could approach economic viability. Ongoing research in this area are demonstrating overpotentials decreasing to 0.7V from 2.1V while maintaining the current density suggests significant savings in operation is likely. At 0.7V the formic acid cost is closer to ~0.4 $/kg suggesting it could already by economically viable. Further cost reductions could come from manufacturing learning that would lower the fixed capital investment [22], and from finding a way to use a lower (cheaper) grade of CO_2, and, of course, cheaper electricity.

Table 40. Practical and lower bounds for the cost of manufacturing formic acid by electrolytic reduction of CO_2.

Input	**Cost/$ $T_{\text{formic acid}}^{-1}$**	**Basis**
Electrolyzer (η=2.1 V)	540	167 kW × 65 $/kW ÷ 20 y
(η=0 V)	*230*	*69.4 kW× 65 $/kW ÷ 20 y*
CO_2 (food grade)	24	0.957 T × 25 $/T
(industrial grade)	9.6	0.957 T × 10 $/T (est.)
Electrical power (η=2.1 V)	123	4.1 MWh × 30 $/MWh
(η=0 V)	*50*	1.67 MWh × 30 $/MWh
Purified water	0	Assumed to be available from the power plant
Total (η=2.1 V)	690	
(η=0 V; industrial grade CO_2)	*290*	

Changing the product to be potassium formate to benefit from its higher commodity price would involve a similar electrolysis process and will require the addition of a potassium salt, such as potassium carbonate or potassium hydroxide, to neutralize the formic acid. Each of these salts sells for ~$0.7/kg [23]. Therefore, the potassium formate would cost between $1 to 1.4/kg and would have to compete with conventional sources that sell the material for $1/kg, which may be favorable if the lower production cost of formic acid is achievable or during times of shortage.

In reality, the costs for either product would be higher because the bare bones estimates above include no provision for other unit operations, installation, labor, or marketing. Even so, this approach appears to offer room to be economically viable. Assuming that the process became viable, perhaps by accessing less-expensive CO_2, then the assumed 135 MW of available power would be sufficient to make 290-690 kt/y of formic acid, or about 25-40% of the global demand (1.2 Mt/y): enough to be noticeable, and thus perturb the market.

5.3 Thermal Decomposition to Make Captive Hydrogen

In this approach, formic acid is produced electrolytically, as in the previous example, but instead of the product being sold, it is stored until needed as a source of hydrogen, which is used to fuel a fuel cell to supply peak electrical power. The approach is similar to that of a reversible fuel cell, except that the fuel is generated and stored at ambient pressure, which promises to enhance safety. However, this is at the cost of lower energy efficiency in making formic acid (Table 39) and of two additional unit operations: storage of formic acid and its thermal decomposition. Formic acid contains 4.4% H_2, so the costs in Table 40 must be multiplied by 23 to convert them to a mass throughput of H_2.

Making a quantity of HCOOH corresponding to storing 1 T of H_2 will require supplying at least 38.3 MWh of electrical energy, E:

$$E = 1000\ kg_{H_2} \times \frac{mol_{H_2}}{0.002\ kg_{H_2}} \times 2\ \frac{mol_{e^-}}{mol_{H_2}} \times 96485 \frac{C}{mol_{e^-}} \times 1.43\ V = 138 \frac{\text{GJ}}{T_{H_2}} = \frac{38.3\text{MWh}}{T_{H_2}} \quad \text{eq. 2}$$

$$E = 1000\ kg_{H_2} \times \frac{mol_{H_2}}{0.002\ kg_{H_2}} \times 2\ \frac{mol_{e^-}}{mol_{H_2}} \times 96485 \frac{C}{mol_{e^-}} \times 3.53\ V = 339 \frac{\text{GJ}}{T_{H_2}} = \frac{94.2\ \text{MWh}}{T_{H_2}} \quad \text{eq. 3}$$

The lower energy and power inputs corresponds to the thermodynamic limit; the higher values correspond to recent experimental results. This compares favorably to ~55 MWh per T H_2 of electrical energy a low temperature electrolyzer operating at 60% efficiency especially considering that new research indicates that ~2V operation may be viable which would translate to 53.6 MWh per T H_2. Of course, a high temperature electrolyzer operating at 95% efficiency would still be superior with an electrical requirement of ~35 MWh per T H_2.

Formic acid has a long, but finite shelf life, which decreases with concentration and temperature [4]. At 40°C, a 99% solution decays by 0.25% over 90 days. The decay rate falls by more than a factor of ten if the temperature is lowered to 20°C. Therefore, the use of thermally insulated or temperature-controlled tanks would permit storage of the intermediate across seasons. Thermal decomposition of formic acid can follow two kinetic pathways (Table 41); the one desired here is dehydrogenation to revert the compound into CO_2 and H_2.

Table 41. Decomposition reactions for HCOOH.

Reaction	Stoichiometry
Dehydrogenation	HCOOH ⇆ H_2 + CO_2
Dehydration	HCOOH ⇆ H_2O + CO

The reactions are catalyzed by both heterogeneous platinum-group metals [24] and transition-metal complexes [6, 25], with the latter exhibiting much higher reaction rates. The desired, dehydrogenation reaction predominates in the presence of polar solvents [26]. Both the acid and its salts can be dehydrogenated [6].

5.3.1 Model Development

A process to make, store and dehydrogenate formic acid or its salts could be designed to produce high-pressure, equimolar mixtures of CO_2 and H_2. The former would not impede the oxidation of the hydrogen in a fuel cell that uses an acidic electrolyte.

The overall energy efficiency of the process would be that of the synthesis step, ~40%, multiplied by the energy efficiency of the fuel cell, ~70%, less small parasitic losses for pumping and temperature control. The overall capital investment for storing and retrieving power would be about double that for a reversible fuel cell (because the forward step and the reverse steps would not be the same), plus the cost of the high-pressure decomposition reactor and its feed pump.

It has been assumed that the decomposition reactor can be sized from kinetics reported in the literature [26]. With a 10 wt% Pd/C catalyst, the reaction is approximately zero order in formic acid vapor and achieves ~80% conversion with a mass contact time of 0.007 g min/mL at 400 K. Production of 1 t/day of H_2 requires the conversion of 500 mol/day of hydrogen (or formic acid) = 16500 m^3/min at 400 K. At that contact time, the decomposition reactor would need to present 80.4 kg of the 10 wt% Pd/C catalyst. A reasonable estimate for the effective catalyst density is 1 kg/L, so an 80 L reactor would be needed, which corresponds to about 35 m of Schedule 160 tubing (ID = 66.7 mm). The reactor tubing itself, if constructed from 304 stainless steel, would cost about $50,000, assuming a Lang installation factor of four. The catalyst packing at the current price of Pd ($49,000/kg) [27] would be at least $400,000; however, it is likely that a much cheaper catalyst could be found, particularly, if the reactor were allowed to operate at a higher temperature, using steam derived from the nuclear power plant.

Therefore, this approach would have an overall energy efficiency of ~30% and would incur a selling price of about $9–18/kg of H_2, which exceeds the target posited by the DOE [28] but is within the range of current hydrogen prices [11]. The electrical power produced by consuming the hydrogen would be correspondingly expensive (Table 42) and at a minimum 90 $/MWh (30 $/MWh ÷ 0.3).

Table 42. Estimate of the cost for producing H_2 from electrolytic formic acid, assuming 10-year straight-line depreciation.

Input	**Cost/$ $T_{H_2}^{-1}$**	**Basis**
Electrolyzer (η=2.1 V)	12,800	3940 kW × 65 $/kW ÷ 20 y
(η=0 V)	*5,200*	*1596 kW× 65 $/kW ÷ 20 y*
CO_2	550	22 T/day × 25 $/T (food grade)
	220	22 T/day x 10 $/T (industrial grade)
Electrical power (η=2.1 V)	2,830	94.2 MWh × 30 $/MWh
(η=0 V)	*1,100*	38 MWh × 30 $/MWh
Purified water	0	Assumed to be available from the power plant
Decomposition reactor	2,500	Installed reactor plus catalyst ÷ 20 y
Process heat	0	Assumed to be available from the power plant
Total (η=2.1 V)	18,700	
(η=0 V)	9,020	

5.4 Direct Electrolysis, High Temperature

In this approach, electrical energy that cannot be fed to the grid is diverted to manufacture formic acid produced by the electrochemical reduction of carbon dioxide. The product formic acid is stored and then used to produce electrical power by using it as fuel for a formic acid fuel cell. As above, the approach is similar to that of a reversible fuel cell, except that the fuel is generated and stored at ambient pressure, which promises to enhance safety, albeit at the cost of the lower energy efficiency of making the formic acid instead of hydrogen and of the cost of two additional unit operations: storage of the formic acid and its reversion. Use of a high temperature (solid oxide) fuel cell affords high energy efficiency in the oxidation of the formic acid, in one study [29], η ≈ 60% at the maximum power density of 6 W/m^2 at 800°C. Moreover, at the high operating temperature, 600–800°C, that fuel cell showed no tendency to coke. A recent estimate[30] for the capital cost of a solid oxide fuel is $92/kW.

Assuming that the CO_2 were recycled, that the system was sized to deliver 1 MW of power with a round-trip efficiency of 24% (= 40% × 60%), and that the daily duty cycle of the system was 50% charging and 50% discharging, then the cost of storing and dispatching the stored power would be about $23/kW.

For reference, the capital investment for a small turbine-powered generator backup generator is about 100 $/kW [31]; therefore, this approach is less expensive, but this analysis ignores operating costs other than the input power.

Table 43. Cost estimate for storing electrical power via production and conversion of formic acid at high temperature.

Input	Cost/$ $MW_{delivered}^{-1}$	Basis
Electrical power input	1,510	4.2 MW × 12h × 30 $/MWh
Formic acid Electrolysis (η=2.1 V)	13,650	4.2 MW × 65 $/kW ÷ 20 y
CO_2	0	Assumed to be recycled
Purified water	0	Assumed to be available from the power plant
Formic acid fuel cell (η=0.6 V)	7,820	1.7 MW × 92 $/kW ÷ 20 y
Total	22,980	24% efficiency round trip efficiency

5.5 Direct Electrolysis, Low Temperature

Formic acid has periodically been considered as a fuel for low-temperature polymer electrolyte fuel cells.[30,31] Its deployment has been impeded by low conversion efficiency resulting from transport of formic acid across the fuel-cell membrane and poisoning of the cathode catalyst by CO generated by the dehydration of formic acid [32].

5.5.1 Model Development

If the electrolyzers that produced and consumed the formic acid operated reversibly, and if the CO_2 released upon oxidizing the intermediate formic acid were completely recycled, then the cost of this approach would be the capital cost of the electrolyzer ($65/kW). More plausibly, the electrolyzer that produced the formic acid and the fuel cell that consumed it would each operate with the ~40% energy efficiency listed in Table 39, meaning that the roundtrip efficiency would be around 16%. A 40% efficient direct formic acid fuel cell would operate at approximately 0.57 V, which is about 84–73% lower than a formic acid electrolyzer. This means that a 1MW formic acid electrolyzer would only produce 0.16–0.28 MW of power in fuel cell mode. Therefore, the capital cost of a reversible direct formic acid fuel cell would optimistically be at a minimum of $232–400/kW.

In that case, assuming that the CO_2 were recycled, that the system was sized to deliver 1 MW of power with a round-trip efficiency of 16%, and that the daily duty cycle of the system was 50% charging and 50% discharging, then the cost multiplier for the stored energy would be 1.32, meaning that there would be at least a 32% energy price penalty for dispatching power stored in this way. The cost of storing and dispatching the stored power would be about $34–43/kW (Table 44).

Table 44. Cost estimate for storing electrical power via production and conversion of formic acid at low temperature.

Input	Cost/$ $MW_{delivered}^{-1}$	Basis
Electrical power input	2,270	6.3 MW × 12h × 30 $/MWh
Formic acid electrolysis (η=2.1 V)	20,475	6.3 MW × 65 $/kW ÷ 20 y
CO_2	0	Assumed to be recycled
Purified water	0	Assumed to be available from the power plant
Formic acid fuel cell (η=0.85 V)	11,600	1 MW × 232 $/kW ÷ 20 y
	20,000	1 MW × 400 $/kW ÷ 20 y
Total	34,345	16% efficiency round trip efficiency
	42,745	

For reference, the capital investment for a small turbine-powered generator backup generator costs about 100 $/kW [31]; this approach promises to be more expensive than high temperature electrolysis but, again, less expensive than a small turbine generator.

References

[1] Markets and Markets, 2018, Formic Acid Market worth $618,808.7 Thousand by 2019, https://www.marketsandmarkets.com/PressReleases/formic-acid.asp, accessed on: 10 December 2018.

[2] R.S. Weber, "Effective Use of Renewable Electricity for Making Renewable Fuels and Chemicals," *ACS Catalysis* Vol. 9 (2019), pp. 946–950.

[3] H.H. Szmant, *Organic Building Blocks of the Chemical Industry; John Wiley & Sons: New York, 1989.*

[4] J. Hietala, A. Vuori, P. Johnsson, I. Pollari, W. Reutemann, and H. Kieczka, "Formic Acid," in *Ullmann's Encyclopedia of Industrial Chemistry*; 6th ed.; B. Elvers, Ed.; Wiley-VCH Verlag: Weinheim, 2016.

[5] BASF, 2013, "Formic acid for deicing," http://formic-acid.basf.us/p02/USWeb-Internet/formic-acid/en_GB/content/microsites/formic-acid/deicing/index, accessed on: 15 March 2019.

[6] K. Müller, K. Brooks, and T. Autrey, "Hydrogen Storage in Formic Acid: A Comparison of Process Options," *Energy & Fuels* Vol. 31 (2017), pp. 12603–12611, doi: 10.1021/acs.energyfuels.7b02997.

[7] X. Lu, D.Y.C. Leung, H Wang, M.K.H. Leung, and J. Xuan, "Electrochemical Reduction of Carbon Dioxide to Formic Acid," *ChemElectroChem* Vol. 1 (2014), pp. 836–849, doi: 10.1002/celc.201300206.

[9] U.S. Environmental Protection Agency (EPA), "Green Power Pricing," 2018, https://www.epa.gov/greenpower/green-power-pricing#fn2, accessed on: 10 June 2018.

[10] Alibaba, "Potassium Formate," 2019, https://www.alibaba.com/showroom/potassium-formate-price.html, accessed on: 17 March 2019.

[12] M. Ruth, H2@Scale Analysis, National Renewable Energy Laboratory, 2017, TV045, https://www.hydrogen.energy.gov/pdfs/review17/tv045_ruth_2017_o.pdf.

[13] A. Bilgic, S. King, A. Lusby, and D.F. Schreitner, "Estimates of U.S. Regional Commodity Trade Elasticities of Substitution," *J Regional Analysis Policy*, Vol. 32 (2002), pp. 79–98.

[14] H.M. Stowe and G.S. Hwang, "Fundamental Understanding of CO2 Capture and Regeneration in Aqueous Amines from First-Principles Studies: Recent Progress and Remaining Challenges," *Industrial & Engineering Chemistry Research*, Vol. 36 (2017), pp. 6887–6899, doi: 10.1021/acs.iecr.7b00213.

[15] D.J. Heldebrant, P.K. Koech, V.A. Glezakou, R. Rousseau, D. Malhotra, and D.C. Cantu, "Water-Lean Solvents for Post-Combustion CO2 Capture: Fundamentals, Uncertainties, Opportunities, and Outlook," *Chem Rev* Vol.117 (2017), pp. 9594–9624, doi: 10.1021/acs.chemrev.6b00768.

[16] P. Koech, D. Malhotra, D.J. Heldebrant, V.-A. Glezakou, R. Rousseau, and D.C. Cantu, 2017, "Capture and Release of Acid Gases Using Tunable Organic Solvents with Aminopyridien," U.S. Pat. Appl. 2017/0203250 A1.

[17] J. Kothandaraman, R.A. Dagle, V.L. Dagle, S. Davidson, E.D. Walter, S. D. Burton, D.W. Hoyt, and D.J. Heldegrant, "Condensed-phase low temperature heterogeneous hydrogenation of CO2 to methanol," *Catal. Sci. Technol*. Vol. 8 (2018), pp. 5098–5103.

[18] Y. Oh and X. Hu, "Ionic liquids enhance the electrochemical CO_2 reduction catalyzed by MoO_2," *Chem Commun (Camb)* Vol. 51 (2015), pp. 13698–13701, doi: 10.1039/c5cc05263g.

[19] Doty Energy, "Commercial CO2 market Today," 2011, http://dotyenergy.com/Economics/Econ_Physical_CO2_Market.htm, accessed on: 18 March 2019.

[20] H. Yang, J.J. Kaczur, S.D. Sajjad, and R.I. Masel, "Electrochemical conversion of CO_2 to formic acid utilizing Sustainion™ membranes," Journal of CO_2 Utilization Vol. 20 (2017), pp. 208–217, doi: 10.1016/j.jcou.2017.04.011.

[21] GinerELX, "Hydrogen Fueling Stations," 2017,https://ginerelx-2938941.hs-sites.com/-temporary-slug-4ce32f8e-1189-4b5b-9ed3-5e9a2e2a34a7?hs_preview=AeaozHnR-4981184696&__hstc=222486980.6d70dad4fcee7551739c2eb15ec3990e.1525217563826.1538774607765.1552936020826.7&__hssc=222486980.1.1552936020826&__hsfp=22981983, accessed on: 18 March 2019.

[22] V. Viswanathan, A. Crawford, D. Stephenson, S. Kim, W. Wang, B. Li, G. Coffey, E. Thomsen, G. Graff, P. Balducci, M. Kintner-Meyer, and V. Sprenkle, "Cost and performance model for redox flow batteries," Journal of Power Sources Vol 247 (2014), pp. 1040–1051, doi 10.1016/j.jpowsour.2012.12.023.

[23] R.S. Weber and J.E. Holladay, "Modularized Production of Value-Added Products and Fuels from Distributed, Waste Carbon-rich feedstocks," Engineering 3 (2017), pp. 330–335, https://doi.org/10.1016/j.eng.2018.05.012.

[24] R.S. Weber and L.J. Snowden-Swan, "The Economics of Numbering-up a Chemical Process Enterprise," *J Adv Manuf Process* Vol. 1 (2019), in press, DOI:10.1002/amp2.10011.

[25] Alibaba, "Potassium Hydroxide," 2019, https://www.alibaba.com/product-detail/potassium-hydroxide_62019982178.html?spm=a2700.7724838.2017115.1.76655ed4tf2Aqd, accessed on: 18 March 2019.

[26] E. Iglesia and M. Boudart, "Structure-Sensitivity and Ensemble Effects In Reactions of Strongly Adsorbed Intermediates. Catalytic Dehydrogenation and Dehydration of Formic Acid on Nickel," *J. Phys. Chem.* Vol. 95 (1991), pp. 7011–7016.

[27] C. Fellay, P.J. Dyson, and G. Laurenczy, "A viable hydrogen-storage system based on selective formic acid decomposition with a ruthenium catalyst," *Angew Chem Int Ed Engl* Vol. 47 (2008), pp. 3966–3968, doi: 10.1002/anie.200800320.

[28] D.A. Bulushev, S. Beloshapkin, J.R.H. Ross, "Hydrogen from formic acid decomposition over Pd and Au catalysts," *Catalysis Today* Vol. 154 (2010), pp. 7–12, doi: 10.1016/j.cattod.2010.03.050.

[29] APMEX, "Palladium Prices," 2019, https://www.apmex.com/spotprices/palladium-price, accessed on: 18 March 2019.

[30] US DOE, "DOE Technical Targets for Hydrogen Production from Electrolysis," 2018, https://www.energy.gov/eere/fuelcells/doe-technical-targets-hydrogen-production-electrolysis, accessed on: 19 March 2019.

[31] N.M. Aslam, M.S. Masdar, S.K. Kamarudin, and W.R.W. Daud, "Overview on Direct Formic Acid Fuel Cells (DFAFCs) as an Energy Sources," *APCBEE Procedia* Vol. 3 (2012), pp. 33–39, doi: 10.1016/j.apcbee.2012.06.042.

[32] A.K. Singh, S. Singh, and A. Kumar, "Hydrogen energy future with formic acid: a renewable chemical hydrogen storage system," *Catalysis Science & Technology* Vol. 6 (2016), pp. 12–40, 10.1039/c5cy01276g.

[33] W.G. Scott, “Small, low-cost, highly efficient gas turbines,” 1997, https://www.power-eng.com/articles/print/volume-101/issue-9/features/small-low-cost-highly-efficient-gas-turbines-provide-the-utility-industry-with-a.html, accessed on: 19 March 2019.

6. METHANOL SYNTHESIS WITH CO_2

6.1 Overview

Methanol synthesis can be performed using carbon dioxide and hydrogen as feedstocks. However, potential sources for providing industrial quantities of carbon dioxide and hydrogen feedstocks are often not located at the same site. Ethanol plants emit quantities of carbon dioxide that could be utilized as a feedstock to a methanol-synthesis process. Separately, an LWR provides sufficient power generation capacity to produce significant quantities of hydrogen using electrolysis-based processes. During periods of low electrical demand, a significant fraction of the nuclear plant output could be diverted to hydrogen production via electrolysis. Although LWRs and ethanol plants could provide industrially significant quantities of hydrogen and carbon dioxide for use as methanol-synthesis feedstocks, the locations of these feedstock generators are most often not located in proximity.

Synthesis of methanol from hydrogen and carbon dioxide requires these reactants to be supplied at a molar ratio of 3:1 (Reaction 1). The potential hydrogen-production capacity that could be provided by a typically sized LWR, with all energy output applied to hydrogen production, would provide more hydrogen than the ratio of CO_2 could react with if produced by a single, typically sized ethanol plant. Therefore, a hydrogen-producing nuclear plant must be paired with multiple ethanol plants to maximize the ability of the nuclear plant to divert energy output to methanol synthesis instead of electricity generation during periods of low electrical demand/pricing.

$$CO_2 + 3H_2 \rightarrow CH_3OH + H_2O \quad (1)$$

To make use of these potential feedstocks, it would be necessary to transport hydrogen from a centrally located LWR to distributed ethanol plants. Alternatively, the carbon dioxide produced by the distributed ethanol plants could be transported to the centrally located nuclear plant. The objective of this analysis is to evaluate the most cost-effective option for transporting methanol synthesis feedstocks to the production site. Two methanol synthesis production process locations are evaluated: (1) at a centralized methanol synthesis plant with close proximity to a light-water nuclear reactor, or (2) at distributed methanol synthesis plants located near ethanol plants.

6.2 Centralized Production

A centralized methanol synthesis facility would utilize electrical power produced by the co-located nuclear plant during time periods when load is low to provide energy input to the methanol synthesis process. The syngas would be supplied using an SOEC operating in co-electrolysis mode, whereby water and carbon dioxide can be simultaneously converted to syngas. The co-electrolysis reaction is described in Reaction 2, and the SOEC operation principle is illustrated in Figure 35:

$$H_2O + CO_2 \rightarrow H_2 + CO + O_2 \quad (2)$$

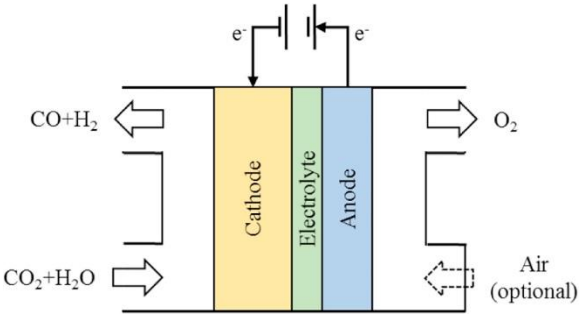

Figure 34. The principle of co-electrolysis in a SOEC [1].

The carbon dioxide feed to the co-electrolysis SOEC would be obtained by transporting carbon dioxide from remotely located ethanol plants to the centralized methanol synthesis facility. Because the methanol synthesis reaction takes place at a pressure of 75 bar [2] the co-electrolysis SOEC is assumed to operate at or above this pressure.

Methanol is formed by the following elementary reaction steps [3]:

$$CO + H_2O \rightarrow H_2 + CO_2 \quad (3)$$

$$CO_2 + 3H_2 \rightarrow CH_3OH + H_2O \quad (4)$$

When these reactions are added, the net stoichiometric equation for reaction of CO to methanol becomes:

$$CO + 2H_2 \rightarrow CH_3OH \quad (5)$$

Although the molar ratio of H_2 to CO is 2:1 in the net methanol synthesis reaction, in practice the reactor feed stream is maintained at a H_2 to CO ratio of 2.45:1 since less than 100% of the syngas is reacted to methanol in each pass through the synthesis reactor [2]. However, the hydrogen and carbon dioxide feedstocks must be supplied to the methanol synthesis process at a molar ratio of 3:1 as described in Reaction 4. This evaluation of feedstock transport assumes that both the distributed and centralized methanol synthesis process will require that hydrogen and carbon dioxide be provided at a molar ratio of 3:1.

6.3 Distributed Production

A distributed methanol-synthesis production facility located at an ethanol plant would use the carbon dioxide produced by the ethanol plant along with hydrogen imported from a centralized hydrogen-production facility as the feedstocks. Carbon dioxide produced by the ethanol plant would be electrochemically reduced to carbon monoxide and oxygen at a pressure equal to that of the methanol-synthesis-reactor operating pressure. Imported H_2 and produce CO would be combined into a syngas stream that would be used for methanol synthesis at the ethanol plant.

In order to establish representative hydrogen and carbon dioxide transport distances and flow rates, potential hydrogen demand data within 150 miles of the representative nucelar plant in the Midwest Region obtained from Elgowainy and Hawkins [4] were evaluated. Data were filtered to obtain estimated future hydrogen demand from ethanol plants that could potentially produce synfuels from byproduct carbon dioxide were a source of hydrogen available. Within a 150-mile radius of the station, 15 ethanol plants were identified. The median future hydrogen demand for these 15 ethanol plants is 117 tonnes/day assuming 341 days of operation per year, with minimum and maximum values of 59 tonne/day and 440 tonne/day, respectively.

Figure 36 is a plot of the number of ethanol plants and the total potential hydrogen demand for all plants within a given radius from the modeled nuclear plant. Based on the average geographic density of the ethanol plants identified in the dataset from Elgowainy and Hawkins [4] (one ethanol plant per 4712 mi^2 based on the 15 plants within a radius of 150 mi^2, or one ethanol plant per 4712 mi^2), a generic correlation to estimate the number of ethanol plants within a specified radius from a central nuclear power plant was developed (solid line in Figure 36).

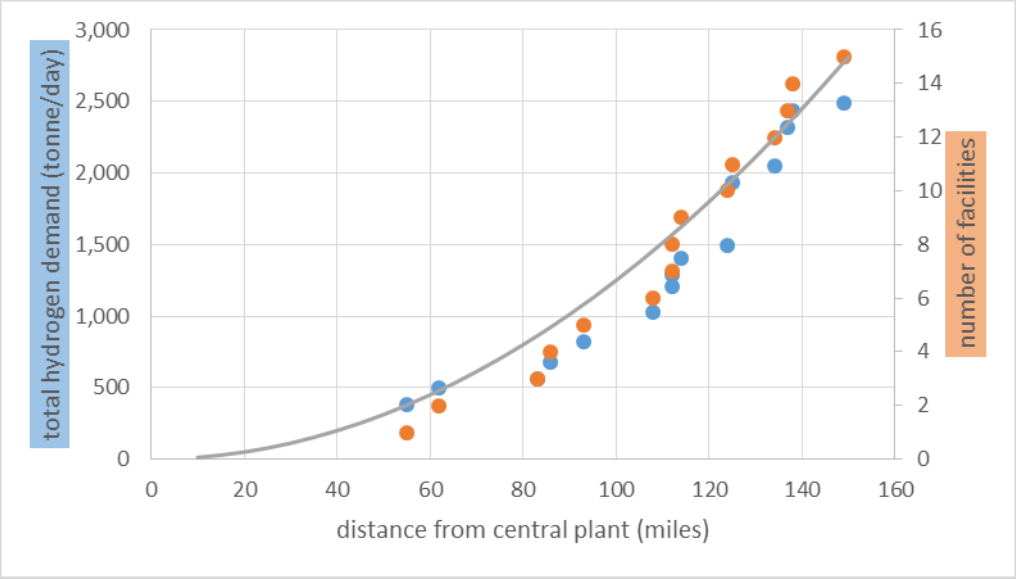

Figure 35. Total potential hydrogen demand and number of ethanol production facilities within specified radius of a representative plant in Midwest.

Hydrogen transport capacities of 100 tonne/day and 400 tonne/day were evaluated; these capacities correspond to ethanol-plant sizes close to the median- and high-potential future demand values reported in Elgowainy and Hawkins [4]. Based on the stoichiometry of Reaction 4, corresponding methanol-production plants would have daily capacities of 530 tonne/day and 2120 tonne/day of methanol product, respectively. For the case of a centralized methanol-synthesis plant where the carbon dioxide is transported from the distributed ethanol plants to the centralized hydrogen-producing nuclear plant, carbon dioxide transport capacities of 727 tonne/day CO_2 and 2910 tonne/day CO_2 were evaluated; these carbon dioxide flow rates correspond to the quantity of CO_2 that would have to be transported to provide the CO_2 feedstock to the methanol-synthesis plants with specified capacities of 530 tonne/day and 2120 tonne/day of methanol product.

Yang and Ogden [5] determined that for systems where a quantity of 100 tonnes/day of H_2 is transported, a pipeline is the lowest-cost option (relative to gas trucks or liquid trucks) regardless of transport distance. Because the flow rates considered in this analysis are equal to or above the threshold value for pipeline transport identified by Yang and Ogden [5], pipelines are the only transport method considered in this preliminary evaluation. This evaluation only considers the simplistic case in which a single pipeline between the centralized facility and the distributed facility is utilized (independent of whether carbon dioxide or hydrogen is being transported) (i.e., no branched pipelines are used).

Inclusion of pipeline booster stations (intermediate compressor stations for boosting pipeline pressure) was not considered in this analysis. Addition of booster stations is an economic decision (i.e., the added capital and operating costs associated with use of booster stations may reduce the pipeline diameter and associated costs by enough to result in lower overall costs). Subsequent analysis would be required to determine whether the use of booster stations could reduce overall transport and compression costs for hydrogen or carbon dioxide.

Transport costs presented are for a single pipeline and the associated compressors and pumps required to pressurize the fluid transported through the pipeline. In the case of the centralized facility, it is likely that hydrogen would be produced at a large scale and transported to multiple distributed facilities. In this case, larger hydrogen compression equipment would be installed, such that each pipeline did not require an independent compressor to pressurize the inlet stream; however, this analysis does not account for the

additional economies of scale that could be realized by supplying multiple pipelines using a single compressor train. Instead, it is assumed that each pipeline is paired with a dedicated compressor.

6.4 Pipeline Transport Considerations

The temperature and pressure conditions at which the carbon dioxide and hydrogen are transported has a significant impact on the required transport-system equipment design, as well as the capital and operating costs associated with the transport system. Transport temperature and pressure determine the phase (liquid or vapor) in which the fluid is transported as well as relevant fluid properties such as density and viscosity. Therefore, selection of the transport mode and operating conditions has a significant impact on transport costs.

6.4.1 CO_2 Transport

A carbon dioxide pipeline design must incorporate several important design considerations. Practical considerations regarding the structural integrity of the pipeline must be considered to ensure safe yet economical pipeline design. Peletiri et al. [6] describe practical minimum and maximum pressures for carbon dioxide pipeline design.

Carbon dioxide has several unique characteristics and fluid properties that must be considered during pipeline design. Carbon dioxide in the liquid or supercritical phase can be transported using smaller-diameter pipes than gaseous carbon dioxide although, if the source carbon dioxide is at low pressure, compression is required to achieve liquid or supercritical phase carbon dioxide. Additional discussion of dense-phase carbon dioxide transport considerations are provided by Peletiri et al. [6]:

In this analysis the carbon dioxide pipeline inlet and outlet pressures are specified as 12 MPa and 10 MPa, respectively. Compression is required to pressurize the carbon dioxide produced by the ethanol plants from atmospheric pressure to the design pipeline inlet pressure of 12 MPa. Carbon dioxide compression has significantly higher energy requirements than carbon dioxide pumping. It was assumed that five stages of compression are required to compress the carbon dioxide to the critical pressure of 7.38 MPa followed by pumping to increase the pressure to the pipeline inlet pressure. The pipeline outlet pressure (delivery pressure) of 10 MPa was specified to deliver carbon dioxide to a methanol synthesis process at a pressure sufficient to feed the synthesis reactor (1090 psi or 7.5 MPa) [2]. Although the specified pipeline outlet pressure is higher than the methanol synthesis reactor operating pressure, a literature review by Knoope [7] indicates that several open-literatures sources suggest an average minimal pressure of 9.2 MPa for long-distance carbon dioxide transport (300 km).

Carbon dioxide mass flow rates of 728 tonne/day and 2910 tonne/day were evaluated; these flow rates were determined by applying the H_2:CO_2 molar ratio of 3:1 for methanol synthesis to the ethanol-plant hydrogen demand design-basis values of 100 tonne/day and 400 tonne/day identified above. The carbon dioxide flow-rate specification assumes that the amount of carbon dioxide each ethanol plant could supply is independent of whether methanol synthesis is performed at the distributed facility (ethanol plant) or the centralized facility (nuclear plant with integrated hydrogen production) (i.e., the total methanol synthesis capacity is independent of whether carbon dioxide or hydrogen is transported).

6.4.2 Hydrogen Transport

Hydrogen has a low molecular weight and a low density in the gaseous phase. Therefore, cost-effective hydrogen-gas transport requires pressurization to achieve high mass-flow rates using economical pipe sizes.

The hydrogen source in this analysis is an HTE process. It is possible to operate HTE processes at elevated pressures (liquid water can be pumped to the HTE process operating pressure using pumps with relatively low capital and operating costs) to achieve efficient HTE process operation, as well as to minimize the additional compression requirements to pressurize hydrogen to the pipeline inlet pressure. According to Yildiz et al. [8] there are several factors to consider when choosing an HTE design pressure:

The product hydrogen should be delivered at a pressure that matches the distribution infrastructure pressure. This can be achieved in three ways:

1. *Electrolyzing steam at atmospheric pressure and compressing the product hydrogen gas up to the distribution infrastructure pressure*
2. *Pumping water up to the distribution infrastructure pressure and electrolyzing steam at this high pressure*
3. *Partially pumping water to be electrolyzed at relatively high pressure and by additional compression of the product hydrogen to match the distribution infrastructure pressure.*

The third strategy identified by Yildiz et al. [8] was employed in this analysis, i.e., the electrolysis feed water was pumped to the relatively high pressure of 3.5 MPa specified for several different hydrogen production processes evaluated by [9] followed by additional compression of the production hydrogen to match the transmission infrastructure pressure of 70 atm (7.1 MPa) evaluated for pipeline transport by Yan and Ogden [5].

As discussed previously, hydrogen mass flow rates of 100 tonne/day and 400 tonne/day were evaluated. These flow rates approximately correspond to the future hydrogen demand for methanol synthesis associated with median- and maximum-sized ethanol plants [4].

6.5 Calculation of Pipeline Diameter

The pipeline length and diameter are two major factors in determining pipeline capital costs. Pipeline length is determined by the logistics of the transport scenario (i.e., the distance between the sources of hydrogen and carbon dioxide). Pipeline inside diameter can be calculated following specification of mass flow rate, fluid properties, and pipeline-inlet and outlet pressures. As previously noted, this analysis did not consider the use of booster stations, so the pipeline diameter calculation is based on the specified inlet and outlet pressures (i.e., the outlet pressure specification defines the maximum allowable pressure drop), which in turn determines the minimum pipeline diameter.

The following equation can be used to calculate the inside diameter of a pipeline for liquid or gas transport [10,11]:

$$D_i = \left\{ \frac{-64 Z_{ave}^2 R^2 T_{ave}^2 f_F \dot{m}^2 L}{\pi^2 [M Z_{ave} R T_{ave} (p_2^2 - p_1^2) + 2 g P_{ave}^2 M^2 (h_2 - h_1)]} \right\}^{1/5} \quad (6)$$

where D_i is the internal pipeline diameter (m), Z_{ave} is the average fluid compressibility, R is the universal gas constant (Pa m³/mol K), T_{ave} is the average fluid temperature (K), f_F is the Fanning friction factor, $\dot{m}$ is the design mass flow rate (kg/s), L is the pipeline segment length (m), M is the molecular weight of the stream (kg/kgmol), g is acceleration due to gravity (m/s²), p is pressure (Pa), h is pipeline elevation (m), where 1 and 2 represent upstream and downstream locations.

Pressure varies non-linearly in the pipeline and must be calculated using the below Equation [10]:

$$P_{ave} = \frac{2}{3}\left(p_2 + p_1 - \frac{p_2 p_1}{p_2 + p_1}\right) \quad (7)$$

Zigrang and Sylvester [12] provide an explicit approximation for the Fanning friction factor:

$$\frac{1}{2\sqrt{f_F}} = -2.0 \log\left\{\frac{\varepsilon/D_i}{3.7} - \frac{5.02}{Re} \log\left[\frac{\varepsilon/D_i}{3.7} - \frac{5.02}{Re} \log\left(\frac{\varepsilon/D_i}{3.7} + \frac{13}{Re}\right)\right]\right\} \quad (8)$$

where ε is the roughness of the pipe (m), and Re is the Reynolds number:

$$Re = \frac{4\dot{m}}{\mu \pi D_i} \quad (9)$$

where μ is the viscosity of the fluid (Pa s).

The Fanning friction factor is a function of the pipeline diameter and the Reynolds number and does not have a direct analytical solution. Therefore, the Fanning friction factor must be iteratively solved along with the pipeline diameter and Reynolds number.

The diameter of the pipeline used to transport the fluid is highly dependent on the fluid transport conditions (temperature and pressure) and the resulting fluid properties. In this analysis REFPROP v9.1[13] was used to calculate temperature and pressure dependent fluid properties.

6.6 Pipeline-based Transport-system Cost Estimate

Several correlations are available in the open literature for estimating the costs of carbon dioxide and hydrogen pipelines. Parker [14] applies multipliers to NG-pipeline capital costs to estimate costs for hydrogen-transmission pipelines. McCollum and Ogden [15] provides a carbon dioxide pipeline capital-cost correlation based on carbon dioxide mass-flow rate; this cost model is not considered applicable for estimating hydrogen pipeline capital costs. McCoy and Rubin [11] provides a cost correlation for carbon dioxide pipeline capital costs based on natural gas pipeline costs. The McCoy and Rubin cost correlation includes factors to account for cost differences in different regions of the U.S.

In this analysis the cost correlation [11] was used to estimate the costs for both carbon dioxide and hydrogen transport pipelines using the calculated diameter for transport of each of these respective feedstocks as input. The calculated pipeline diameter was rounded up to the closest nominal diameter in order to calculate pipeline costs. The McCoy and Rubin correlation includes contributions for materials, labor, right-of-way, and miscellaneous costs. As noted in various literature sources including Parker [15] and Fekete et al. [16], hydrogen pipelines require upgraded materials with additional costs relative to natural gas or CO_2 pipelines; the additional costs for hydrogen pipelines are not accounted for in this analysis and the costs estimated using the correlation in McCoy and Rubin [11] will therefore be lower-bound estimates of the hydrogen-pipeline costs. Pipeline annual O&M costs were estimated as 2.5% of the pipeline installed capital cost [15].

Compressor and pump equipment sizing and capital costs were calculated based on correlations presented in McCollum and Ogden [15]. Annual O&M costs for compression and pumping equipment were estimated as 4% of the compressor and pump installed capital costs [15]. Electrical power for compressor and pump operation was assumed to cost $0.05/kWh.

Annualized costs were calculated using a capital recovery factor of 10%, which corresponds to a weighted average cost of capital of 7.8% with a 20-year capital recovery period.

6.7 Results

The nominal pipeline diameter for transport of carbon dioxide (centralized production) and hydrogen (distributed production) are plotted as a function of pipeline diameter in Figure 37. Using the pipeline operating pressures specified in this analysis, hydrogen pipeline transport always requires equal- or larger-diameter pipe size than carbon dioxide transport.

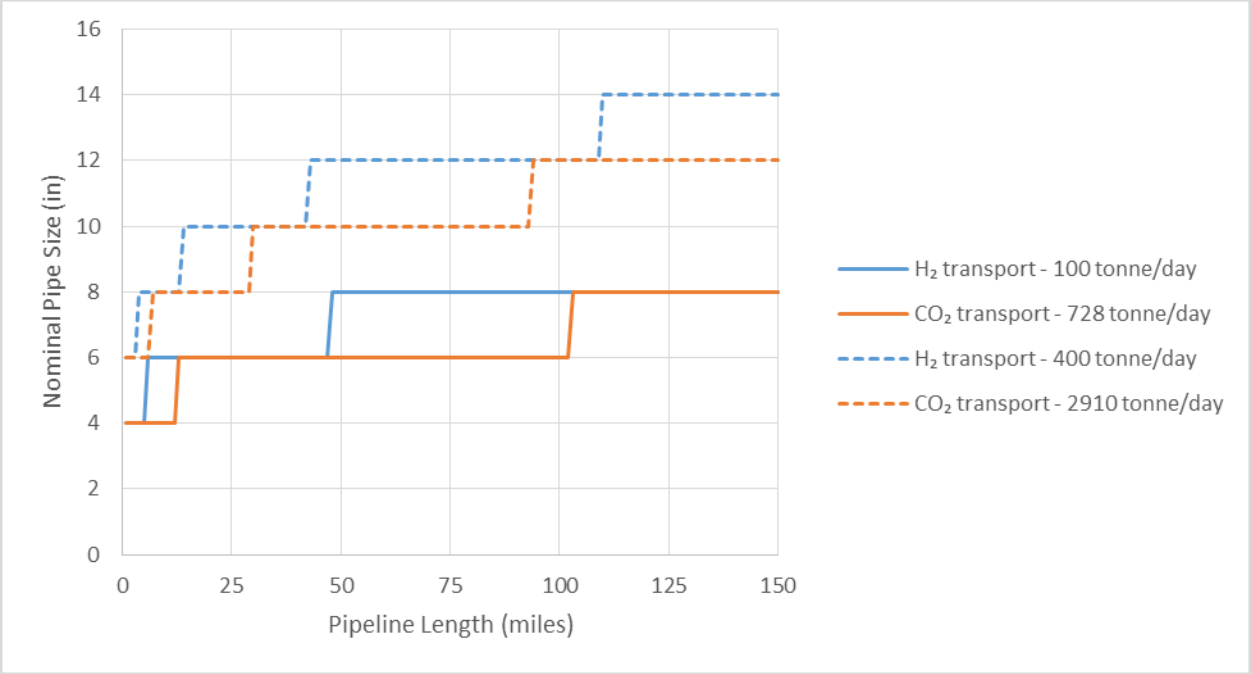

Figure 36. Hydrogen and carbon dioxide pipeline diameter as function of pipeline length.

The larger-diameter pipes required for hydrogen transport will generally result in higher capital costs (Figure 38); in practice the capital costs for hydrogen transport would be further exacerbated by the higher materials costs required for high-strength steel used for hydrogen pipeline construction (additional costs for upgraded pipe materials associated with hydrogen transport are not accounted for in this analysis).

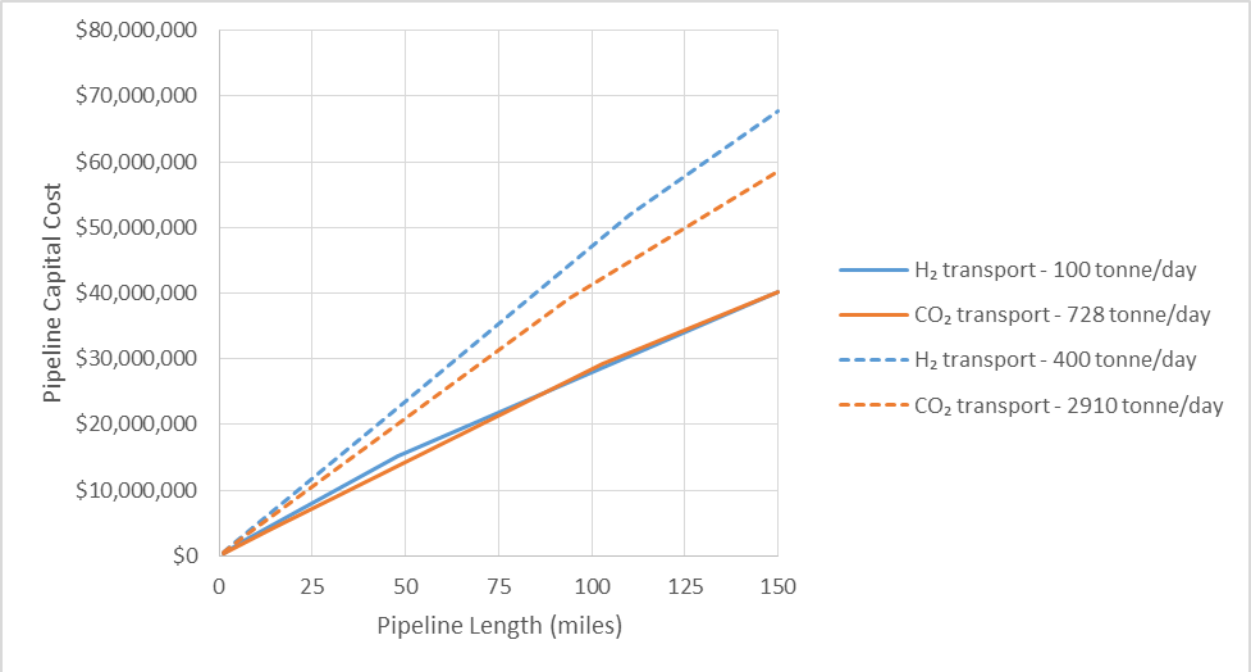

Figure 37. Hydrogen and carbon dioxide pipeline capital cost as function of pipeline length.

Annualized transport and compression costs for the four scenarios evaluated (distributed vs centralized methanol production at median [530 tonnes methanol per day] and large scale [2120 tonnes methanol per day]) are shown in Figure 39.

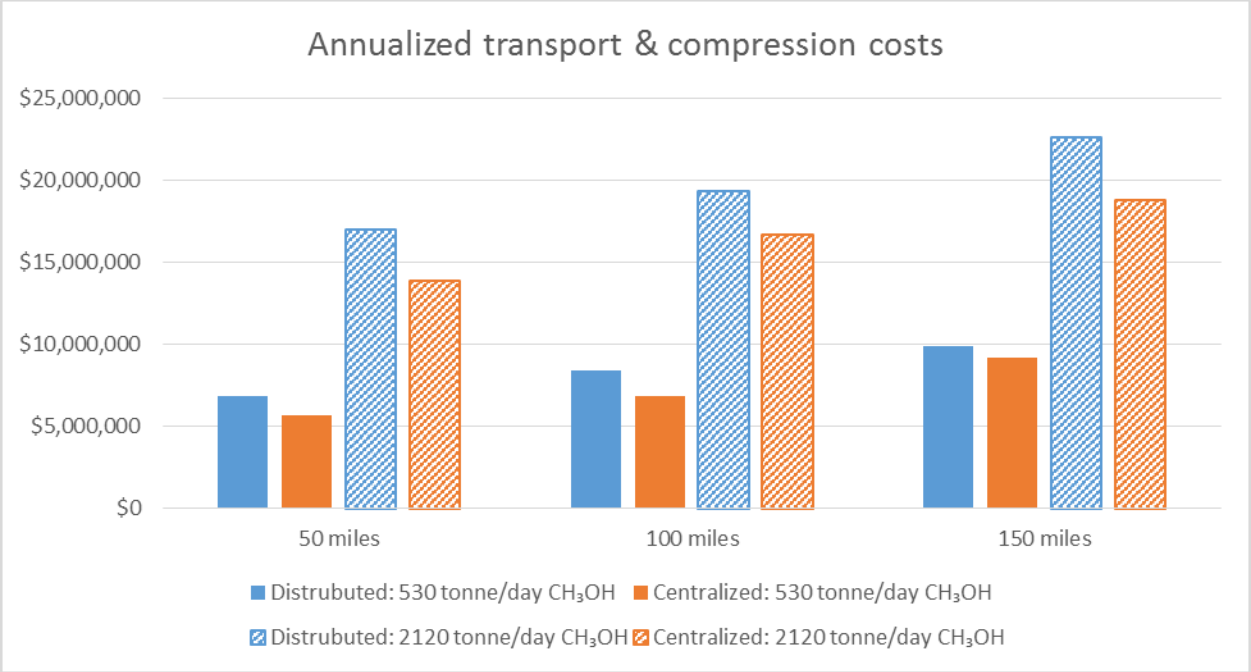

Figure 38. Annualized transport and compression costs for centralized and distributed methanol production. Centralized production requires carbon dioxide transport, distributed production requires hydrogen transport.

Detailed feedstock transport and compression costs for distributed vs centralized methanol production are provided in Table 45 (530 tonnes methanol per day) and Table 46 (2120 tonnes methanol per day). The feedstock flow rate listed in each column is sufficient to support the specified capacity of methanol production; the carbon dioxide production rate at the distributed facility provides the basis for specification of reactant transport flow rates. An LWR could have hydrogen-production capacity sufficient to supply a flow rate of hydrogen greater than that required for the specified capacity of methanol production; in this case, multiple pipelines would be required to transport feedstock to/from multiple ethanol plants, and the system's total methanol-production capacity would scale up accordingly.

Table 45. Feedstock transport and compression costs for distributed versus centralized methanol production: 530 tonnes/day of methanol production.

Methanol Production	Distributed	Distributed	Distributed	Centralized	Centralized	Centralized
Transported Material	H_2	H_2	H_2	Co_2	Co_2	Co_2
Mass Flow Rate (Tonne/Day)	100	100	100	728	728	728
Pipeline Length (Miles)	50	100	150	50	100	150
Capital Costs						
Pipeline	$15,760,570	$28,459,184	$40,280,143	$12,180,737	$22,038,039	$40,280,143
Transport Compression	$1,185,524	$1,185,524	$1,185,524	$14,363,735	$14,363,735	$14,363,735
Transport Pumping	0	0	0	$162,604	$162,604	$162,604

Process Feed Compression	$15,683,569	$15,683,569	$15,683,569	$1,266,876	$1,266,876	$1,266,876
Total	$32,629,663	$45,328,277	$57,149,236	$27,973,952	$37,831,254	$56,073,358
Annual Capital Recovery Charge ($/Yr)	**$3,262,966**	**$4,532,828**	**$5,714,924**	**$2,797,395**	**$3,783,125**	**$5,607,336**
Operating Costs						
O&M: Pipeline ($/Yr)	$394,014	$711,480	$1,007,004	$304,518	$550,951	$1,007,004
O&M: Compression And Pumping ($/Yr)	$674,764	$674,764	$674,764	$631,729	$631,729	$631,729
Energy Cost						
Transport Compression ($/Yr)	$633,492	$633,492	$633,492	$1,188,457	$1,188,457	$1,188,457
Transport Pumping ($/Yr)	$0	$0	$0	$32,887	$32,887	$32,887
Feed Compression ($/Yr)	$1,881,821	$1,881,821	$1,881,821	$689,036	$689,036	$689,036
Total Annualized Costs ($/Yr)	**$6,847,057**	**$8,434,384**	**$9,912,004**	**$5,644,022**	**$6,876,185**	**$9,156,448**
Levelized Transport Cost ($/Tonne)	**$208.43**	**$256.75**	**$301.74**	**$23.61**	**$28.76**	**$38.30**

Table 46. Feedstock transport and compression costs for distributed vs centralized methanol production: 2120 tonnes/day of methanol production.

Methanol Production	Distributed	Distributed	Distributed	Centralized	Centralized	Centralized
Transported Material	H_2	H_2	H_2	CO_2	CO_2	CO_2
Mass Flow Rate (Tonne/Day)	400	400	400	2911	2911	2911
Pipeline Length (miles)	50	100	150	50	100	150
Capital Costs						
Pipeline	$22,957,341	$41,378,349	$67,716,897	$19,347,415	$41,378,349	$58,488,881
Transport Compression	$2,030,719	$2,030,719	$2,030,719	$24,949,327	$24,949,327	$24,949,327
Transport Pumping	0	0	0	$440,414	$440,414	$440,414
Process Feed Compression	$27,213,892	$27,213,892	$27,213,892	$2,172,361	$2,172,361	$2,172,361
Total	**$52,201,951**	**$70,622,960**	**$96,961,507**	**$46,909,517**	**$68,940,452**	**$86,050,983**
Annual Capital Recovery Charge ($/Yr)	**$5,220,195**	**$7,062,296**	**$9,696,151**	**$4,690,952**	**$6,894,045**	**$8,605,098**

Operating Costs						
O&M: Pipeline ($/Yr)	$573,934	$1,034,459	$1,692,922	$483,685	$1,034,459	$1,462,222
O&M: Compression And Pumping ($/Yr)	$1,169,784	$1,169,784	$1,169,784	$1,102,484	$1,102,484	$1,102,484
Energy Cost						
Transport Compression ($/Yr)	$2,533,968	$2,533,968	$2,533,968	$4,753,829	$4,753,829	$4,753,829
Transport Pumping ($/Yr)	$0	$0	$0	$131,547	$131,547	$131,547
Feed Compression ($/Yr)	$7,527,284	$7,527,284	$7,527,284	$2,756,144	$2,756,144	$2,756,144
Total Annualized Costs ($/Yr)	**$17,025,165**	**$19,327,791**	**$22,620,110**	**$13,918,640**	**$16,672,507**	**$18,811,324**
Levelized Transport Cost ($/Tonne)	**$129.57**	**$147.09**	**$172.15**	**$14.56**	**$17.44**	**$19.67**

6.8 Conclusions

Based on the assumptions and methods used in this analysis, transporting methanol synthesis reactants to a centralized production location would be less expensive than transporting methanol synthesis reactants to distributed production locations. Methanol synthesis at a centralized production location requires carbon dioxide byproduct from distributed ethanol production facilities to be compressed and transported via pipeline to the centralized location. Carbon dioxide can be compressed to a liquid phase and transported using smaller diameter piping than hydrogen at the pipeline operating pressures recommended in the open literature. Additionally, pipeline transport of hydrogen requires a pipeline constructed of more expensive materials (the additional material costs are not accounted for in this analysis).

Although carbon dioxide compressor capital costs and compression-energy requirements are large, carbon dioxide compression at the distributed ethanol plants must be performed regardless of whether the methanol-synthesis reactor is located at a centralized or distributed plant; i.e., the carbon dioxide must be compressed to approximately 7.5 MPa either for pipeline transport or to achieve the methanol synthesis reactor-inlet conditions. Although pipeline transport of the carbon dioxide requires additional pressurization to pressures of approximately 12 MPa, this pressurization can be achieved using liquid-phase pump equipment for which the capital and operating costs are significantly lower than for compression such that they do not have significant impact on the analysis results.

This analysis does not consider the cost of constructing and operating the methanol synthesis process, but constructing the methanol synthesis process at a centralized location would enable economies of scale to be achieved, both in terms of capital costs as well as operating costs (e.g., operations personnel, maintenance, etc.). Additionally, the locating the methanol-synthesis reactor at the centralized location would enable the process to leverage utilities associated with the nuclear plant, such as cooling water, process steam, and process heat from the nuclear plant.

References

[1] R. Andika et al., "Co-electrolysis for power-to-methanol applications," *Renewable and Sustainable Energy Reviews,* Vol. 95, 2018, pp. 227–241.

[2] Idaho National Laboratory. "Nuclear-Integrated Methanol-to-Gasoline Production Analysis," TEV-667, May 2010.

[3] Alan English, Jerry Rovner, John Brown, and Simon Davies, "Methanol," *Kirk-Othmer Encyclopedia of Chemical Technology*, John Wiley & Sons, 2005.

[4] A. Elgowainy and T. Hawkins, *Summary of Potential Hydrogen Demand Analysis for H2@Scale*, Argonne National Laboratory, January 2019.

[5] C. Yang and J. Ogden, "Determining the lowest-cost hydrogen delivery mode," *International Journal of Hydrogen Energy*, Vol. 32, 2007, pp. 268–286.

[6] S. P. Peletiri, N. Rahmanian, and I. M. Mujtaba, "CO_2 Pipeline Design: A Review," *Energies* Vol. 11 (2018), pp. 2184; doi:10.3390/en11092184.

[7] M.M.J. Knoope, A. Ramirez, A., and A.P.C. Faaij, "A state-of-the-art review of techno-economic models predicting the costs of CO_2 pipeline transport," *International Journal of Greenhouse Gas Control,* Vol. 16, 2013, pp. 241–270.

[8] B. Yildiz, K. J. Hohnholt, and M. S. Kazimi, "Hydrogen Production Using High-Temperature Steam Electrolysis Supported by Advanced Gas Reactors with Supercritical CO_2 Cycles," *Nuclear Technology*, Vol. 155, No. 1, 2006, 1–21, doi: 10.13182/NT06-A3742

[9] McKellar, et al (2007), Technical Evaluation Study: HTGR-Integrated Hydrogen Porduction via Steam Methane Reforming (SMR) Process Analysis, INL TEV-953, January, 2011

[10] M. Mohitpour, H. Golshan, and A. Murray, *Pipeline Design & Construction*, ASME Press, New York, NY, 2003.

[11] S. T. McCoy, and E. S. Rubin, "An engineering-economic model for pipeline transport of CO_2 with application to carbon capture and storage," *International Journal of Greenhouse Gas Control* Vol. 2 (2008), pp. 219–229.

[12] D. J. Zigrang, and N. D. Sylvester, "Explicit approximations to the solution of Colebrook friction factor equation," *AIChE J.* Vol. 28, No. 3, 1982, pp. 514–515.

[13] https://www.nist.gov/srd/refprop

[14] N. Parker, *Using natural gas transmission pipeline costs to estimate hydrogen pipeline costs*, UCD-ITS-RR-04-35, 2004, pp. 1–85.

[15] D. L. McCollum and J. M. Ogden, *Techno-economic models for carbon dioxide compression, transport, and storage & Correlations for estimating carbon dioxide density and viscosity*. UCD-ITS-RR-06-14, 2006, pp. 1–87.

[16] J. R. Fekete, J. W. Sowards, and R. L. Amaro, "Economic impact of applying high strength steels in hydrogen gas pipelines," *International Journal of Hydrogen Energy,* Vol. 40, 2015, pp. 10547–10558.

7. THERMAL ENERGY STORAGE

Thermal-energy storage (TES) enables thermal-energy use and can reduce strains on energy infrastructure during peak usage periods, weather events, and other outages, ultimately improving resiliency and reducing costs. Economic stressors have been forcing nuclear energy sources to consider operating in a load-follow mode. For nuclear reactors, load-follow operation can be undesirable due to the associated thermal and mechanical stresses placed on the fuel and other reactor components. Various methods of TES can be coupled to nuclear (or renewable) power sources to help absorb grid variability caused by daily load-demand changes and renewable intermittency. Studies have shown the thermal energy can then be recovered, either as a supplement to the power plant during peak demand times, cooling demands, or used for other ancillary applications such as hydrogen production [1,2,3,4].

TES can be classified into three main types: sensible heat storage, thermochemical storage, and latent heat storage. Sensible heat storage (SHS) systems work by raising the temperature of a storage medium, usually a solid or a liquid. The storage materials undergo no change in phase over the temperature range of the storage process. A good SHS material has high heat capacity, relative molecular stability, and durability over the temperature range of interest. Thermochemical storage is a newer technology that relies on heat to drive reversible chemical reactions [5]. Latent heat storage is an approximately isothermal process which takes advantage of the heat of fusion of the storage material as it changes phase.

Current technology readiness levels (TRLs) dictate that SHS is the only of these three types of TES to be considered with nuclear reactors in the near term (i.e., a 3 to 7-year timeframe) [6]. SHS can be deconstructed into two operating modes: charging and discharging. A two-tank TES system is a common configuration for liquid SHSs. In the charging mode, cold fluid is pumped from a cold tank through an intermediate heat exchanger (IHX), heated, and stored in a hot tank while the opposite occurs in the discharge mode. Such systems have been successfully demonstrated in the solar-energy field as a load management strategy [7].

7.1 Potential Nuclear System Integration Points

The performance of a TES system is a strong function of the connection point to the secondary side of the nuclear plant. For plants incorporating once-through steam generators the turbine control valves (TCVs) act as pressure-control valves to maintain steam-generator pressure at a given set point. Shown in Figure 39 turbine bypass valves (TBVs) can be configured such that bypass steam can either be taken off the steam line at the pressure equalization header upstream of the TCVs (Aux 1), downstream of the TCVs prior to entering the high-pressure turbine (Aux 2), or at some low-pressure turbine tap (Aux 3). If taking steam upstream of the TCVs, the steam conditions are approximately constant, but the system is only able to bypass ~50% nominal steam flow before losing pressure control. If more steam flow is desired, then placing the taps downstream of the TCVs is an option that has no steam-flow limitation. However, steam conditions downstream of the TCVs are a strong function of the load profile. Taking bypass steam downstream of the TCVs can result in highly varying steam pressures and temperature entering the TES system, making storage challenging. Further, if the TBVs are placed downstream of the TCVs, then TBV operation must be uniform to maintain symmetric operation of the TCVs.

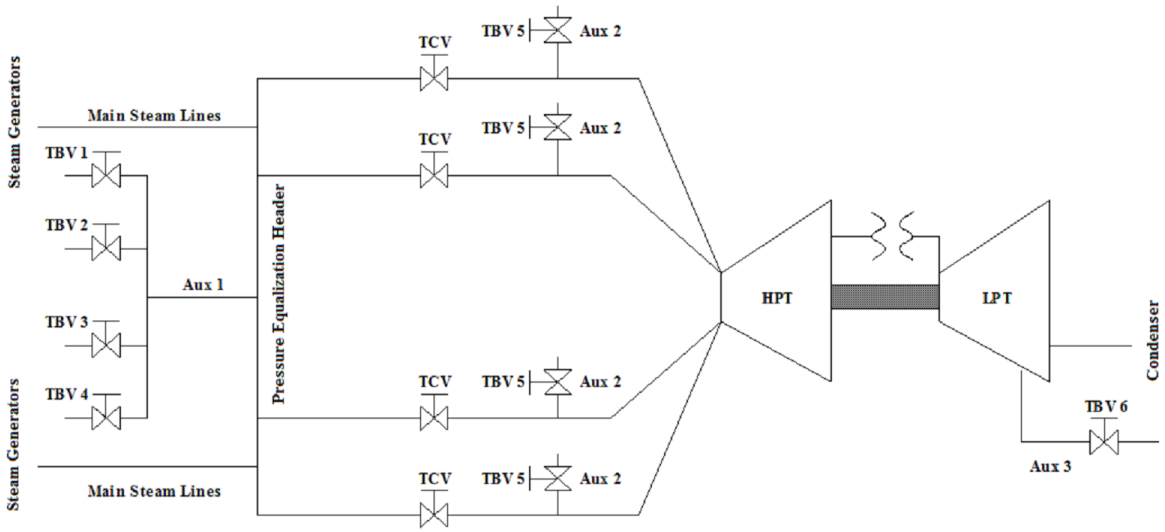

Figure 39. Bypass steam options.

For plants incorporating U-tube steam generators, the control strategy is different, but the trends remain the same. If the bypass is taken prior to the TCV, the steam conditions sent to the TES system are approximately constant. And if bypass is taken after the TCVs, highly varying pressures and temperatures can occur, thus decreasing the TES systems effectiveness.

7.2 Thermal Energy Storage Technology Options

In the realm of thermal integration technologies, there are several different options depending on steam conditions, size requirements, and the availability of waste heat. The technologies presented in this section are a summary of the most technologically mature systems that would be readily accessible in the near term for nuclear-system integration. The authors fully acknowledge that, as time progresses, the technologies presented below may become antiquated as newer energy-storage options near commercialization.

7.2.1 Single/Two-Tank Sensible Heat Storage

Sensible heat TES is a technology that is in commercial use in concentrated-solar-power plants (CSPs) [7]. In the solar industry, an array of parabolic solar reflectors in concentric circles about a collector in which a medium, either molten salt or thermal oil, is heated to produce steam to make electricity. During periods where electricity demand is low, the heated fluid is stored for later use. Current CSP plants have storage tanks to allow for upwards of 15 hours of storage [8].

In commercial use, there are two main types of sensible heat thermal storage designs. Single tank thermocline designs and two-tank designs, both of which can be used with or without packed bed filler material to increase heat density and eliminate the need for massive tank designs. Two-tank designs are the most commercially available and readily understood systems. These designs have separate tanks that hold hot and cold fluid separately. An advantage of two-tank systems is the relative simplicity in their design and the reduced thermal degradation achieved. Single tank thermocline systems involve having the hot and cold fluid present within a single tank and relying on density differentials to thermally stratify the fluid, thus developing a thermocline between the hot and cold fluid.

Designs for both have been put forth for use with nuclear reactors. A potential configuration of the two-tank system with nuclear reactors can be seen in Figure 40. An in-depth look at single-tank thermocline operation is not presented here as it is effectively synonymous with two-tank operation. In the charging mode configuration of a proposed two-tank TES system, an outer loop interfaces with the reactor's balance of plant directly through four parallel auxiliary TBVs connected at the pressure-equalization header, each staged to open at a certain percent of the maximum auxiliary-flow demand. Bypass steam is directed through an IHX and discharged to the main condenser or some other low-pressure process [9]. An inner loop containing a TES fluid consists of two large storage tanks, along with several pumps to transport the TES fluid between the tanks, the IHX, and a steam generator. Flow bypass valves are included in the discharge lines of both the hot and cold tanks to prevent deadheading the pumps when the flow control valves are closed. Common TES fluid properties are given in Table 47. While the two-tank system can utilize numerous TES fluids, the configuration proposed by Frick [3] utilizes Therminol-66. Therminol-66 was chosen because it is readily available, can be pumped at low temperatures, and offers thermal stability over the range -3–343°C, which covers the anticipated operating range of the TES system (203–260°C). Other benefits of using Therminol-66 include its material safety data sheet (MSDS) classification as a nonhazardous material [10]. In addition, as hydrocarbons do not readily exchange hydrogen atoms with other materials [11], tritium migration would be mitigated in the rare event of simultaneous leaks in the steam generator and an IHX tube allowed activated primary water to mix with the TES fluid. In this event, the TES tanks would act as holding tanks for the activated water. Molten salts are often considered for SHS systems due to their low-cost, high-heat transfer properties, and general thermal stability. However, many of the standard salts freeze at temperatures (141°C for Hitec) just outside typical operating bounds required for integration with LWRS systems (~170°C); therefore, entire system-heat tracing would be required.

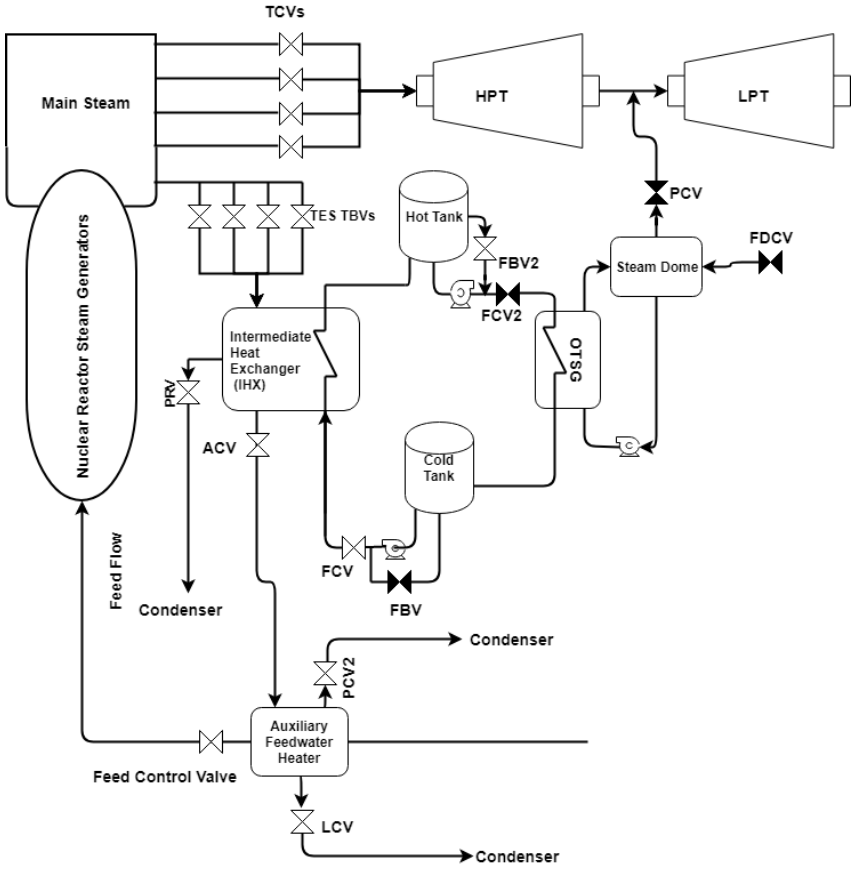

Figure 40. Schematic of a PWR connected to a two-tank sensible heat TES system, discharge mode.

Table 47. Properties of possible TES fluids at ~260°C.

Heat Transfer Fluid	Density (kg/m^3)	Heat Storage ($kJ/m^3{}^\circ C$)	Operating Range (°C)
Therminol-66 [12]	840	2033	-2.7–343.3 (27–650°F)
Therminol-68 [13]	854	2048	-25.5–360 (-14–680°F)
Therminol-75 [14]	906	1984	79.44–385 (175–725°F)
Hitec [15]	1889	2456	142–540

The TES system is designed to allow the reactor to run continuously at ~100% power over a wide range of operating conditions. During periods of excess capacity, bypass steam is directed to the TES unit through the auxiliary bypass valves, where it condenses on the shell side of the IHX. TES fluid is pumped from the cold tank to the hot tank through the tube side of the IHX at a rate sufficient to raise the temperature of the TES fluid to some set point. The TES fluid is then stored in the hot tank at constant temperature. Condensate is collected in a hot well below the IHX and drains back to the main condenser or can be used for some other low-pressure application, such as chilled-water production, desalination, or feed heating. Pressure-relief lines connect the shell side of the IHX with the condenser to prevent overpressurization of the heat exchanger during periods of low condensation rate. A nitrogen cover gas dictates tank pressure. Tank sizes are a direct function of the designed temperature difference (ΔT) between the hot tank and the cold tank. Smaller tank sizes can be achieved by increasing the ΔT between the tanks.

Converse to the charging mode, during periods of peak demand, or when process steam is desired, the system is discharged by pumping TES fluid from the hot tank to the cold tank through the tube side of an once-through steam generators producing a saturated liquid-vapor mixture. This two-phase mixture flows into a steam dome, where it is separated into gas and liquid phases. As illustrated in Figure 40, this saturated steam can then be reintroduced into the power-conversion cycle for electricity production or directed to some other application through the pressure-control valve at the exit of the steam dome. For operation as an electrical-peaking unit, steam is assumed to be reintroduced prior to the moisture separator and reheaters before entering the low-pressure turbine. This allows the flow streams from the steam dome and high-pressure turbine exhaust to combine and eliminates any moisture that may be present prior to entering the low-pressure turbine. Additionally, at the bottom of the intermediate heat exchanger is a well of high-grade waste heat that can be utilized to help minimize reactor oscillations due to feedwater-temperature changes associated with typical load-following operation. This is accomplished by sending the high-grade waste heat to an auxiliary feedwater heater at the end of the feed train to boost feed temperature prior to the feed's entering the steam generators. A recent study was done on the dynamic response of such a system; it showed temperature oscillation in feedwater temperature can be drastically reduced [16].

7.2.2 Chilled-water Storage

Chilled-water storage is often overlooked as an effective TES method. Chilled water is regularly used in large manufacturing facilities, college campuses, and district heating and cooling systems to satisfy cooling demands. Traditionally, electric chillers make chilled water via the vapor-compression cycle. The chilled water is pumped to air handlers throughout a facility to satisfy comfort-cooling needs. During warmer months of the year, a large portion of a facility's electricity demand is generated from associated heating, ventilation, and air-conditioning (HVAC) equipment. Because building cooling loads regularly peak during the early to late afternoon hours, the HVAC equipment is sized to accommodate these peak loads. At night or during early morning hours, when cooling loads are low, excess chiller capacity exists. Moreover, these peak facility-cooling loads often coincide with peak electricity demands, thereby putting further strain on utilities. In the form of chilled water storage, TES is a way to combat peak cooling loads

by shifting them from on-peak to off-peak hours [17]. Stratified chilled-water storage tanks have emerged as an effective option for storing chilled water [18]. In a stratified chilled-water storage tank, warm water and cold water are stored in the same vessel, with no solid component between the warm and cold volumes of water. Differences in density between cold and warm water cause a thin thermocline, or sharp temperature gradient, to form. Excess chilled water produced when facility cooling demands are low is deposited in the bottom of the tank via diffusers. Because the tank is a constant-volume device, charging the tank with cold water means simultaneously removing warm water from the top of the tank to be sent to the chillers. Conversely, discharging the cold water to be used during times of peak facility cooling loads results in warm water being deposited in the top of the tank. Therefore, a fully charged tank implies the tank is full of chilled water while a fully discharged tank implies the tank is full of warm water. In terms of thermal-needs single effect, lithium bromide chillers utilize steam or hot water at or below 205 kPa (15 psig) and the affinity between an absorbent and a refrigerant to create a chilling effect. Therefore, absorption chillers become particularly attractive when a source of waste heat that would normally be rejected to the environment or some other low-temperature sink is available. Potential sources of this heat are turbine tap extraction or waste heat from an ancillary process connected upstream of the turbine, such as large-scale TES or hydrogen production.

Frick and Misenheimer [1,9] described and simulated such an arrangement with nuclear reactors. Through the integration of a two-tank sensible heat system, a well of high-grade waste condensate is collected at times of low electric demand. The high-grade waste condensate is sent to a flash vessel, where steam is produced and sent to the absorption chillers as depicted in Figure 41. Once in the flash vessel, the condensate is separated into liquid and vapor. The vapor can then be utilized in four single-effect lithium bromide chillers to chill water for a 1,000,000 ft^2 adjacent office space.

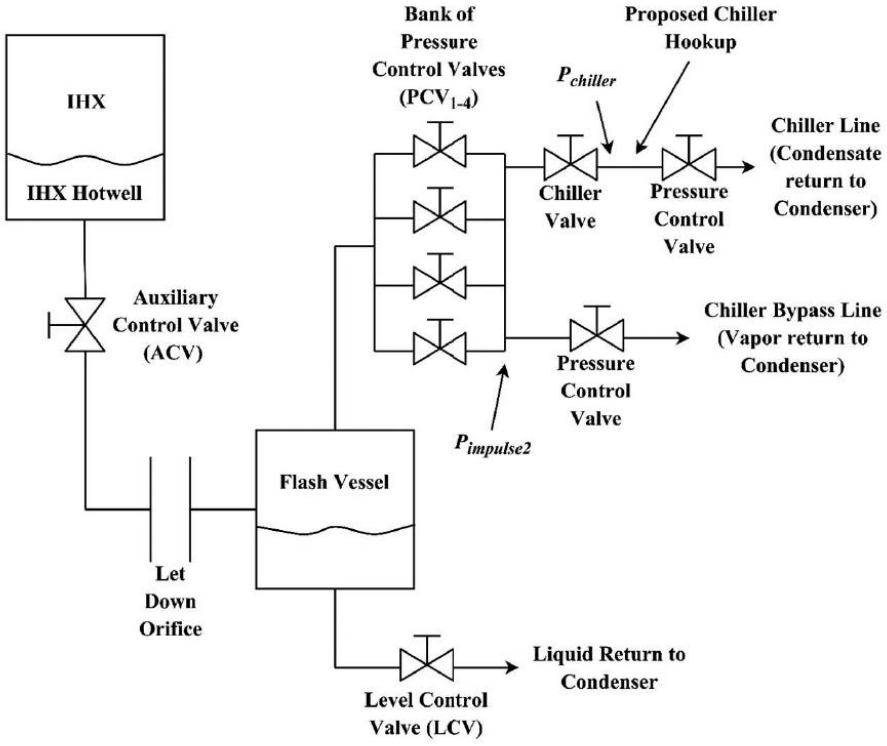

Figure 41. Flash-vessel configuration.

This configuration has the effect of utilizing additional waste heat and reducing the cooling load required for a given facility. Additionally, it has the effect of load shifting the cooling demand on the

electric grid. Traditionally cooling loads are highest during the middle of the day when, depending on the region's solar capacity, electric prices can be the highest. Through the installation of absorption chillers, in addition to other thermal storage devices, utilities establish the flexibility not only to store high-grade thermal energy for later use in either the electricity market or ancillary process market but can also to shift cooling loads from peak times to off-peak times.

7.2.3 Steam Accumulators

Another commercially available technology for the mass storage of thermal energy from nuclear reactors is steam accumulators. A steam accumulator is a pressure vessel nearly full of water that is heated to its saturation temperature by steam injection Figure 42.

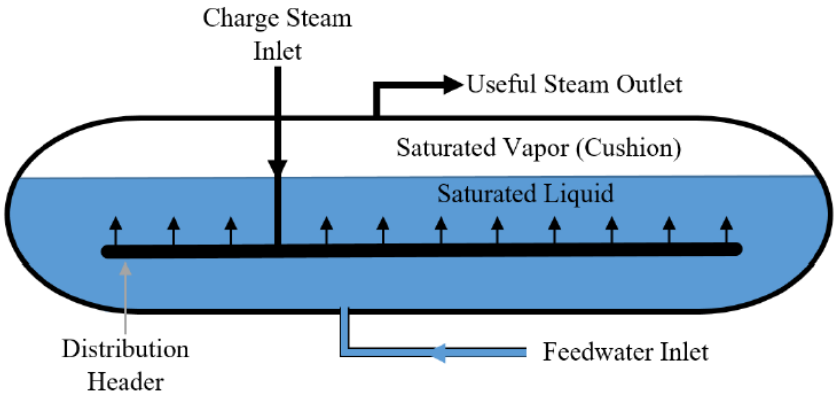

Figure 42. Steam accumulator [19].

Heat is stored as high-temperature, high-pressure water. In addition to its fairly high thermal conductivity, liquid water has a high volumetric heat-storage capacity of up to 1.2 kWh/m^3 [20]. When steam is needed, valves open, and some of the water is flashed to steam and sent to a turbine [21], producing electricity, while the remainder of the water decreases in temperature. Steam accumulators have been used as pressure buffers in steam plants for over a century. The first large steam accumulator built to produce peak electricity was the Charlottenburg Power Station, built in Berlin in 1929 with a peak electricity output of 50 MWe and a storage capacity of 67 MWh. The steam was provided by a coal-fired boiler, and the accumulator had a separate turbine. This accumulator had 16 tanks, each 4.3 meters in diameter and 20 meters high [22]. There are multiple commercial suppliers of steam accumulators, but not at the size that would be associated with an LWR.

There are two classes of accumulators. The variable pressure accumulator is a single-tank accumulator with sliding pressure during operation and is the most commercially available accumulator design. The more-complex expansion accumulator may be of interest for very large accumulators but is not generally used. The expansion accumulator involves two tanks: an accumulator tank that operates at constant pressure and an evaporator tank that delivers constant pressure steam. During discharge hot pressurized water is transferred from the accumulator tank to the expansion tank while cold water is added at the bottom of the accumulator tank to maintain a constant pressure with a thermocline separating the hot and cold water [22].

A potential configuration for use with nuclear reactors recently proposed by North Carolina State University [19] is illustrated in Figure 43. The steam accumulator is connected to the steam generator and, during times when excess electric demand is low, rather than downpower the reactor, instead bypasses excess steam to the steam accumulator for later use. While it is not shown in the configuration presented by North Carolina State, the steam accumulator could additionally choose to discharge steam in the form

of process steam to an ancillary process, such as hydrogen production, multi-stage flash desalination, or pulp and paper production.

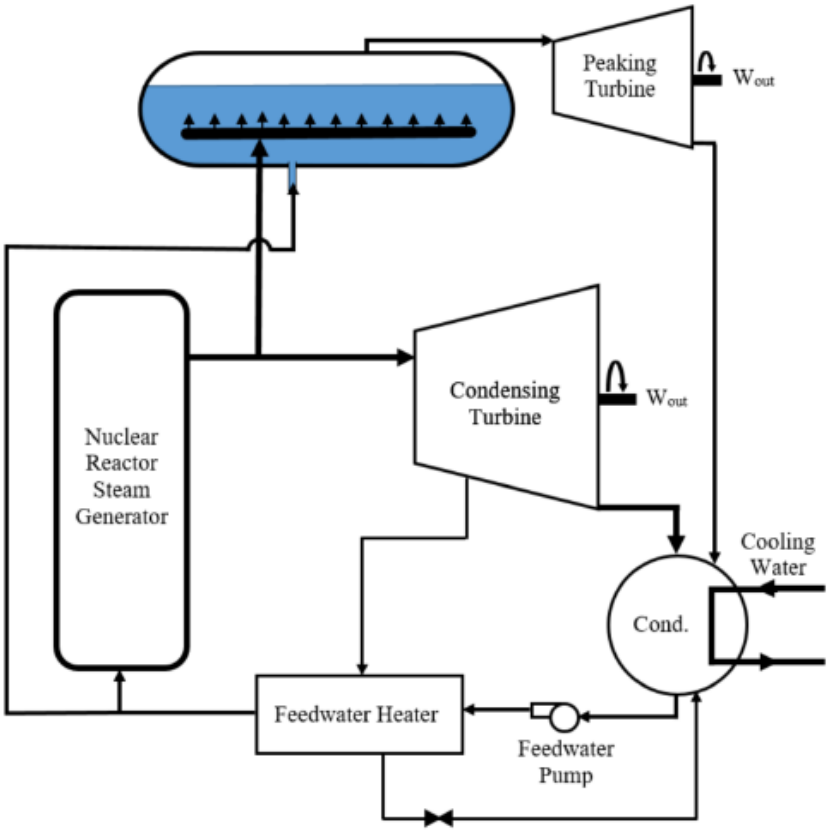

Figure 43. Potential integrated configuration of nuclear with steam-accumulator.

While the configuration presented above shows a single steam accumulator, it could instead be broken down into several smaller steam accumulators that may be at a more economical price point. An advantage of steam accumulators is the high TRL associated with them.

7.3 Latent-heat Storage Research and Development

Latent-heat TES has the advantage of power density, meaning far more heat can be condensed into a much smaller region. This can help to lower economic costs. However, to this point there have been very few breakthroughs in the realm of latent heat storage. This option will be explored in future technical and economic assessments.

References

[1] Konor Frick, Corey T. Misenheimer, J. Michael Doster, Stephen D. Terry, and Shannon Bragg-Sitton, "Thermal Energy Storage Configurations for Small Modular Reactor Load Shedding," *Nuclear Technology*, Vol. 202, No. 1 (2018), 53–70, doi: 10.1080/00295450.2017.1420945.

[2] M. Bragg-Sitton, R. Boardman, C. Rabiti, J. S. Kim, M. McKellar, P. Sabharwall, J. Chen, M.S. Cetiner, T. J. Harrison and L. A. Qualls, *Nuclear-Renewable Hybrid Energy Systems: 2016 Technology development program plan*, INL, Idaho Falls, ID, INL/EXT-16-38165, 2016.

[3] K. Frick, *Modeling and Design of a Sensible Heat Thermal Energy Storage System for Small Modular Reactors*, Ph.D. Dissertation, North Carolina State University, Department Raleigh, North Carolina, 2018, https://repository.lib.ncsu.edu/bitstream/handle/1840.20/34975/etd.pdf.

[4] S. Bragg-Sitton, R. Boardman, J. Collins, M. Ruth, O. Zinaman and C. Forsberg, *Integrated Nuclear Renewable Energy Systems: Foundational Workshop Report*, Idaho National Laboratory, 2014.

[5] S. Kuravi, J. Trahan, D. Y. Goswami, M. Rahman and E. Stefanakos, "Thermal energy storage technologies and systems for concentrating solar power," Progress in Energy and Combustion Science, vol. 39, pp. 285- 319, 2013.

[6] J. Coleman, S. Bragg-Sitton, Eric Dufek, Sam Johnson, Joshua Rhodes, Todd Davidson, and Michael Webber., "An Evaluation of Energy Storage Options for Nuclear Power," INL/EXT-17-42420. June 2017

[7] K. Powell and T. Edgar. "Modeling and control of a solar thermal power plant with thermal energy storage," *Chemical Engineering Science*, Vol. 71, 2012, pp. 138–145.

[8] Concentrating Solar Power, *Renewable Energy Technologies: Cost Analysis Series*, Volume 1: Power Section Issue 2/5, International Renewable Energy Agency, 2012.

[9] C. Misenheimer, *Modeling Chilled-Water Storage System Components for Coupling to a Small Modular Reactor in a Nuclear Hybrid Energy System*, Ph.D. Dissertation, North Carolina State University, Raleigh, North Carolina, 2017.

[10] Therminol-66; MSDS 150000093438 [Online]; Eastman Chemical Company: 200 South Wilcox Drive, Kingsport, Tennesee, 37660-5280, April 11, 2017, http://ws.eastman.com/ProductCatalogApps/PageControllers/MSDS_PC.aspx?Product=71093438, (accessed Dec 04, 2017).

[11] OpenStax College, "Chemistry OpenStax College," March 11, 2015, <http://cnx.org/content/col11760/latest/>.

[12] "Therminol 66: High Performance Highly Stable Heat Transfer Fluid," Applied Chemistry, Creative Solutions, Solutia, Inc., St. Louis, Missouri; https://www.therminol.com.

[13] "Therminol 68: Highly Stable Low Viscosity Heat Transfer Fluid," Applied Chemistry, Creative Solutions, Solutia, Inc., St. Louis, Missouri; https://www.therminol.com.

[14] "Therminol 75: Synthetic, Aromatic, High-Temperature Heat Transfer Fluid," Applied Chemistry, Creative Solutions, Solutia, Inc., St. Louis, Missouri; https://www.therminol.com.

[15] Nicholas Boerema, Graham Morrison, Robert Taylor, and Gary Rosengarten, “Liquid Sodium versus Hitec as a heat transfer fluid in solar thermal central receivers, *Solar Energy* Vol. 86 (2012), 2293-2305.

[16] Konor Frick, J. Michael Doster, and Shannon-Bragg Sitton. “Auxiliary Feedwater Reheating to Mitigate Primary and Secondary Side Thermal Stressors.”, in *11th International Topical Meeting on Nuclear Plant Instrumentation, Control and Human Machine Interfacing, Orlando, FL. 2019*.

[17] R. K. SURI et al., “Experimental Investigation of Chilled-Water Storage Technique for Peak Power Shaving,” *Int. J.Refrig.* Vol. 12, p. 213. https://doi.org/10.1016/0140-7007(89)90046-7.

[18] M. R. Al-Marafie, “Stratification Behaviour in a Chilled-Water Storage Tank,” *Int. J. Refrig.* Vol. 10 (1987); https://doi.org/10.1016/0140-7007(87)90125-3.

[19] M. Medrano, A. Gil, I. Martorell, X. Potau, and L. F. Cabeza, “State of the art on high-temperature thermal energy storage for power generation. Part 2—Case studies,” *Renewable and Sustainable Energy Reviews* Vol. 14, No. 1, (2010), pp. 56–72.

[20] A. LaPotin, and E. Schneider, “An Economic Model of a Steam Accumulator Storage System for Nuclear Power Plants,” *Transactions of the American Nuclear Society, November 2016.*

[21] M. Tucker. “Integration of Large-Scale Steam Accumulators for Energy Storage in Nuclear Hybrid Energy Systems”. Masters of Science Thesis. North Carolina State University, Raleigh, NC, 2017.

[22] *Light Water Reactor Heat Storage for Peak Power and Increased Revenue: Focused Workshop on Near Term Options,* Center For Advanced Nuclear Energy Systems, MIT-ANP-TR-170, July 2017.

8. CONCLUSIONS AND RECOMMENDATIONS

This study verifies a modeled nuclear power plant located in the Midwest can support growth in the industrial-manufacturing sector and, therefore, provides a good opportunity to assess the value proposition of direct use of nuclear energy by industry. Projected growth in the hydrogen market for fuel-cell vehicles, petroleum refineries, iron-ore reduction, and biofuels and ammonia synthesis provide opportunities to scale hydrogen production to nuclear power plant proportions. The transportation industry is looking to begin operating bus fleets in the northern and southeastern Ohio regions. The new Cleveland Cliffs hot-briquetted iron plant will perform iron-ore reduction in the area, beginning in 2020. This plant will reform natural gas into hydrogen and carbon monoxide to directly reduce iron ore into a product that can be refined into iron and steel by electric-arc mini mills; could be supplemented with hydrogen produced by the power provided from a the modeled nuclear power plant to reduce the emissions associated with natural-gas reforming. Similarly, hydrogen can be sent to refineries in the region to help reduce carbon dioxide emissions. New ammonia plants are also a possible outlet for hydrogen production. Finally, the carbon dioxide (CO_2) produced at ethanol plants can be converted into methanol and synthetic fuels with H_2. Affordable, clean hydrogen is desired for each of these applications.

The DOE target for hydrogen production is $2.00/kg. Projections in this report indicate a nuclear power plant can meet and even exceed this target. In fact, the outcomes of the analysis indicate an LWR electricity/hybrid plant can also outperform conventional natural-gas steam reforming (referred to by industry as steam-methane reforming) under specific conditions. For the purposes of this evaluation, it was assumed that natural gas SMR plants would be located in proximity to industrial users. However, because the electrolysis plant is close coupled to the nuclear plant, it was assumed hydrogen produced near the LWR site must be compressed and delivered to the set of industrial users. Hence, this evaluation fairly compares the market case for LWR electricity/hydrogen hybrids with the incumbent process.

Four conditions that need to be met for LWR electricity/H_2 hybrids to compete with conventional natural gas SMR plants are

1. *A consistent, reliable, and low-cost energy will be available for the life of the project*. Many LWR power plants already meet this condition, as follows:

    a. Hydrogen is produced with a relatively high on-line capacity factor, while allowing the power-generation station to participate in the electricity market as reserve capacity to further increase revenue. The exact availability of electricity production can be determined using the tools being developed by the DOE Office of Nuclear Energy to optimize system-wide operating schedules.
    b. Low-temperature water-splitting electrolysis, based on emerging PEM technology—which requires only an electrical connection only to the nuclear power plant—is competitive with small-scale natural-gas SMR hydrogen plants (~23 tpd) when the cost of electricity purchased from the power plant is around $33–36/$MW_e$-hr or less before other considerations, such as carbon-emissions tax credits, are taken into account. In this case, parity with natural gas SMR is achieved at the cost of producing hydrogen for $2.93/kg-$H_2$.
    c. High-temperature steam splitting electrolysis or HTE (which requires electricity and thermal energy from the plant) achieves the DOE target for a large centralized hydrogen plant (~534 tpd) when electricity is sold to the hydrogen plant for under $44/$MW_e$-hr. The thermal energy duty of HTE for an LWR is less than 7% of the total thermal energy that is used for power production. LWR operating experiences to date indicate this would have little to no impact on the operation of the LWR.
    d. HTE becomes competitive with an equally large natural gas SMR plant when the cost of electricity is under $25–27/$MW_e$-h; therefore, other financial incentives may be necessary for the nuclear power plant to be profitable when coupled to a large centralized hydrogen plant.

For example, with a nominal capacity payment of \$132.4/MWe-day and an equivalent-demand forced outage rate (EFORd) of 1.67%, HTE is competitive with natural gas SMR when electricity sells for around \$30/MW_eh.

e. Hydrogen produced by the energy from a nuclear power plant is valued as a clean-energy carrier for transportation fleets, fuels, and chemical production. Thus, credits under clean-fuels standards or CO_2-reduction credits will spur investments in small and large electrolysis plants connected to an LWR. A carbon credit of \$10/tonne-CO_2 avoided could reduce the cost of hydrogen produced by electrolysis \$0.10/kg-H_2. Similarly, a carbon credit of \$40/tonne-CO_2 avoided could similarly reduce the cost of hydrogen produced by electrolysis \$0.40/kg-H_2.
f. By participating in both a typical capacity-payment market while earning a CO_2 emissions credit of about \$40/tonne CO_2 avoided, hydrogen generation by a centralized HTE plant will rival natural gas SMR when the cost of electricity is under \$40/MW_e-h.
g. The solid-oxide cells used for HTE can be built to operate in reverse, as fuel cells that burn H_2 to produce electricity. Analysis of reversible solid-oxide fuel-cell/electrolysis cell was not evaluated in this study because it is mainly applicable to LWRs in regions where renewable energy will force baseload plants to run flexibly or in hybrid-systems operation.

2. *The capital and operating costs of electrolysis stacks are reduced to under \$100/kWe for HTE solid-oxide stacks and less than \$86/kWe for PEM stacks (DC power input rating). This condition is plausible based on the following analysis assumptions and outcomes.*

    a. This assessment applied DOE models to calculate the cost of hydrogen production. These are based on scalable electrolysis modules comprised of multiple stacks.
    b. Stack component-manufacturing rates reach a volume of around 300-tpd hydrogen annual production capacity additions (or about 500 MWe added production per year).
    c. Balance of plants systems and other capital costs are bounded by the Aspen process-model capital-cost estimates completed for this assessment.

3. *The market for hydrogen in the Midwest near the representative nuclear plants is large and can be supplied from a central hydrogen production plant.*

    a. This condition can be met by establishing an industry complex of hydrogen users in the modeled nuclear plant. This study indicates market opportunities already exist for both high-value/low-volume hydrogen, beginning immediately and growing exponentially, while high-volume/lower-value hydrogen markets are possible in 3–7 years, as both LTE/PEM and HTE electrolysis technology matures. The Midwest Region in a prime area for a complex of new hydrogen-using industries that would have access to commerce transport by shipping, railroads, and highways in this area.
    b. This report proposes a strategy that commences with low-temperature electrolysis supplying hydrogen of high value, but initially relatively low volume of around 50 tpd-H_2 needed by the transportation industry, and then transitioning to a high-volume but relatively lower-value merchant hydrogen market of around 500 tpd-H_2.
    c. The associated cost of pipeline hydrogen delivery adds approximately \$0.21/kg-H_2 for a high-capacity hydrogen pipeline under 50 miles or \$0.30 for a pipeline under 150 miles.

4. *Policy and/or regulatory conditions spur the transition from electricity production to nuclear electricity/hydrogen hybrid operations.*

    a. In order to optimize revenue for a nuclear power plant in the Midwest, or even to achieve revenue adequacy, it may be necessary to authorize capacity payments for the duration of

transitioning from day-ahead scheduling to a plant that responds to market signals for electricity production and non-electrical products manufacturing.

b. Policy incentives for clean energy can especially promote and accelerate LWR supported electrolysis of around 50 tpd-H_2 production.
c. Hybrid operations may require authorization of state or federal power regulators and management agencies to participate in grid markets while selling electricity to the hybrid-plant user at some value nominally lower than the wholesale electricity market. Market rate structure differs by region, depending on regulated versus deregulated power generation and transmission requirements and governing public-utility commissions.
d. Access to thermal energy requires an engineering study and analysis of NRC license authorization.

This assessment documents for the first time a comparison of a future electrochemical process referred to as non-oxidative deprotonation (or NPD) to produce polyethylene with a modular/scalable technology that is similar to HTE. A new NPD process under development at Idaho National Laboratory is especially tailored for LWR hybrid operations. Growth in the plastics and resins markets provides incentive for capital investments in plants that are supplied electricity and thermal energy from a nuclear power station.

This preliminary evaluation indicates the capital cost of new NDP process is about 30% less than a conventional ethane cracking facility that produces PE feedstock. Operating costs can be reduced from $673 to $429 for each tonne of PE produced, resulting in a saving of about 40%. In addition, with electricity and thermal energy supplied by an LWR, the CO_2 footprint is reduced by 98%. A net energy saving of 41.7 GJ/tonne-C_2H_4 produced is transformational, taking credit for the pure hydrogen stream that is coproduced by NPD.

The study emphasizes four important drivers for LWR hybrid systems:

1. *The existing fleet of nuclear reactors can reliably produce cost-competitive, moderately high-pressure steam (5.2 MPa, ~300°C) for the projected life of a hybrid plant large capital investment project.* Engineering calculations indicate the cost of steam generation and delivery by an existing LWR is already lower than the cost of producing steam with a new industry-scale natural-gas package boiler. In addition, while the cost of natural-gas production could stay at historically low costs for many years, this is dependent on several factors and the price of natural gas could rise any time before resource scarcity is realized. The cost of nuclear fuel on the other hand is projected to remain flat for decades to come with little or no volatility in price up to 40–60 years of future LWR operations. This assumes LWR upgrades for license extension remain within plant maintenance and refurbishing activities. **In short, LWR hybrid plants can provide low-cost energy to U.S. energy-intensive manufacturing industries, and this can help maintain American competitiveness.**

2. *Nuclear energy has very low emissions and should therefore be valued as a clean energy source with the same considerations as alternative energies.* Hybrid LWR operations can allow nuclear plants to operate at their nameplate capacities while compensating for the variability of intermittent wind and solar energy additions to the electricity grid. **The synergy of nuclear and renewable energy sources can help reduce both U.S. Clean Air Act criteria air pollutant emissions as well as CO_2 emissions.**

3. *Hybrid systems can be used for daily and seasonal stored energy*. **LWRs hybrids are especially suitable for thermal- and chemical-energy storage, with the possibility of producing power that matches diurnal-demand cycles or peak-season demands.**

4. *Nuclear power generating stations provide important reliability, and hybrid systems can help maintain grid resiliency that is becoming increasingly important with the build-out of renewable*

energy. **Hybrid LWR plants that mainly switch power production between large electrical loads and the electricity grid can be used not just to balance generation and demand on a short time scale (possibly minute-by-minute) to help regulate reactive power (*VAR*) and frequency (*f*) at the transmission level of the grid.**

This report includes the following recommendations.

Recommendation 1: It is important to continue forward with R&D activities that help develop enabling interfaces for LWR hybrid energy systems. Attention to the fourth principle is being addressed by various organizations, including the DOE Grid Modernization Initiative, DOE Fuel Cell Technology Office, and DOE Nuclear Energy Program. These efforts are helping to illustrate the value of assets like large nuclear power generating stations beyond the traditional grid market. It will be important to continue these efforts. The INL Systems Integration Laboratory and the DOE Tri-Lab Consortium efforts of INL [1], the National Renewable Energy Laboratory, and the National Energy Technology Laboratory will also help achieve this objective.

This TEA is mainly focused on hydrogen (H_2) generation for associated markets in the Midwest as a possible beginning for conversion of a nuclear power plant into a hybrid facility or an industry complex. Preliminary evaluations of polymers production—based on polyethylene feedstock production—and two important chemical commodities, methanol and formic acid, are also considered. In addition, because the value of the heat produced by an LWR is compelling, a section of this report summarizes LWR heat extraction and thermal-energy storage to provide an initial understanding of pertinent technology-development needs. Finally, interest in utilizing biogenically produced CO_2 from any the numerous ethanol plants in the Midwest as a feedstock to produce formic acid, methanol, and also urea fertilizer is growing. Therefore, a pipeline-transport tradeoff analysis is included in this report to elucidate the value of a large-scale CO_2-utilization hybrid system located near an LWR, versus a distributed plant that would not have access to the thermal energy that can be provided by the LWR.

Recommendation 2: Region-specific and location-specific TEAs are needed for LWRs in other regions, especially where solar and wind energy are on the rise. The advent of low-cost solar energy in the southern states and wind energy along the corridor stretching from Texas to the Northern Plains is projected to have significant impact on LWR operations. Therefore, case-specific TEAs are needed to identify the best hybrid systems based on the optimal business case for these locations.

Recommendation 3: It will be beneficial to continue analysis that quantify tradeoffs between hydrogen production, as a distributed system, tied to an LWR with a dedicated electricity transmission line versus hydrogen delivery from a centralized plant through a pipeline. Development of systems design and optimization tools will help scale hybrid systems to achieve the highest profitability of the overall system.

Recommendation 4: Given that the value of LWR steam and thermal energy is high, it will be beneficial to undertake engineering studies of systems that extract and deliver steam or thermal energy to industrial users, including high-temperature steam electrolysis and polyethylene production. A front-end engineering and design study by an engineering and plant-construction firm will certify thermal-energy extractration is technically feasible and economically competitive. These studies must account for future capacity expansions and the impact of these expansions on grid prices.

Recommendation 5: This study emphasized the need to evaluate hydrogen compression and delivery options and their associated costs. Cursory attention was given only to pipeline delivery under the assumption that any large source of hydrogen would be sent to a constant user within a reasonable distance to a centralized plant. Tube trailers may be a good option for carrying hydrogen to fuel cell vehicle filling stations. Hydrogen liquefaction could be used to carry hydrogen to large volume customers at relative long distances, such as an oil refinery. Also, the benefits of running a dedicated power line to a

location where hydrogen could be generated on-site by low-temperature electrolysis should be compared to delivery of hydrogen from a centralized plant.

Recommendation 6: The importance of thermal energy storage provides impetus to develop the type of storage systems described in Section 7. Engineering design and prototype testing in a thermal energy delivery test loop will help accelerate thermal-energy storage-technology development and reduce commercial risks of deployment.

Recommendation 7: The high reward for polyethylene production, and also formic acid production, provides incentive for investments in R&D that raises the technical readiness level from between 2 and 3 to levels of 4–5. In order to proceed with pilot-scale testing investments are required for commercial-scale use of these transformational processes.

Recommendation 8: Pilot-plant testing of integrated energy systems are needed to start the conversion of LWR operations to hybrid systems. Pilot-plant testing will help LWR station owners and operators develop procedures to jointly operate the industrial plant where, at minimum, electricity is dispatched from the LWR electrical-transmission operator to the electricity grid or the industrial user. Similarly, thermal integrations in a tightly coupled system may require interaction between the LWR operators and the steam or heat users. A pilot-plant system will address technical, operational, and license-authorization matters. The pilot-plant platform can also be used to establish response characteristic of the systems. These characteristics must be known to calibrate physics-based models that are useful for full-scale systems analysis. This information is also important for updating probabilistic risk assessment that consider the interactions of full-commercial hybrid plant operations.

Recommendation 9: Potential technical impacts of hybrid-system operations on LWR power-generation systems should be evaluated using appropriate models that can account for changes in the quantity of thermal energy (with steam extraction from the power-systems loop) or quality of steam (with heat extraction from main steam).

Recommendation 10: A commercialization strategy for hybrid scaling to full commercial operations will help large capital-investment groups understand opportunities for growth. The strategy will also inform policy makers and regulators about economic-development opportunities and impacts that can be realized.

Recommendation 11: The importance of policies and regulations that value clean energy need to be pursued. Nuclear energy should be considered, documented, and treated as a low carbon clean energy source and as vital long-term stable part of the nation’s energy grid security and resiliency policy. Policies and procedures that support this end should be encouraged. This will provide a compelling argument for the hybrid systems addressed in this study. For example, either a credit for avoided pollutant emissions or capacity payments to a nuclear power plant would help establish a clear business case for selling hydrogen to existing hydrogen users in the vicinity of the plant and perhaps more important, for providing hydrogen to a new world-class ammonia plant or a new direct-reduction ironmaking plant seeking to sell low-carbon products. Any credits granted to the electricity generated by a nuclear power station, the hydrogen product, or the final commodity will enhance the market case for LWR hybrid operation. Similarly, provisions for reserve-capacity payments may also help reduce the cost of hybrid operations by optimizing the profitably of cooperating partners.

Reference

[1] Arent, D. et al., *Summary Report of the Tri-Lab Workshop on R&D Pathways for Future Energy Systems*, INL/Ext-18-52273, July 24-25, 2018.